ISSN 8755-6839

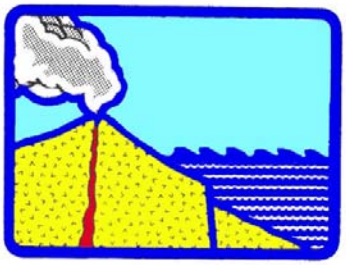

SCIENCE OF
TSUNAMI HAZARDS

The International Journal of The Tsunami Society
Volume 24 Number 5 Published Electronically 2006

THIRD TSUNAMI SYMPOSIUM PAPERS - III

OBJECTIVE: **The Tsunami Society** publishes this journal to increase and disseminate knowledge about tsunamis and their hazards.

DISCLAIMER: Although these articles have been technically reviewed by peers, **The Tsunami Society** is not responsible for the veracity of any statement, opinion or consequences.

Submit manuscripts of articles, notes or letters to the Editor. If an article is accepted for publication the author(s) must submit a scan ready manuscript, a Doc, TeX or a PDF file in the journal format. Issues of the journal are published electronically in PDF format. Recent journal issues are available at

http://www.sthjournal.org.

Tsunami Society members will be advised by e-mail when a new issue is available. There are no page charges or reprints for authors.

Issues of the journal from 1982 thru 2005 are available in PDF format at

http://epubs.lanl.gov/tsunami/

and on a CD-ROM from the Society to Tsunami Society members.

ISSN 8755-6839 **http://www.sthjournal.org**

Published Electronically by The Tsunami Society in Honolulu, Hawaii, USA

MODEL PREDICTIONS OF GULF AND SOUTHERN ATLANTIC COAST TSUNAMI IMPACTS FROM A DISTRIBUTION OF SOURCES

Bill Knight
West Coast and Alaska Tsunami Warning Center
Palmer, AK, USA

ABSTRACT

The West Coast and Alaska Tsunami Warning Center now issues tsunami warnings for the US Gulf and US /Canadian Atlantic coasts. Because there is less historical data for these regions than for the Pacific, numerical models have been used to make predictions of wave amplitudes, travel time, and "reach". Hypothetical tsunami sources are placed in the Atlantic, the Gulf of Mexico, and in the Caribbean, with the resulting waves advanced forward in time 12 to 24 hours. Model results are presented in relation to warning center procedures.

INTRODUCTION

Four initial sea level disturbances were created using Okada's formulas (1985) in conjunction with their associated hypothetical earthquakes. The model earthquakes are also truly "model" in the sense that they do not necessarily correspond to expected magnitude, likelihood of rupture, or precise location on known thrust faults. They have been chosen in part to excite various ocean basins and to present worst case conditions.

The 2D depth averaged model developed at the University of Alaska, Fairbanks (Kowalik et al., 2005) has been used to propagate the initial disturbance to all points along the US Gulf and Atlantic coasts. All computations were done on a uniform 15 second mesh, and 15 second bathymetric / elevation data was used wherever it was available (NOAA / NGDC). In regions where no data was available, bathymetry values were interpolated from the 1 minute Gebco dataset. The model space was a 40 degree square with radiation conditions applied in the open ocean and run-up conditions at the coast.

The results presented here were obtained from inspection of approximately 130 synthetic mareograms along the Gulf and Atlantic coasts generated during the model runs. The source summary is shown in Table 1. Numbers also correspond to locations on the model domain map on the following page (Fig 1).

Table I – source summary

1) *Puerto Rico trench*: 66W, 18N, Mw 9.0
2) *Caribbean Sea*: 85W, 21N, Mw 8.2 – translated from the Swan fault to mouth of Gulf near Cancun
3) *North Panama Deformed Belt*: 66W, 12N, Mw 9.0
4) *Gulf of Mexico*, offshore of Veracruz: 95W, 20N, Mw 8.2 (no known credible source)

The model sources are aligned with local strike where applicable.

Figure I – model domain with source locations (depths and elevations in Meters)

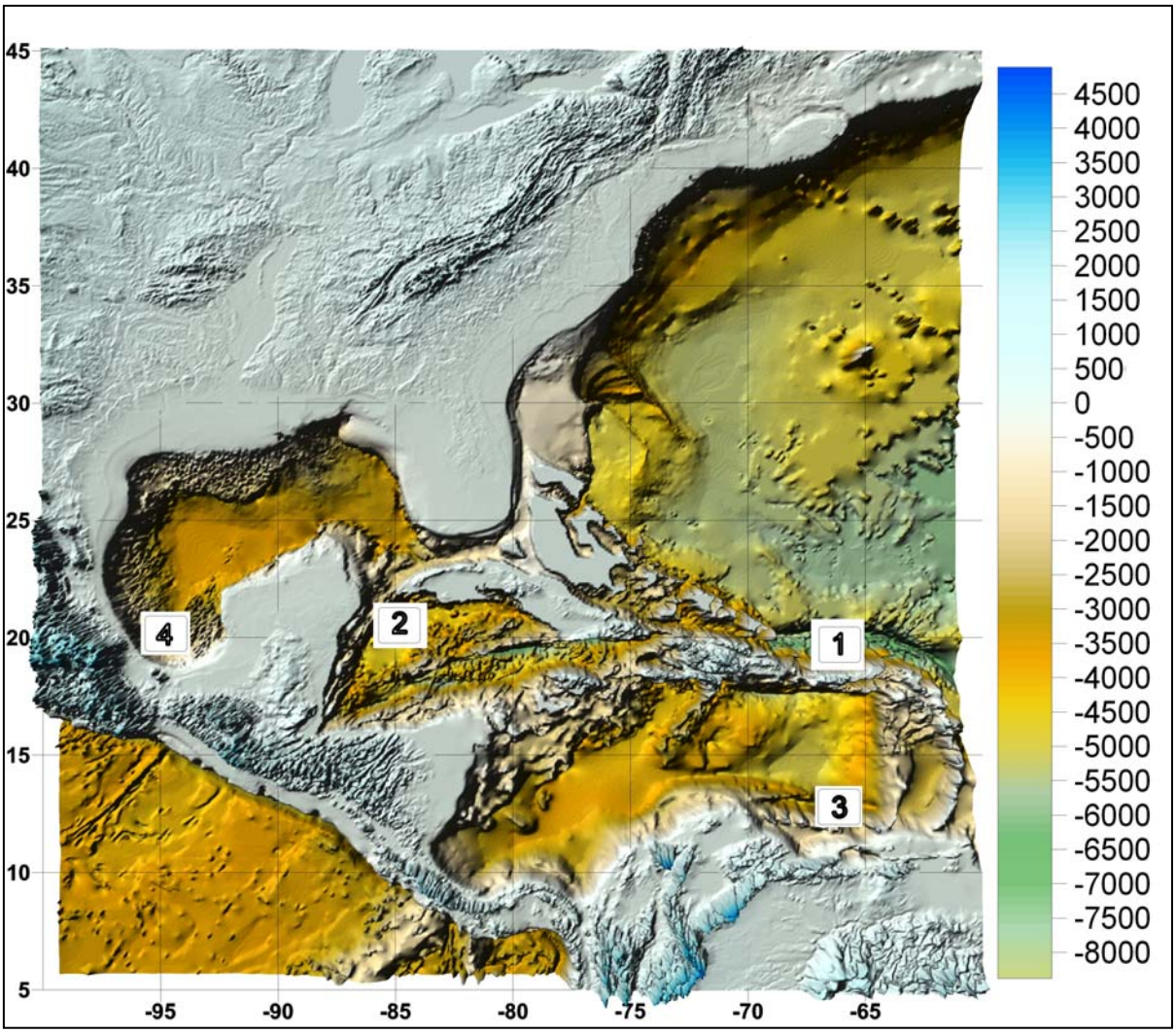

Source #1 results and discussion:
Typical synthetic mareograms are shown below in Figure 2.

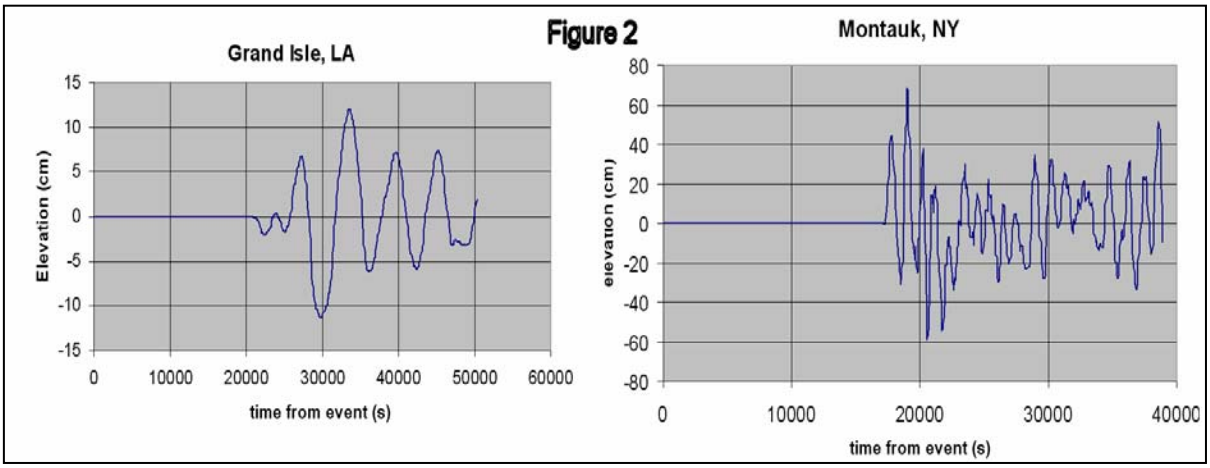

Atlantic and Gulf mareograms form distinct groups that show unique features. Gulf amplitudes are low (under 25 cm) and have leading edge depressions. Wave arrivals along the Atlantic are all leading edge elevations and the amplitudes can be higher (over 150 cm). The leading edge difference can be explained by the orientation of the source.

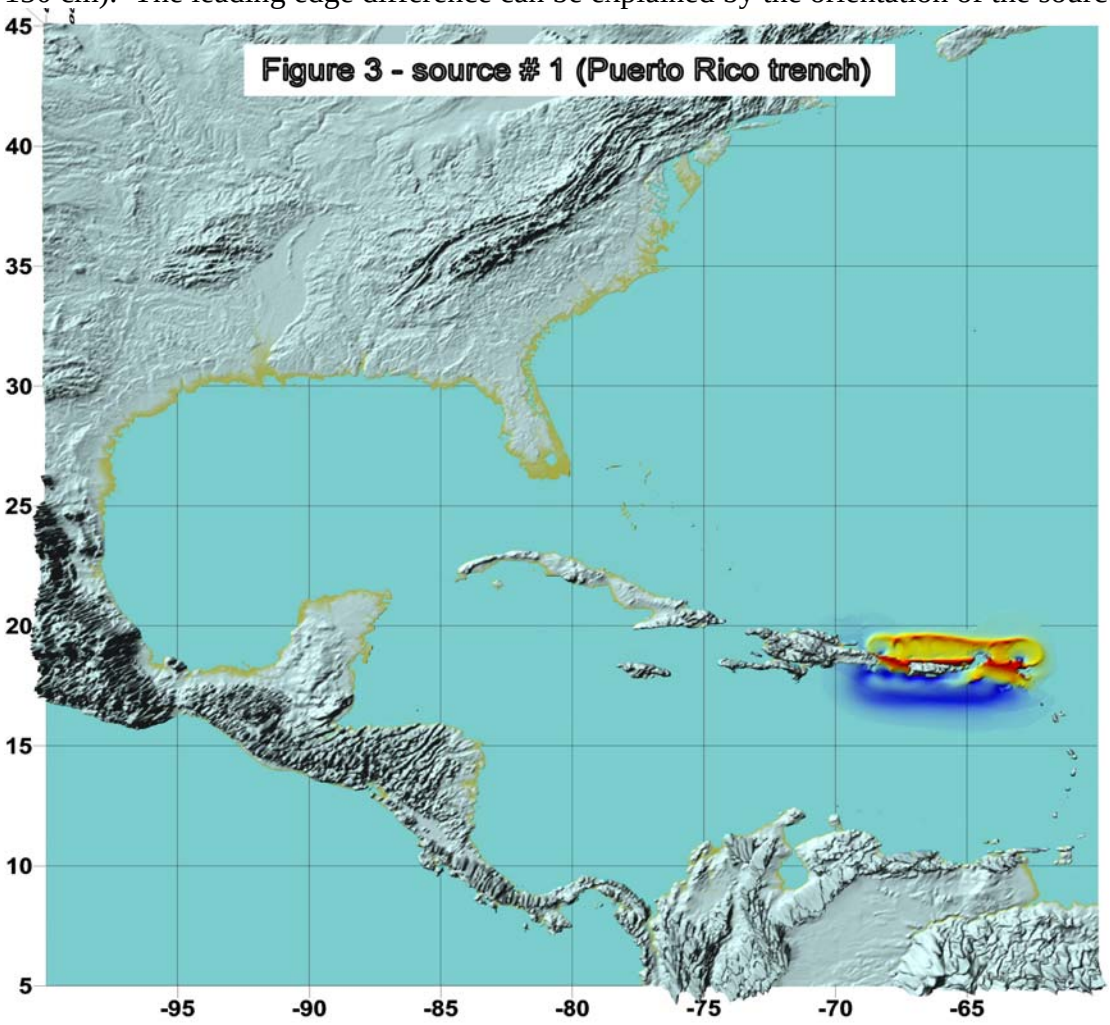

Initial uplift is dipolar as shown in figure 3 above (red is uplifted ocean, blue is down dropped).

Propagation into the Gulf takes two routes, one through the Caribbean and the other through the Straits of Florida. The Caribbean route is faster by about 1 hour, and the first impact is therefore the leading edge depression. Energy transfer into the Gulf is computed with the energy flux vector $\rho d \vec{V}(g\zeta + \frac{1}{2}V^2)$ (Kowalik & Murty, 1993). Evaluating this flux across both the Caribbean and the Straits of Florida shows that more energy moves into the Gulf through the latter pathway, even though it arrives later. This is important because the duration of wave action in the Gulf is increased and because travel times computed from first arrivals may be misleading.

Evaluation of the energy fluxes was done along the planes shown in Figure 4a below.

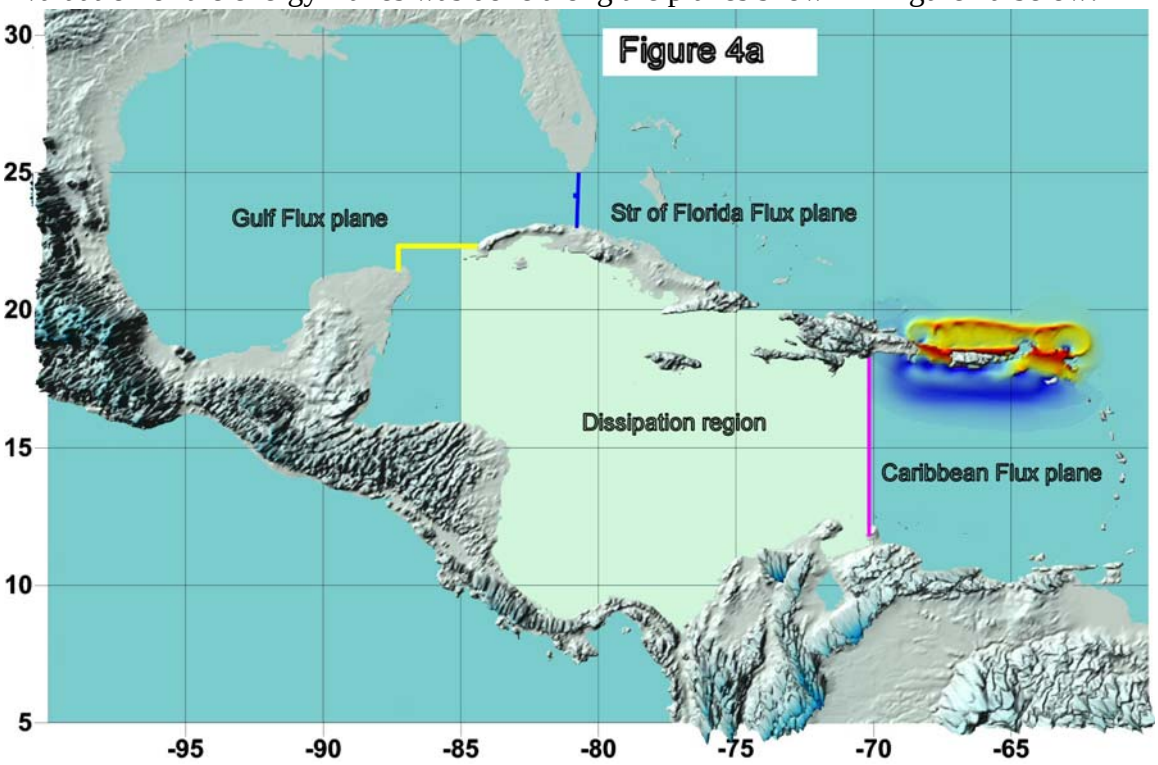

Energy loss was also computed in the part of the Caribbean Sea labeled "dissipation region" by integration of the bottom friction term over the region and up to time t. Results from the three flux planes along with dissipation are plotted in Figure 4b below. Energy flow into the Atlantic was about 10X larger than the energy entering the Caribbean through the magenta plane, and was not included in the plot. Note that the reduction of energy into the Gulf through the Caribbean is well explained by the dissipation curve. Flux through the Straits of Florida winds up being larger than what enters through the Gulf / Caribbean pathway. A complete mareogram summary for

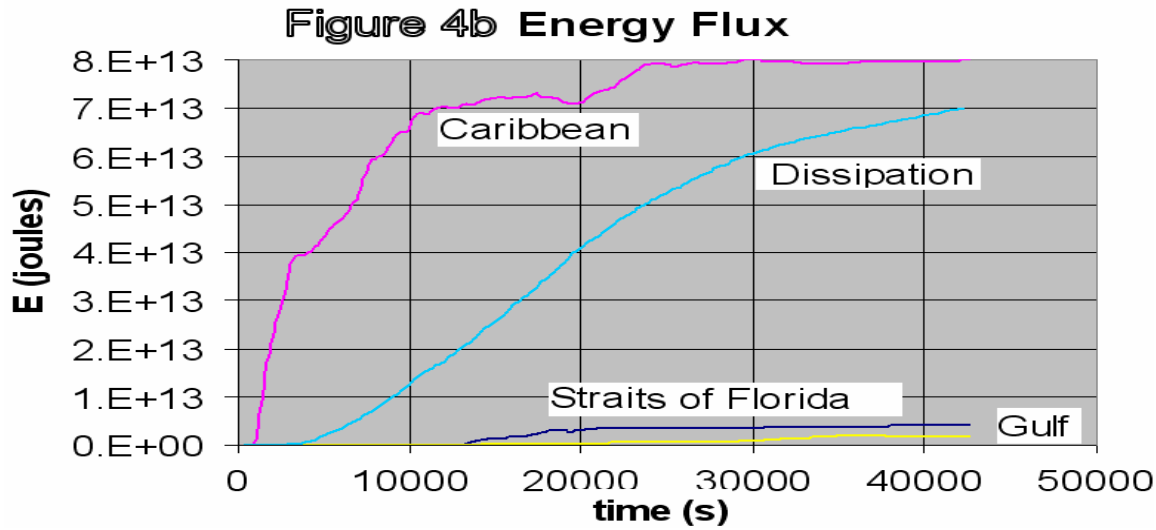

Source 1 is shown in Table 2 on the following page.

Table 2: Source 1 mareogram summary:

Location	Region	Travel Time (hr-min)	Peak Height(cm)	Initial Motion	Period (hr-min)
Brownsville_TX	Gulf	6hours 22min	4	depression	2 hours 3 min
Corpus Christi_TX	Gulf	6 hours 45 min	4	depression	1 hour18 min
Galveston_TX	Gulf	8 hours 2 min	6	depression	1 hour 58 min
High Island_TX	Gulf	8 hours 30 min	3	depression	1 hour 57 min
Eugene Island_LA	Gulf	8 hous 10 min	3	depression	1 hour 56 min
Port Fourchon_LA	Gulf	5 hours 52 min	10	depression	2 hours 3 min
Grand Isle_LA	Gulf	6 hours	12	depression	1 hour 38 min
Waveland_MS	Gulf	10 hours 36 min	1	depression	
Biloxi_MS	Gulf	8 hours 28 min	5	depression	2 hours 5 min
MS_AL Border	Gulf	9 hours 35 min	3	depression	2 hours 2 min
Destin_FL	Gulf	5 hours 38 min	7	depression	1 hour 55 min
Suwanee_FL	Gulf	8 hours 37 min	3	depression	2 hours 2 min
Panama Beach_FL	Gulf	5 hours 47 min	5	depression	1 hour 54 min
Panama City_FL	Gulf	6 hours 20 min	11	depression	2 hours 2 min
Clearwater Bc_FL	Gulf	6 hours 58 min	8	depression	1 hour 6 min
St Petersburg_FL	Gulf	7 hours 48 min	5	depression	2 hours 56 min
Tampa_FL	Gulf	8 hours 28 min	5	depression	2 hours 28 min
Port Manatee_FL	Gulf	7 hours 28 min	5	depression	1 hour 28 min
Bonita_FL	Gulf	7 hours 37 min	25	depression	1 hour 50 min
Naples_FL	Gulf	7 hours 28 min	23	depression	1 hour
Virginia Key_FL	Atlantic	2 hours 57 min	15	elevation	49 min
Ocean Reef_FL	Atlantic	3 hours 13 min	28	elevation	1 hour 40 min
Jupiter_FL	Atlantic	2 hours 47 min	54	elevation	1 hour 2 min
Flagler_FL	Atlantic	4 hours 18 min	117	elevation	1 hour 10 min
Vaca Key_FL	Atlantic	4 hours	13	elevation	1 hour 11 min
St Simons_GA	Atlantic	5 hours 30 min	40	elevation	1 hour 13 min
Altamaha_GA	Atlantic	5 hours 33 min	47	elevation	1 hour 15 min
So Santee_SC	Atlantic	4 hours 32 min	77	elevation	1 hour 22 min
Springmaid_SC	Atlantic	4 hours 57 min	129	elevation	1 hour 8 min
Charleston_SC	Atlantic	4 hours 57 min	49	elevation	1 hour 15 min
Surf City_NC	Atlantic	4 hours 23 min	112	elevation	1 hour 8 min
Beaufort_NC	Atlantic	3 hours 38 min	147	elevation	45 min
Oregon Inlet_NC	Atlantic	3 hours 45 min	38	elevation	42 min
Duck_NC	Atlantic	3 hours 57 min	140	elevation	drained
Currituck_NC	Atlantic	4 hours 15 min	102	elevation	36 min
Chesapeake B_VA	Atlantic	7 hours 12 min	6	elevation	46 min
Annapolis_MD	Atlantic	10 hours 28 min	3	elevation	~2 hours
Cape Henlopen_DE	Atlantic	4 hours 52 min	64	elevation	42 min
Cape May_NJ	Atlantic	5 hours	68	elevation	45 min
Atlantic City_NJ	Atlantic	4 hours 45 min	155	elevation	45 min
Montauk, NY	Atlantic	4 hours 48 min	68	elevation	16 min
Bar Harbor_ME	Atlantic	5 hours 33 min	71	elevation	6 min
D41424 (32.4N, 73W)	Atlantic	1 hour 52 min	35	elevation	
D41420 (23.3N, 67.6W)	Atlantic	32 min	131	elevation	
D41421 (23.4N, 63.9W)	Atlantic	31 min	175	elevation	
D7-2 (38.6N, 68 W)	Atlantic	2 hours 10 min	78	elevation	
D42407 (23.4N, 63.9W)	Caribbean	10 min	-61	depression	
D8-1 (25.4N, 86.8W)	Gulf	3 hours 27 min	-2	depression	
Bermuda	Atlantic	1 hour 57 min	511	elevation	12 min
Limetree_StCroix	Caribbean	1 min	240	depression	15 min
Punta_Guayanilla	Caribbean	0 min	173	elevation	21 min

Source2-4 results:
The remaining source mareograms are presented qualitatively as indicator plots.

Source 2 –mareogram summary (source in Caribbean Sea near Cancun)

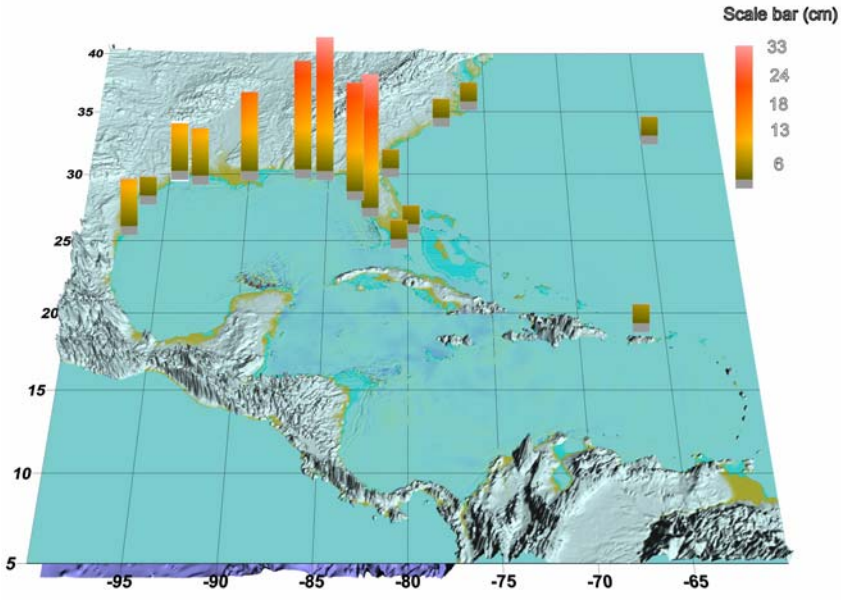

Note that the Gulf amplitudes are all under 30 cm, reflecting in part the fact that significant wave energy is lost to bottom friction in the Caribbean Sea.

Source 3 mareogram summary (source near Venezuela)

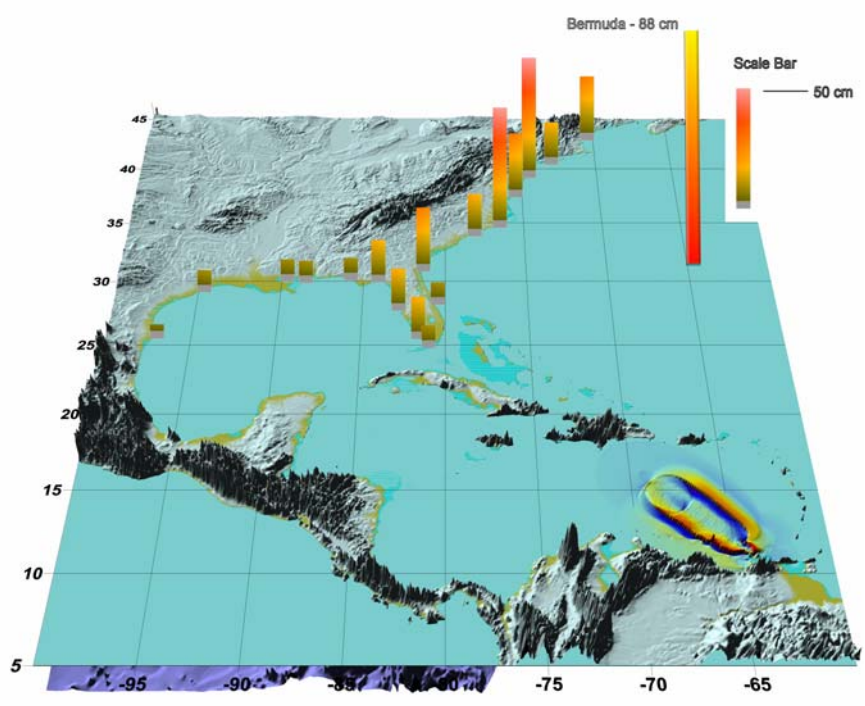

The largest Atlantic coast amplitudes are under 50 cm, with the Gulf coast run-ups reduced from these values to a maximum of 15 cm. The wave energy is well dissipated by bottom friction and spread in time by multiple reflections in the Caribbean, resulting in lower than expected amplitudes both on the Gulf and the Atlantic coasts.

Source 4 mareogram summary (Gulf source near Veracruz).
Note the amplitudes are all under 35 cm, and there is very little leakage of wave energy into the Atlantic.

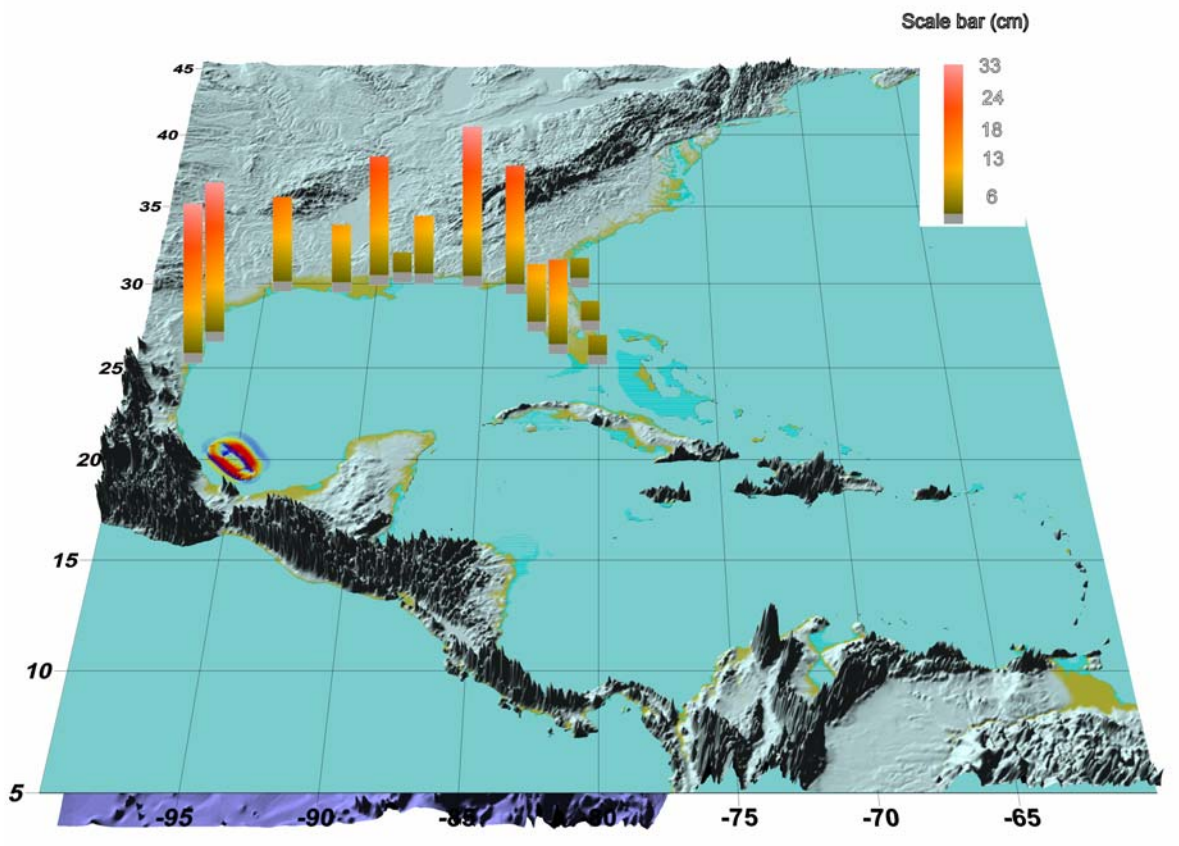

SUMMARY

The Atlantic and Gulf coasts are nearly independent since the hydrodynamic connection between basins is through the narrow Straits of Florida and through the Caribbean, where bottom friction losses appear to be large. Sources outside the Gulf are not expected to create a tsunami threatening to the Gulf coast. Thus the Gulf coast would not need to be included in a warning for a non-Gulf source (unless a Gulf DART buoy records an unexpected large amplitude wave). For Atlantic sources, warnings could be issued for the Atlantic coast alone. Both Gulf and Atlantic coasts appeared to be well shielded from the large model Caribbean source. This would argue for warnings to be issued only with extreme caution for this source region.

The Puerto Rico trench source is the most threatening of the modeled scenarios, but even here, the Gulf should not need to be placed in a warning. The short travel time to Atlantic DART buoys, along with the large amplitude signal and short travel time to Bermuda should provide timely check points for a possible expansion of a tsunami warning to the northern Atlantic states.

REFERENCES

Okada, Y: SURFACE DEFORMATION DUE TO SHEAR AND TENSILE FAULTS IN A HALF SPACE, 1985 Bulletin of the Seismological Society of America (75) 4

Kowalik, Z, Knight, W., Logan, T., and Whitmore, P.: 2005, NUMERICAL MODELING OF THE GLOBAL TSUNAMI: Indonesian Tsunami of 26 December 2004. *Science of Tsunami Hazards*, 23(1), 40-56

Kowalik, Z. and Murty, T.S.: 1993, *Numerical Modeling of Ocean Dynamics*, World Scientific

http://www.ngdc.noaa.gov/mgg/coastal/coastal.html (download site for US coastal bathymetry and elevation)

MOMENTUM AS A USEFUL TSUNAMI DESCRIPTOR

Harold G. Loomis
Honolulu, HI

ABSTRACT

In looking at the videos of the Indonesian tsunami coming ashore at various locations, I thought, "That's a lot of water with a lot of momentum, and that's what does the damage." Perhaps the momentum of a tsunami might be a physical quantity to focus on. Only external forces on the designated body of water create its momentum. Within the body of water, turbulence, internal friction and laminar flow involve internal forces and are not relevant.

This could be particularly useful in the generating area. There could be external forces on a designated body of water from a landslide, a pyroclastic flow, an explosion, from steam generation and from chunks of matter falling into the ocean. The horizontal components of those forces result in horizontal momentums. Ultimately when the wave moves out from the generating area and the internal turbulence and laminar flow get dissipated by friction, in the remaining long wave motion the wave height is simply related to the horizontal momentum. The horizontal momentum contribution to the directionality of the wave would be narrower than that due only to the initial vertical displacement.

Focusing on the momentum description of the tsunami introduces many new kinds of physical problems that are interesting in themselves.

INTRODUCTION

The main idea in this paper is to focus on the momentum of a tsunami. The momentum contained in the largest positive wave crest is a measure of its damaging potential and might be used as a measurement of tsunami magnitude. Since there is little history of thinking about tsunami momentum, many unanswered questions arise. Some are answered quickly with obvious conventional thinking, but others may be difficult. Some momentum questions may lead to worthwhile theoretical considerations. Other momentum questions might be answered with the computer. Giving some thought to questions about momentum would at least broaden the range of considerations that go into tsunami research.

You might look at the tsunami phenomena this way: In one kind of source a vertical uplift distorts the surface of the ocean which results in wave propagation (momentum) in all directions The net horizontal momentum from this is zero, but in any given direction there is a momentum associated with the wave moving in that direction. Add to this the effects of other external forces caused by landslides, horizontal displacements, steam generation and other possible external forces on the designated body of water and additional horizontal momentums are added. Think of a ray from the source to a given location where the effect of the tsunami is to be calculated. Propagate the tsunami along the ray keeping track of changes in the momentum due to external horizontal forces on the water and of the spreading and focusing of momentum due to bathymetric features. This then is the momentum delivered to a destination. It is this momentum which is the agent of destruction.

Momentum is another statement of Newton's Second Law, namely,

$$\vec{F} = m\vec{a},$$

or integrating over time

$$\int \vec{F} dt = \Delta\left(m\vec{v}\right).$$

The impulse imposed on the left, equals the change in momentum on the right. This paper concentrates on the change in momentum on a body of water from the external forces upon it. Let a body of water be specified and $\vec{k}$ be a unit vector in a given direction, then

$$\int \left(\oint \vec{F} \cdot \vec{k}\right) dt = \Delta\left(m\vec{v}\right),$$

where $\vec{v}$ is in the direction of $\vec{k}$ and $\oint$ is the surface integral around the body of water.

GENERATION OF THE TSUNAMI

Landslides. The tsunami of April 1, 1946 has long been an enigma. That tsunami was larger than the size of the earthquake could account for and more directional than most other tsunamis. It was proposed by several researchers that a landslide was part of the generating mechanism. The dimensions of that landslide and the thrust of it have been estimated[1]. The question is (still), what forces are induced on the water by the landslide? I think there are 3 components to these forces which are, in principle, calculable: The first is the leading edge of the landslide pushing against the water in front of it. The second is the turbulent surface of the landslide pushing along the underside of the ocean through friction, and finally, the forces on the water connected with the trailing edge of the landslide. I don't know the solution to any of these problems, but they are three worthwhile topics for research in the tsunami field. Note that the forces due to this landslide are very directional where as the effect of the vertical deformation is less so.

Horizontal displacements. It has been speculated that the whole side of a volcano (viz. Cumbra Vieja[2] in the Canary Islands) collapsing into the ocean would produce a large tsunami. A similar physical problem was when the side of the mountain slid into Lituya Bay in Alaska[3]. I separate this situation out from undersea landslides because one could assume that the total momentum of the earth moving into the water ends up being transferred to the ocean. An insight to this problem can be gained by a simple model. Compare the wave generated by a piston thrusting horizontally into the water with the wave from a piston thrusting vertically into the water. Let the total water displacement be the same in each case and calculate the effect of the additional horizontal momentum in the first case.

Pyroclastic flow. It is not clear how much horizontal momentum is contained in a pyroclastic flow from a volcano, but it is clear that all of that momentum goes into the momentum of the water. Frequently, the pyroclastic flow is not contemporary with the other mechanisms of generation, but when it is, it should be included in the calculations of the resultant tsunami.

Explosions and steam. The heat of a lava flow when it hits the water generates steam. In some cases that steam produces a significant force on the

[1] Gerard Fryer, personal communication
[2] Pararas-Carayannis (2002b)
[3] Mader

water. A volcano collapsing at or below sea-level is like an explosion[4]. The case of an asteroid hitting the ocean can be treated like an explosion. These clearly impart a horizontal impulse and are a part of the tsunami generation.

MID-OCEAN MOMENTUM CALCULATIONS[5]

In the linear long wave theory, a wave, $\eta(x,t)$, in water depth *h*, has particle velocity *v* given by

$$v = \eta\sqrt{g/h}\,,$$

so the momentum/unit width is given by

$$M = (h+\eta)\eta\sqrt{g/h}\,.$$

Taking only the first order term, the momentum/unit width in the direction of travel is

$$M = C\eta$$

where

$$C = \sqrt{gh}\,,$$

is the celerity of the wave! This almost seems intuitively obvious except that the reason for the η is not from the additional wave elevation, but because the particle velocity is proportional to η. One might assume, then, that for any traveling wave form where the particle velocity in the wave is proportional to the wave height above it has the same, or nearly the same rule.

The total momentum/unit width of the tsunami is the integral of *M* along some portion of the wave, say, the first positive crest. For a sinusoidal long wave of semi-amplitude H in water of constant depth *h* and wavelength *L* is

$$M = C\cdot(2/\pi)HL$$

How does the momentum change during transmission? The bottom friction is a force opposite to the direction of the particle velocity, *v,* which decreases

[4] Mader and Gitling (2006)
[5] Loomis (2002)

the momentum in the part of the wave where η is positive and increases the momentum (i.e. decreases the negative momentum) where η is negative. However, particle velocities are small in deep water and this effect would be small. Only as the particle velocity becomes large as the wave enters shallow water or crosses the shoreline would this be significant.

There is another bottom force, namely the horizontal component of the bottom pressure. In the long-wave linear theory, the wave height is small compared to the depth and the incremental force due to the wave height is negligible is constant along the length of the wave and has no effect. In fact, using just the linear long-wave theory, there is no change in momentum from changes in bathymetry. Why this is so is not entirely clear and needs more thinking. The issue arises again below in the discussion of shoaling.

There is, however, the spreading of the wave front propagating on the surface of a sphere. This accounts for the diminution of wave heights and thus, momentum, with distance.

When the bottom changes across the direction of travel, this produces forces at right angles to the direction of travel which would bend the wave. To the extent that this distorts a straight portion of the wave front into a convex or concave shape it results in scattering or focusing the momentum. This effect is automatically taken care of in calculating the normal propagation of the wave.

How about the change in momentum due to propagation from deep water to the shoreline? In the region where the long-wave linear theory applies, (say approximately $h \geq 10m$), the wave height is inversely proportional to $\sqrt{h}$ and the celerity is directly proportional to $\sqrt{h}$ and these are directly off-setting. So, the momentum is unchanged due to this shoaling.

In other words, the momentum leaving the generating area and headed for a distant shore arrives at an offshore point virtually undiminished except for spreading, small frictional losses, and the cumulative effect of the focusing and spreading effects of bathymetry. When the wave gets into quite shallow water the amplitude and particle velocity become larger and at some point the linear theory is not a good approximation. The definition of "shallow" here depends on the wave height. I would consider a wave with deep water height of 1m. to be treatable by shallow water theory until the water depth gets to be 10m.

Terminal Effects. Consider the total momentum contained in the first crest of a tsunami coming ashore. This momentum is scattered or reversed by

forces on the moving water of objects in its path and of the ground itself. These forces are exactly the same but in opposite direction to the forces of the water on the objects, i.e. the destructive force of the tsunami. Thus, the total momentum is a measure of the destructive capability of the tsunami. There are three (at least) kinds of forces to consider. The horizontal forces of the ground on the water (both friction and the horizontal component of pressure) are not destructive. They simply serve to slow the water down and to some extent, reverse the direction of the momentum. The second kinds of forces are those of irregular objects such as brush or trees and junk in general on the water. These forces tend to disorganize the water flow and, in effect, dissipate the organized momentum of the rushing water. The third category of forces are those of buildings, cliff faces, and other large objects. Consider forces on the water which cause the momentum to reverse direction. This would require an impulse that is twice the momentum of the oncoming water. In the process of reversing direction, the wave amplitude is the sum of the incident wave and the reflected wave so that the water level is doubled in amplitude at the reflecting surface. This phenomenon can account for the reports of most large wave heights. In the case of the Indonesian tsunami, the home videos (which certainly pictured well the rushing water and corresponding momentum) showed water levels which judging by its relationship to buildings that it was rushing by of heights of maybe 8 to 14 ft, whereas reported wave heights which would be where the highest water effects were noted were typically double that, or more. The "or more" part of that might be the result of splashes which can reach higher levels.

REFERENCES

Charles L. Mader and Michael Gittings, "Numerical Model for the Krakatoa Hydrovolcanic Explosion and Tsunami," Science of Tsunami Hazards, Vol.24, No. 3, (2006)

Charles L. Mader, "Modeling the 1958 Lituya Bay Tsunami, Science of Tsunami Hazards, Vol. 17, (1999)

Harold G. Loomis, "The Momentum of a Tsunami," Science of Tsunami Hazards, Vol.20, No.1, (2002)

George Pararas-Carayannis, "Near and Far-Field Effects of Tsunamis Generated by …Krakatoa in 1883," Science of Tsunami Hazards, Vol.21, No.4, (2003)

George Pararas-Carayannis, "Evaluation of the Threat of Mega Tsunami Generation from Slope Failures of Island Volcanoes on La Palma, Canary Island…..," Science of Tsunami Hazards, Vol.20, No.5 (2002b)

FINITE VOLUME METHODS AND ADAPTIVE REFINEMENT FOR GLOBAL TSUNAMI PROPAGATION AND LOCAL INUNDATION.

David L. George and Randall J. LeVeque
Department of Applied Mathematics
University of Washington
Seattle, WA 98195 U.S.A.

ABSTRACT

The shallow water equations are a commonly accepted approximation governing tsunami propagation. Numerically capturing certain features of local tsunami inundation requires solving these equations in their physically relevant conservative form, as integral conservation laws for depth and momentum. This form of the equations presents challenges when trying to numerically model global tsunami propagation, so often the best numerical methods for the local inundation regime are not suitable for the global propagation regime. The different regimes of tsunami flow belong to different spatial scales as well, and require correspondingly different grid resolutions. The long wavelength of deep ocean tsunamis requires a large global scale computing domain, yet near the shore the propagating energy is compressed and focused by bathymetry in unpredictable ways. This can lead to large variations in energy and run-up even over small localized regions.

We have developed a finite volume method to deal with the diverse flow regimes of tsunamis. These methods are well suited for the inundation regime—they are robust in the presence of bores and steep gradients, or drying regions, and can capture the inundating shoreline and run-up features. Additionally, these methods are *well-balanced*, meaning that they can appropriately model global propagation.

To deal with the disparate spatial scales, we have used adaptive refinement algorithms originally developed for gas dynamics, where often steep variation is highly localized at a given time, but moves throughout the domain. These algorithms allow evolving Cartesian sub-grids that can move with the propagating waves and highly resolve local inundation of impacted areas in a single global scale computation. Because the dry regions are part of the computing domain, simple rectangular cartesian grids eliminate the need for complex shoreline-fitted mesh generation.

INTRODUCTION

We will describe a type of finite volume numerical method that is useful for solving a class of hyperbolic equations, specifically the nonlinear shallow water equations. These equations are one of the commonly accepted approximations governing tsunami propagation and inundation. They can present various difficulties for numerical methods depending on the flow regimes of the solution—which can vary greatly. For instance, the shallow water equations can often accurately describe global propagation of tsunami waves as well as general features of inundating waves at the shoreline or flooding onto dry land. These equations even admit solutions with propagating bores or discontinuities that approximate breaking waves, which may exist in the runup regions depending on local bathymetry. Although the validity of the shallow water approximation becomes more tenuous in the inundation and flooding regimes, these equations still perform surprisingly well at describing basic features of these flows, and are often the most efficient and least expensive practical model [11, 12].

Many methods have been developed for the shallow water equations; however, numerical methods differ in their utility for different flow regimes—often a method that works well for one regime may fail to be useful for other regimes. Our goal has been to develop a method that is robust and accurate for solving these equations in any of the diverse regimes.

THE SHALLOW WATER EQUATIONS

The shallow water equations can be derived in a number of ways and in a variety of forms, all of which rely on the basic assumption that the flow is vertically hydrostatic, or equivalently, that the vertical acceleration of water particles is negligible. The validity of this assumption can be demonstrated for flows with long wavelengths compared to depth. It may be a reasonable approximation for other flows as well, at least for the depth averaged horizontal velocities. Once this approximation is accepted, the most physically relevant and generally valid form of the equations is as an integral conservation law for mass and momentum, which in one dimension is

$$\begin{aligned} \tfrac{d}{dt}\textstyle\int_{x_1}^{x_2} h\,dx + (hu)_{xl}^{xr} &= 0 \\ \tfrac{d}{dt}\textstyle\int_{x_1}^{x_2} hu\,dx + \left(\tfrac{1}{2}gh^2 + hu^2\right)_{xl}^{xr} &= -\textstyle\int_{x_1}^{x_2} ghb_x\,dx, \end{aligned} \tag{1}$$

where h is the water depth, u is the horizontal velocity, g is the gravitational constant and b is the bottom surface elevation. The integral conservation law (1) is often used to deduce a set of PDEs for mass and momentum

$$\begin{bmatrix} h \\ hu \end{bmatrix}_t + \begin{bmatrix} hu \\ \frac{1}{2}gh^2 + hu^2 \end{bmatrix}_x = \begin{bmatrix} 0 \\ -ghb_x \end{bmatrix}, \tag{2}$$

where the subscripts imply differentiation. This set of PDEs can be manipulated further to yield the most common form of the shallow water equations

$$\begin{aligned} \eta_t + u(\eta - b)_x &= 0 \\ u_t + u(u)_x + g\eta_x &= 0, \end{aligned} \tag{3}$$

where η is the elevation of the water surface, $\eta = h + b$. The system (3) is the most commonly used form for modeling tsunamis since it is the least problematic for global propagation, however, it is not always valid in the near shore region as will be described below.

HYPERBOLIC SYSTEMS OF CONSERVATION LAWS

The system (2) belongs to a broader class of conservation laws of the form

$$\tfrac{d}{dt}\int_{x_1}^{x_2} q(x,t)\,dx + f(q(x_2,t)) - f(q(x_1,t)) = \int_{x_1}^{x_2} \psi(q,x)\,dx, \quad \forall (x_1,x_2), \tag{4}$$

where $q \in \mathbb{R}^m$ is a vector of conserved quantities, $f(q) \in \mathbb{R}^m$ is the flux of these quantities, and ψ is a source term. If the solution $q(x,t)$ is differentiable, then (4) can be manipulated into the form

$$\int_{x_1}^{x_2} \left[q_t(x,t) + f(q(x,t))_x - \psi(q,t)\right] dx = 0, \quad \forall (x_1,x_2), \tag{5}$$

which implies the PDEs

$$q_t(x,t) + f(q(x,t))_x = \psi(q,t). \tag{6}$$

If ψ is nonzero, (4) is sometimes referred to as a *balance law* due to the contribution from the source term. However, we will refer to (4) as a conservation law, and in the special case that $\psi \equiv 0$

$$q_t(x,t) + f(q(x,t))_x = 0, \tag{7}$$

a *homogeneous* conservation law. The systems (6) and (7) are hyperbolic if the Jacobian $f'(q)$ has real eigenvalues and a full set of eigenvectors. Physical systems exhibiting wave propagation are often described by hyperbolic systems, and the wave speeds are generally the eigenvalues of the Jacobian. The shallow water equations are hyperbolic with eigenvalues $u \pm \sqrt{gh}$.

The PDE form (6) is valid only if the solution is differentiable, however, (4) admits nondifferentiable—even discontinuous—solutions. Standard finite difference methods based on (6) will, in general, not only fail to converge to the correct solutions to (4), they will often develop instabilities or nonphysical oscillations near steep gradients in the solution. Additionally, due to discontinuities, solutions to (4) can be non-unique. The physically relevant solution must be isolated by additional admissibility conditions, sometimes called *entropy conditions*. For a numerical method to converge to the correct,

possibly discontinuous, solution to the conservation law, it must be consistent with (4) and additional entropy conditions (see for example [9, 6]).

For modeling global tsunami propagation, (3) is the most convenient and least problematic form of the shallow water equations. The steady state—a pool of motionless water—will be preserved by any standard finite difference method since u and η are identically zero. However, in the near shore and inundation regions, steep gradients or turbulent bores may develop rendering (3) problematic. A numerical method for the integral conservation law (1) is therefore preferable for modeling flows in the near shore and inundation region. However, this presents a new set of numerical challenges for accurate global propagation.

FINITE VOLUME METHODS

Various classes of numerical methods have been developed to deal with the difficulties of solving hyperbolic systems of the form (4), most of which are finite volume methods. A finite volume numerical solution consists of a piecewise constant function Q_i^n that approximates the average value of the solution $q(x,t^n)$ in each grid cell $\mathscr{C}_i = [x_{i-1/2}, x_{i+1/2}]$. A conservative finite volume method updates the solution by differencing numerical fluxes at the grid cell boundaries

$$Q_i^{n+1} = Q_i^n - \frac{\Delta t}{\Delta x}\left[F_{i+1/2}^n - F_{i-1/2}^n\right], \tag{8}$$

where

$$F_{i-1/2}^n \approx \frac{1}{\Delta t}\int_{t_n}^{t_{n+1}} f(q(x_{i-1/2},t))\,dt, \tag{9}$$

and

$$Q_i^n \approx \frac{1}{\Delta x}\int_{x_{i-1/2}}^{x_{i+1/2}} q(x,t^n)\,dx, \tag{10}$$

where we have assumed the grid cells are of fixed length Δx. Note that (8) is a direct discrete representation of the integral conservation law (4) over each grid cell (neglecting source terms), using approximations to the time averaged fluxes at the boundaries. The essential properties of the finite volume method then, come from the approximation for the numerical fluxes (9).

Much research has been devoted to establishing stable and accurate numerical fluxes, and fluxes that allow convergence to smooth solutions as well as physically admissible discontinuities such as shocks or bores (see [9]). One of the most successful strategies is to solve *Riemann problems*, which consist of the original conservation law and constant initial data with a single jump discontinuity. These problems are solved at each grid cell interface with the numerical solution data to determine the numerical flux at each time t^n. The flux $F_{i-1/2}^n$ is then the solution to the Riemann problem at $x_{i-1/2}$, with initial data Q_i^n and Q_{i-1}^n.

Riemann solutions to homogeneous conservation laws often have a simple structure that can be solved exactly or approximated. For solutions to conservation laws with a source term (4), the standard approach is to use *fractional stepping*, which splits the problem at each timestep into an update for the homogeneous part, followed by an integration of the source term

$$Q_i^{n*} = Q_i^n - \frac{\Delta t}{\Delta x}\left[F_{i+1/2}^n - F_{i-1/2}^n\right] \tag{11}$$

$$Q_i^{n+1} = \Delta t \Psi(Q_i^{n*}, x_i), \tag{12}$$

where Ψ is some numerical approximation to the source term $\psi(q,t)$. Fractional stepping works well for many applications, however, it is well known [2, 8] that it fails to numerically preserve *nontrivial* steady states or small perturbations to those steady states, which exist when a large nonzero flux gradient nearly balances the source term

$$f(q(x,t))_x \approx \psi(q,x), \tag{13}$$

implying $q_t(x,t) \approx 0$ in (4). The failure of fractional stepping for this situation is not surprising, considering that (11) and (12) must precisely cancel in order to preserve Q_i^n, and these two terms come from unrelated types of numerical approximations.

This eliminates fractional stepping as a viable technique for solving (1), when modeling tsunami propagation. Deep ocean tsunamis have small amplitudes, often less than a meter, while the depth of the ocean can approach 4000 meters. This means that tsunamis in the deep ocean are tiny perturbations to the steady state, which arises from the balance of the hydrostatic pressure gradient and the source term

$$(\frac{1}{2}gh^2)_x = -ghb_x. \tag{14}$$

Tsunami propagation results from tiny deviations to (14), and would be completely lost in the numerical noise of fractional stepping.

WAVE PROPAGATION METHODS

An alternative implementation of (8) comes from considering the structure of the Riemann solution, rather than simply using the Riemann solution to determine a numerical flux. Riemann solutions for hyperbolic systems typically consist of a set of m waves propagating away from the initial discontinuity. These waves carry jumps in the solution vector, and therefore the solution can be numerically updated directly by averaging the effect of the waves onto the grid cells. This *wave propagation* update on Q_i can be written

$$Q_i^{n+1} = Q_i^n - \frac{\Delta t}{\Delta x}\left[\mathscr{A}^+\Delta Q_{i-1/2} + \mathscr{A}^-\Delta Q_{i+1/2}\right], \tag{15}$$

where $\mathscr{A}^-\Delta Q_{i+1/2}$ is the net effect of the waves moving to the left from $x_{i+1/2}$, and $\mathscr{A}^+\Delta Q_{i-1/2}$ is the net effect of the waves moving to the right from $x_{i-1/2}$. The method

(15) is more general than (8), since it also applies to hyperbolic systems other than conservation laws (see [9] for a description of wave propagation methods). For conservation laws the *fluctuations* must satisfy

$$f(Q_i) - f(Q_{i-1}) = \mathscr{A}^- \Delta Q_{i-1/2} + \mathscr{A}^+ \Delta Q_{i-1/2}. \tag{16}$$

The wave propagation algorithm (15) uses Riemann solutions to directly update the solution rather than determine interface fluxes. This methodology suggests an alternative treatment of source terms as well; rather than treating source and flux terms separately, the effect of the source term can be added directly to the updating waves in the fluctuations $\mathscr{A}^{\pm}\Delta Q$. In this case (15) is still the form of the numerical method for a system with a source term, and

$$f(Q_i) - f(Q_{i-1}) - \Delta x \tilde{\Psi}(Q_{i-1}, Q_i, x_{i-1/2}) = \mathscr{A}^- \Delta Q_{i-1/2} + \mathscr{A}^+ \Delta Q_{i-1/2}, \tag{17}$$

where $\tilde{\Psi}(Q_{i-1}, Q_i, x_{i-1/2})$ is some consistent approximation to the source term. Consistency requires that (17) be satisfied, however it does not guarantee that steady states will be preserved. A method is sometimes termed *well balanced*, if it maintains exactly certain discrete data that result from the discretization of a true steady state solution. This requires the updating fluctuations in (15) be *deviations* from the steady state. When near a steady state this implies

$$f(Q_i) - f(Q_{i-1}) - \Delta x \tilde{\Psi}(Q_{i-1}, Q_i, x_{i-1/2}) \approx \mathscr{A}^- \Delta Q_{i-1/2} \approx \mathscr{A}^+ \Delta Q_{i-1/2} \approx 0. \tag{18}$$

A RIEMANN SOLVER FOR TSUNAMI MODELING

Ensuring (18) requires appropriate Riemann solvers that incorporate the source term correctly. We accomplish this for the shallow water equations by using approximate Riemann solutions based on an augmented homogeneous hyperbolic system

$$\tilde{q}_t + A(\tilde{q})\tilde{q}_x = 0, \tag{19}$$

where $\tilde{q} = (\ h, \quad hu, \quad \frac{1}{2}gh^2 + hu^2, \quad b\ )^T$ and $A \in \mathbb{R}^{4\times 4}$. The system (19) is derived such that its solutions are also solutions to the shallow water equations with a source term, yet (19) is homogeneous. By using certain approximate Riemann solutions to (19) to determine updating fluctuations ($\mathscr{A}^{\pm}\Delta Q$) the method (15) is well balanced, and is able to accurately resolve small perturbations to steady states and model global tsunami propagation on the deep ocean.

By proper construction of the approximate Riemann solutions to (19), the method also converges correctly to discontinuous solutions to the shallow water equations, such as propagating bores, without converging to entropy violating solutions to (4). Additionally, the Riemann solver is robust near vanishing depths or dry regions and is able to robustly capture inundation and runup (see [5] for details).

TWO DIMENSIONAL GRIDS AND SHORELINES

In two dimensions finite volume grid cells are typically rectangles, $\mathscr{C}_{ij} = [x_{i-1/2}, x_{i+1/2}] \times [y_{j-1/2}, y_{j+1/2}]$, though more complex shapes are possible. For tsunami modeling we use uniform Cartesian grids in computational space, using latitude and longitude coordinates, that map to the sphere. The algorithms described for one dimension can be be logically extended to two dimensions by solving Riemann problems normal to cell interfaces (for details see [9, 5]). Since the algorithms are robust to the existence of dry states, there is no special reference to the shoreline, grid cells in dry regions simply have $h = 0$. Additionally, the Riemann problem between a cell with water and a dry cell, or the *dambreak problem*, is automatically solved by (19), so grid cells simply fill-up or drain out of water as waves move onto shore. This simplifies calculations near the shore for a couple of reasons: first, no special grid fitting to the shoreline is needed—simple rectangular grids are used; and second, no special shoreline tracking is needed—inundation is calculated as cheaply and automatically as any part of the grid.

ADAPTIVE MESH REFINEMENT

The numerical difficulties associated with simultaneously modeling global propagation and inundation described so far are due to diverse *flow regimes*. An additional difficulty arises due to the diverse spatial scales of these flows. On the deep ocean, tsunami wavelengths are often on the order of several hundred kilometers requiring a large computational domain. In the near shore region tsunami energy is compressed and focused by bathymetry in often unpredictable ways, requiring grid spacing that is orders of magnitude smaller. A standard approach to such a difficulty is to use fixed telescoping grids at the shoreline. This may be satisfactory for certain case studies of particular regions of interest, however, for global or large scale modeling it is less than ideal for several reasons. First, it requires some *a priori* knowledge or assumptions about the level of refinement that will be needed in certain areas. Second, refined grids must be integrated throughout the computation, even when there are no waves present in the region—these trivial steady state calculations on fine grids increase the computational cost and can decrease the length of timesteps. Finally, a fixed resolution for the offshore or deep ocean reduces the efficiency, and hence the resolution, with which propagating waves can be resolved.

For these reasons we have used adaptive refinement methods previously developed for compressible inviscid gas dynamics, where often sharp gradients and moving shock waves needing high degrees of refinement are present in small isolated parts of the domain at a given time (see [3]). Obviously fixed telescoping grids would not work for this application since the shock waves move throughout the entire domain. Global scale tsunamis are similar in the sense that waves move throughout the entire domain needing various levels of refinement at different times and locations, yet no single area needs a fixed level of refinement for the entire computation. These algorithms use evolving Cartesian subgrids that are simple rectangles with various levels of spatial and temporal refinement. These

moving subgrids may appear at any time, or disappear, depending on the level of refinement needed in a specific area. Adaptive mesh refinement allows a very coarse grid to cover parts of the domain where no waves are present, allowing higher refinement levels to track moving waves in the deep ocean. As waves approach the shoreline and compress, still higher refinement level grids can appear capturing the inundation and run-up. The adaptive refinement methods described in [3] have been modified for this application, for proper treatment of shorelines and steady states associated with tsunami modeling.

MODELING THE INDIAN OCEAN TSUNAMI

Our numerical methods are implemented in TSUNAMICLAW part of the freely available CLAWPACK [7] software package. We used our single grid algorithms to model benchmark problems in the 2004 International Long Wave Workshop [10]. These benchmark problems involved near-shore features, such as comparisons to analytical run-up solutions (see [4]), and wave tank scale models of the 1993 Okushiri Island tsunami in Japan.

We are currently using our adaptive code to model the Indian Ocean tsunami of 2004. The tsunami is numerically generated by dynamically moving the seafloor according to a temporal-spatial model of the Sumatra-Andaman fault rupture, provided by the Seismolab at Caltech [1]. An example simulation is shown in Figure 1. This simulation used 40×40, $1^\circ \times 1^\circ$ grid cells on the coarsest grid (top left). A second level refined by a factor of 8, was used to track the deep ocean tsunami propagation (top right). Third level grids, allowed near Sri Lanka and the eastern coast of India, were again refined by a factor of 8, resulting in approximately 1 minute grid cells. Grid lines are omitted from these levels for clarity. This calculation ran in 28 minutes of computing time on a personal single processor Dell desktop.

We have used higher level grids in some regions allowing resolution onto 25 meter grid cells for inundation modeling. Because of the limited availability of digital bathymetry in the Indian Ocean region, we have had to manually digitize nautical charts in these regions—a process that is time consuming and labor intensive.

ACKNOWLEDGEMENTS

This work was supported in part by NSF grants DMS-0106511 and CMS-0245206, and by DOE grant DE-FC02-01ER25474. The authors would like to thank Marsha Berger and Donna Calhoun for their assistance and contribution to the adaptive refinement routines, Harry Yeh for advice and assistance, and the Caltech Seismolab for providing their fault rupture data.

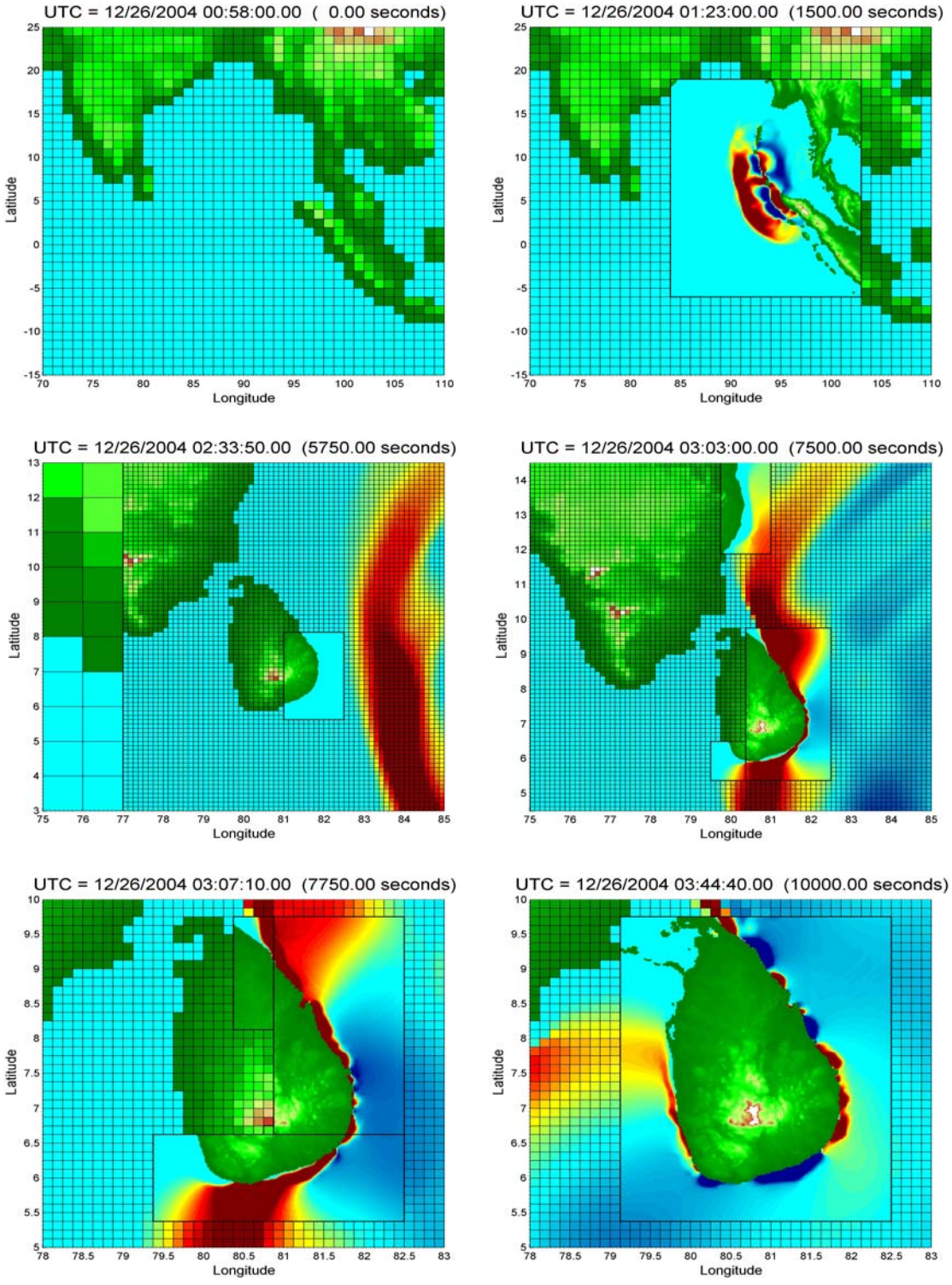

Figure 1: Simulation of the Indian Ocean Tsunami with three grid levels.

References

[1] C.J. Ammon et al. Rupture process of the 2004 Sumatra-Andaman earthquake. *Science*, 308:1133–1139, 2005.

[2] D. Bale, R. J. LeVeque, S. Mitran, and J. A. Rossmanith. A wave-propagation method for conservation laws and balance laws with spatially varying flux functions. *SIAM J. Sci. Comput.*, 24:955–978, 2002.

[3] M. J. Berger and R. J. LeVeque. Adaptive mesh refinement using wave-propagation algorithms for hyperbolic systems. *SIAM J. Numer. Anal.*, 35:2298–2316, 1998.

[4] G. Carrier, T. Wu, and H. Yeh. Tsunami run-up and draw-down on a plane beach. *Journal of Fluid Mech.*, 475:79–99, 2003.

[5] D.L. George. *Finite volume methods and adaptive refinement for tsunami propagation and inundation*. PhD thesis, University of Washington, 2006.

[6] T. Hou and P. LeFloch. Why non-conservative schemes converge to the wrong solutions: Error analysis. *Math. of Comput.*, 62:497–530, 1994.

[7] R. J. LeVeque. The CLAWPACK software package. `http://www.amath.washington.edu/ claw`.

[8] R. J. LeVeque. Balancing source terms and flux gradients in high-resolution Godunov methods: The quasi-steady wave propagation algorithm. *Journal of Computational Physics*, 146:346–365, 1998.

[9] R. J. LeVeque. *Finite Volume Methods For Hyperbolic Problems*. Cambridge University Press, 2002.

[10] R. J. LeVeque and D. L. George. High-resolution finite volume methods for the shallow water equations with bathymetry and dry states. In P. Liu, editor, *Proceedings of Long-Wave Workshop, Catalina*, page to appear, 2004.

[11] Charles L. Mader. *Numerical Modeling of Water Waves*. CRC Press, 2004.

[12] Eleuterio F. Toro. *Shock Capturing Methods for Free Surface Shallow Flows*. John Wiley and Sons, Chichester,United Kingdom, 2001.

TSUNAMI PROPAGATION ALONG TAGUS ESTUARY (LISBON, PORTUGAL) PRELIMINARY RESULTS

M. A. Viana-Baptista, P. M.. Soares
Instituto Superior de Engenharia de Lisboa
CGUL-IDL, Portugal

J. M. Miranda,
University of Lisbon, CGUL-IDL, Portugal.

J. F. Luis
University of Algarve, CIMA, Portugal.

ABSTRACT

In this study we present preliminary results of flood calculation along Tagus Estuary, a catastrophic event that happened several times in the past, as described in historical documents, and that constitutes one of the major risk sources for Lisbon coastal area. To model inundation we used Mader's SWAN model for the open ocean propagation with a 2 km grid, and Imamura's TSUN2 with a 50 m grid covering the entire estuary. The seismic source was computed with the homogeneous elastic half space approach. Modelling results agree with historical reports. Synthetic flood areas correspond to the sites where there are morphological and sedimentary evidences of two known major events that stroke Lisbon: 1531-01-26 and 1755-11-01 tsunamis.

INTRODUCTION

Research undertaken on tsunami risk in Portugal heavily relies on historical records for large events and on tide gauge data for a small number instrumental events that occurred in the XX Century. Nevertheless, historical plus instrumental data corresponds to a short time series in comparison with the long recurrence intervals that may characterize events of extreme tsunami flooding. The compilation of the Portuguese/European GITEC database (Baptista et al., 1998) includes events since 60 BC. The most destructive tsunamis listed along Tagus Estuary - Lisbon are the 1531.01.26 - local tsunami in Lisbon and the well known 1755.01.11 transoceanic event.

Large tsunami events are quite well described in Portuguese historical reports. The city of Lisbon, one of the main harbours in Europe during the XVII and XVIII centuries was severely damaged by two tsunami generated by strong magnitude earthquakes: 1531-01-26 (Justo and Salwa, 1998) and 1755-11-01 (Baptista et al., 1998). Although the location of the source area of these tsunamis may be quite different, and the coastal areas affected also distinct, the effects along the Tagus estuary are well known and described in coeval sources.

Tsunami propagation inside estuaries and coastal bays is a subject of major importance for risk evaluation. Strong non linear effects are present and focusing, reflection and amplification of the waves may occur in different points of the estuary. The effects of a tsunami event similar to the ones that occurred in 1531 or 1755 are not yet assessed, due to the large unknowns on their sources, the unavailability of high resolution bathymetric and topographic data and the difficulties involved in the assessment of the morphological and bathymetric changes in the Estuary.

In this work we use a new morphological compilation prepared for the Lisbon Estuary area and we present a series of modelling results concerning potential inundation areas. We also compare the results obtained with known records for large events and briefly discuss the impact of morphological changes on the effects of tsunami waves in the main populated areas of Lisbon.

MAIN HISTORICAL FLOODS IN LISBON

The 26th January 1531 Lisbon tsunami

On the 26 January 1531 an earthquake was felt in Lisbon and along Tagus margins. The epicentre coordinates, inferred from isosseimal map are 38.9N, 9.0W (Martins and Mendes-Victor, 1990) and the maximum intensity is evaluated in X MSK making it one of the most disastrous earthquakes in the history of Portugal. The source location of this event is uncertain, some authors place it offshore Iberia, while others place it north of Lisbon, up estuary (Justo and Salwa, 1998).

The downtown of Lisbon and several dwellings along estuary were flooded by the river. Although written reports in Lisbon at that time are scarce, several coeval sources document the event (Surius, 1567, in Babinet 1861). The distinction between a tsunami like event or a storm it is sometimes not clear in the texts, but the simultaneity of the

earthquake definitively states the occurrence of a tsunami. The reports state that the Tagus divided some islands in the estuary into smaller ones; others report the occurrence of strong flux and reflux and that it was possible to see the sands of the bottom (Codice, 8009). This fact is also stated by different authors later in the 18th century prior to the 01-11-1755 event, so we can believe that the information on the event was not biased by the occurrence of the great earthquake. The report from Couto (1736) clearly states the great damage observed in the port. Moreira de Mendonça (1758) compares this event with the 1755 concluding that for the city the 1531 event was even more catastrophic than the later one. Mendonça (1758) reports the flux of the Tagus and distinguishes between the damage observed inside and outside estuary and describes that ships were destroyed in the sea.

The 1th November 1755 Lisbon tsunami

On the 1st November 1755 a magnitude 8.75 (Abe, 1989) earthquake occurred offshore Iberia and generated a transoceanic tsunami that ravaged the north Atlantic area. The effects along the coast of Iberia are well documented and the tsunami damage at downtown Lisbon is described by several British citizens that lived in Lisbon at the time. These reports are compiled in a unique work: "The 1755 Lisbon earthquake, British Accounts", where we can read:"(…) There was another great shock after this that pretty much affected the river, but, I think not so violent as the preceding, though several people afterwards assured that as they were riding on horseback, in the great road to Belem, one side of which lays upon the river, the waters rushed in so fast that they were forced to gallop as fast as possible to the upper grounds for fear of being carried away (…) "(…) A large quay, piled up with goods near the Custom House sunk the first shock, with about 600 persons upon it, who all perished (…)" see figure 1A.

Figure 1. A - The sunk of "Caes da Pedra" (GEO – Gabinete de Estudos Olissiponenses, Lisboa); B - Inundation area at Lisbon downtown as described by contemporary sources.

Also the Portuguese reports describe the tsunami (Baptista, 1998): "(...) a lot of people run to the river bank trying to escape from the ruins. Suddenly the sea came in through the bar and flooded the river banks…*"*(Mendonça, 1758). According to Silva (1756) "the river waters with their ebb and flow flooded the "Custom House", the square and the "Vedoria"), see figure 1B. Baptista et al. (1998), evaluated the run-in distance along Lisbon downtown and describe in detail the tsunami observations in Lisbon. In Figure 1B we present the inundation area as described by coeval sources.

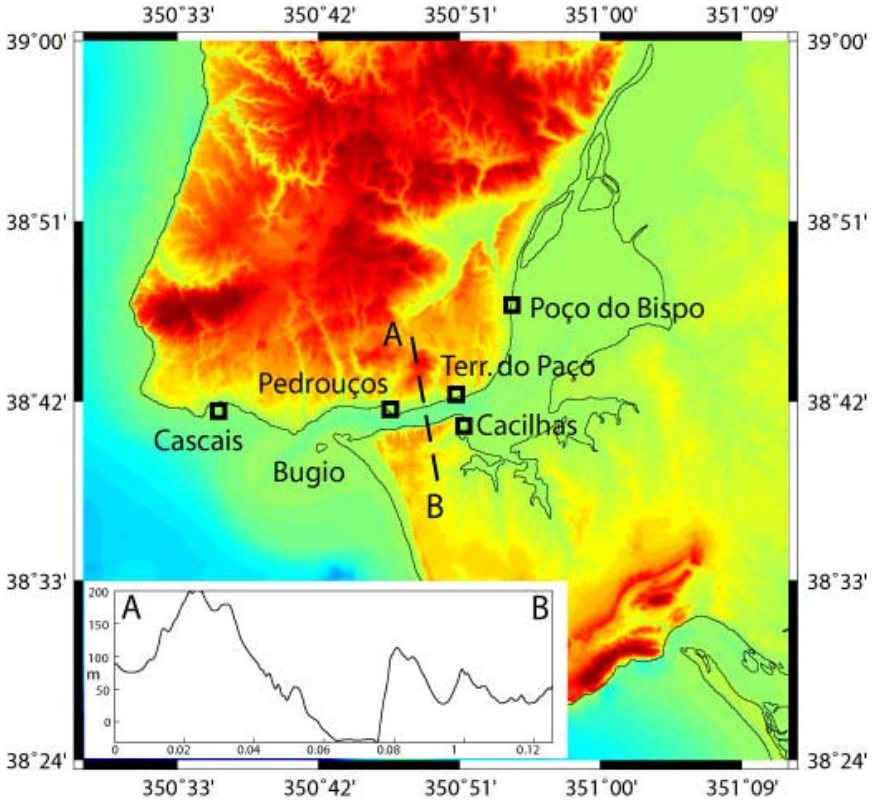

Figure 2. Present Bathymetry of the Estuary.

Instrumental Events

On the 20th century two tsunami events, both with source location offshore in the Atlantic, were registered by the mareographic stations installed not only along the Portuguese west coast, but also inside the estuary. However, the small amplitude of the tsunami waves in the estuary (e.g. 29 cm (peak to peak) for the 26-05-1975 and 85 cm (peak to peak) for the 28-02-1969 event, according to Lynnes and Ruff, 1985) prevented any significant inundation.

Detailed studies on the tsunami frequency content for the 1969 and 1975 events are presented in Baptista et al., (1992). Preliminary results on the 1969.02.28 event, along Tagus estuary are presented in Heinrich et al., (1994); the tsunami arrival time and the shape of the first peaks at Cacilhas and Pedrouços,Tagus Estuary (see figure 2) are quite well reproduced by modelling.

MODELLING

To model tsunami open ocean propagation, between the source and Lisbon area, we use the shallow water non-linear model based on SWAN code (Mader, 1988, 2001). This model solves the non-linear long wave equations of the fluid flow, using an explicit in time finite difference scheme (see Mader, 2001). Calculation was preformed in geographical coordinates. The bathymetric grid was obtained from Smith and Sandwell (1997). The final grid resolution used for open ocean propagation is 2 km with a time step of 5 sec.

Propagation inside estuary and flooding was computed with TUNAMI N2 code, authored by F. Imamura. Bathymetric data collation was made with swath bathymetry data for the whole river bed and photogrammetric digital elevation models of the scale 1:10000 for the on-shore areas. The vertical data for both data sources were taken into account. A grid spacing of 50 m and a time step of 1 sec were used in the computations. Figure 2 shows the compilation used for this study. The geometric relationship between the two grids is represented in figure 3.

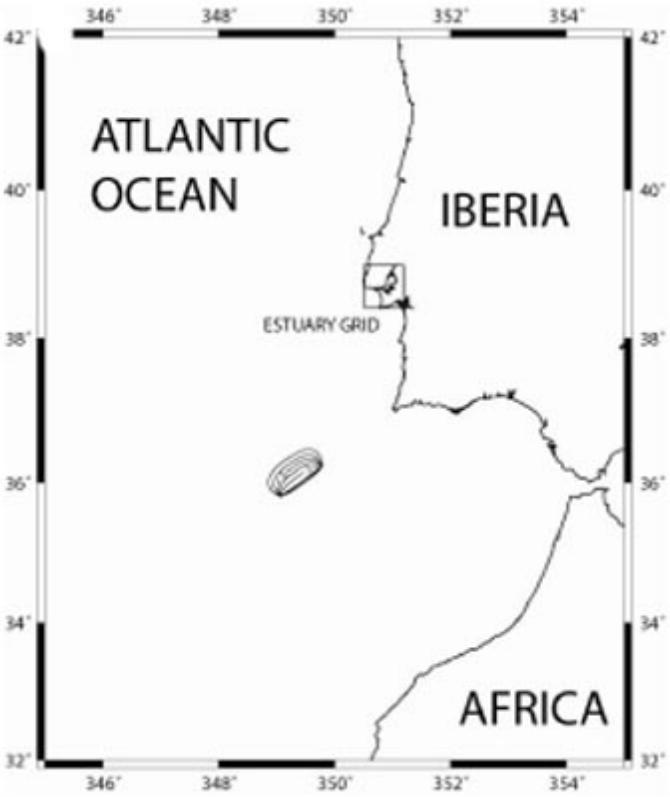

Figure 3. Grid's nesting for the propagation in open ocean (2 km grid spacing) and estuary propagation and flood (50 m grid spacing).

In this preliminary study we used as the "candidate" source the one that generated the 28-02-1969 event (Fukao, 1973) that we can consider as well defined by seismology and tsunami studies. A slip of 10 meter was fixed, to account for an event larger than 1969 and able to produce a significant effect in Lisbon.

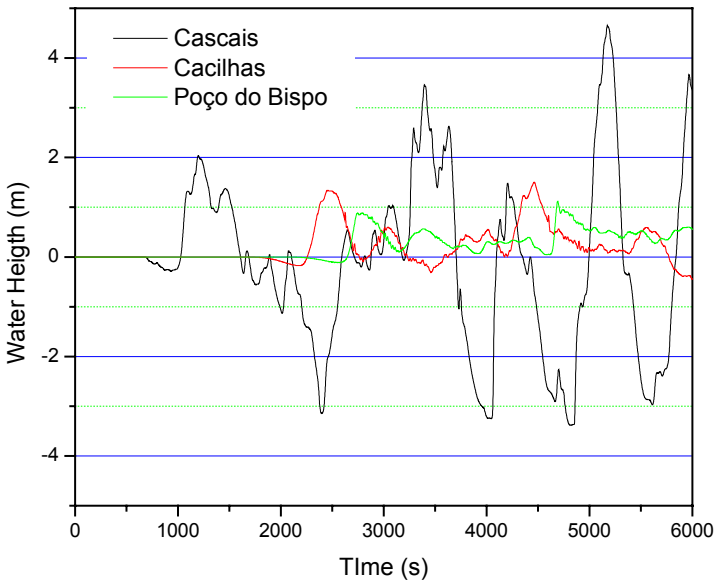

Figure 4. Water height computed at three locations, one outside the estuary (Cascais) and two other inside (Poço do Bispo and Cacilhas).

In figure 4 we show synthetic tsunamis for three locations, one outside the estuary, in Cascais, where it is located the oldest Portuguese tide station; two along estuary: Cacilhas (on the south bank of the river, opposite to Terreiro do Paço and Poço do Bispo (cf. figure 2 for locations). It can be concluded that tsunami wave slows down and its height decreases inside the estuary, as a consequence of the geometry of the river bed. Between Bugio Castle/Lighthouse and Cacilhas (see figure 2 for location), the propagation is strongly affected by the Tagus "bottleneck", generating in Poço do Bispo a wave less than 1 meter height.

The computation of the flood area is plotted in figure 5. It is clear that large inundation occurs along the Trafaria coast (outside the estuary), Seixal and Alcochete (upper estuary). Along Trafaria segment the run-in is larger than 1 km and a large devastation should be expected.

DISCUSSION AND CONCLUSIONS

The study of tsunami propagation along Tagus estuary is certainly different today than in 1531 or even 1755. In order to reproduce tsunami observations of the 1531 or 1755 events we must take into account the heavy changes produced on the river banks and river-bed between 16th and 18th century and between 18t^{h} and 21th century. These changes were mainly due to defensive and civil construction (Baldaque da Silva, 1893)

that deeply constrained the section between Bugio and Cacilhas and increased sedimentation rates. Before the XVIII century the width of the channel was much larger, so that tides affected largely up-river (Baldaque da Silva, 1893). A tsunami entering the estuary would have certainly a much bigger impact and would propagate significantly upriver, as is known from historical documents.

Figure 5. Inundation at Tagus Estuary.

Even in what concerns the impact in downtown Lisbon, the comparison between figures 1 and 4 shows that relevant differences exist and only in case of combined effect of high water and tsunami wave, or a large local event (similar to 1531?), a great impact should be expected far away from the waterfront.

The flood prediction obtained for Trafaria segment agrees with the well documented landscape changes presented by historical nautical charts and maps Pais (1992). This author presents a comparison between two maps prior to 1755 and an 19th century map and concludes that before 1755 the sea cliffs were connected to the beach limiting the shoreline; after 1755 there was a change in the coast line position, that is similar to the present one.

The inundated areas inside the estuary also match the places where geological signatures of flooding associated with the 1st November AD 1755 tsunami has been tracked in the sedimentary record (cf. Andrade et al., 2003).

AKNOWLEDGEMENTS

This study was supported by TESS project POCTI/CTE-GIN/59996/2004.The authors wish to thank: Professor Antonio C. Mineiro and Dr. Alan Ruffman for the fruitful discussions; Dr. Charles Mader and F. Imamura for code availability.

REFERENCES

Abe K., 1979. Size of Great Earthquakes of 1837-1974 Inferred from Tsunami Data: Journal of Geophysical Research, V. 84, P. 1561-1568.

Andrade C, Maria C. Freitas, J. M. Miranda, M.A. Baptista, Mário Cachão, Pedro Silva, José Munhá, Recognizing Possible Tsunami Sediments In The Ultradissipative Environment Of The Tagus Estuary (Portugal). Congresso Coastal Sediments' 03, Florida, USA

Babinet, 1861. Note dans les Comptes Rendus de la academie des Sciences de Paris, tomo LII, pp 369.

Baldaque da Silva A.A., 1893. Estudo Histórico Hydrográfico sobre a barra e o Porto de Lisboa. INL(Imprensa Nacional de Lisboa-1893). Biblioteca Nacional de Lisboa, Portugal.

Baptista M.A., P.M.A. Miranda, L. Mendes Victor, (1993). Maximum Entropy Analysis of Portuguese Tsunami: The Tsunamis of 28/02/1969 and 26/04/1975. Sc of Tsunami Hazards, vo.10, nº1.

Baptista, M.A., P.M.A. Miranda, J. M. Miranda and L.M. Victor, 1998: "Constrains on the source of the 1755 Lisbon tsunami inferred from numerical modelling of historical data". J. of Geod., 25, 159-174.

Baptista M. A. (1998) Génese Propagação e Impacte de Tsunamis na Costa Portuguesa". PhD Thesis University of Lisbon, Faculdade de Ciências.

British Accounts, The Lisbon Earthquake of 1755. Anonymous Letter, Lisbon, Nov, 18th 1755. ed. The British Society in Portugal, Ed Lisóptima, Lisboa, Portugal, pp. 157-189.

Códice 8009 - Breve notícia de alguns terramotos. Arquivo Nacional da Torre do Tombo. Lisboa-Portugal.

Couto, Diogo (1736) Décadas da Ásia, Que tratam dos mares, Que descobriram armadas, que desbaratarão exércitos, que vencerão e das acções heroicas e façanhas béllicas, que obrarão os Portugueses nas conquistas do oriente, tomo I, Lisboa, Oficina de Domingues Gonçalves, pp 198.

Fukao, Y. (1973). Thrust faulting at a lithosphere plate boundary. The Portugal earthquake of 28.02.1969. Earth and Planet. Sc. Lett., vol.18, pp 205-216.

Heinrich P., M. A. Baptista, P.M.A. Miranda, 1994. Numerical Simulation of 1969 Tsunami along the Portuguese Coasts. Preliminary Results. Sc of Tsunami Hazards, vol.12,nº1, 13-23.

Imamura, F. (1995), "Tsunami Numerical Simulation with the Staggered Leap-frog Scheme (Numerical Code of TUNAMI-N1 and N2)", Disaster Control Research Center, Tohoku University, 33 pp.

Justo, J. L. and C. Saiwa. The 1531 Lisbon Earthquake, Bulletin of the Seismological Society of America, Vol. 88. n. 2, pp. 319—328, 1998.

Lynnes C. S., Ruff L.J. ,(1985). Source process and tectonic implications of the great 1975 North Atlantic earthquake. Geophys. J. R. Astr. Soc., 82, 497-510.

Mader, C. Numerical modelling of water waves. Los Alamos Series in Basic and Applied Sciences, pp 206. 1988, 2001

Mader, C. Modelling the Lisbon Tsunami. Sc of Tsunami Hazards, 19, 93–116. 2001.

Mansinha, L. and Smylie, D. E.: The Displacement Field of Inclined Faults, BSSA, 61, 1433–1440, 1971.

Martins, I. and L. A. Mendes-Victor (1990): "Contribuição para o estudo da sismicidade em Portugal Continental". Publ. IGIDL, 18, Universidade de Lisboa.

Moreira de Mendonça (1758). Historia Universal dos Terramotos que tem havido no mundo de que ha noticia desde a sua creção até ao século presente. Biblioteca Nacional de Lisboa, Portugal.

Pais J.P. (1992). Paisagem protegida da arriba fossil da Costa da Caparica. Liberne - Boletim da Liga para a Protecção da Natureza, nº42, pp5-9.

Smith, W.H.F. & Sandwell, D. T. Global Seafloor Topography from Satellite Altimetry and Ship Depth Soundings, Science Magazine 277 (5334), 1997.

TSUNAMIGENIC SOURCES IN THE BAY OF PLENTY, NEW ZEALAND

Roy A. Walters
National Institute of Water & Atmospheric Research Ltd.
PO Box 8602
Christchurch, New Zealand
r.walters@niwa.co.nz

James Goff
National Institute of Water & Atmospheric Research Ltd.
PO Box 8602
Christchurch, New Zealand
j.goff@niwa.co.nz

Kelin Wang
Pacific Geoscience Centre
Geological Survey of Canada
9860 West Saanich Road
Sidney, B.C. V8L 4B2, Canada
kwang@nrcan.gc.ca

ABSTRACT

New Zealand sits in a precarious position astride the boundary between the Pacific and Australian Plates. There is a wide range of potential tsunamigenic sources in this area including fault movements, submarine landslides, volcanic activity, and other mechanisms. In addition, considerable prehistoric information indicates that large tsunamis have inundated the coastline several times in the past. A part of our work has been directed toward using historic and prehistoric tsunami data to evaluate possible sources. Several types of dislocation models and submarine landslide models are used to simulate the displacement of the sources. A finite element numerical model is used to simulate generation, propagation and runup of the resultant tsunami. As an example, we present results for the Bay of Plenty, northeast coast of the North Island, New Zealand. The range of source types includes local faults, subduction zone rupture, volcanic eruptions, sector collapse of seamounts, and submarine landslides. A likely major source is a subduction zone event along the Tonga-Kermadec Trench. Data from paleotsunami deposits have guided the model in determining appropriate source characteristics and establishing the most significant event for this region.

Introduction

In a geophysical sense, New Zealand sits in a precarious position astride the boundary between the Pacific and Australian Plates (Figure 1). To the north in the Tonga-Kermadec-Hikurangi trench, the Pacific Plate is subducting from the east at a rate of ~40 mm/yr. To the south in the Puysegur trench, the Australian Plate is being subducted from the west with a convergence rate of ~35 mm/yr. Hence, there are a wide range of potential tsunamigenic sources including upper plate and subduction zone fault movements, submarine landslides on the oversteepened continental shelf slope, volcanic activity in the volcanic arc stretching northeast from the North Island, sector collapse of seamounts, and other mechanisms.

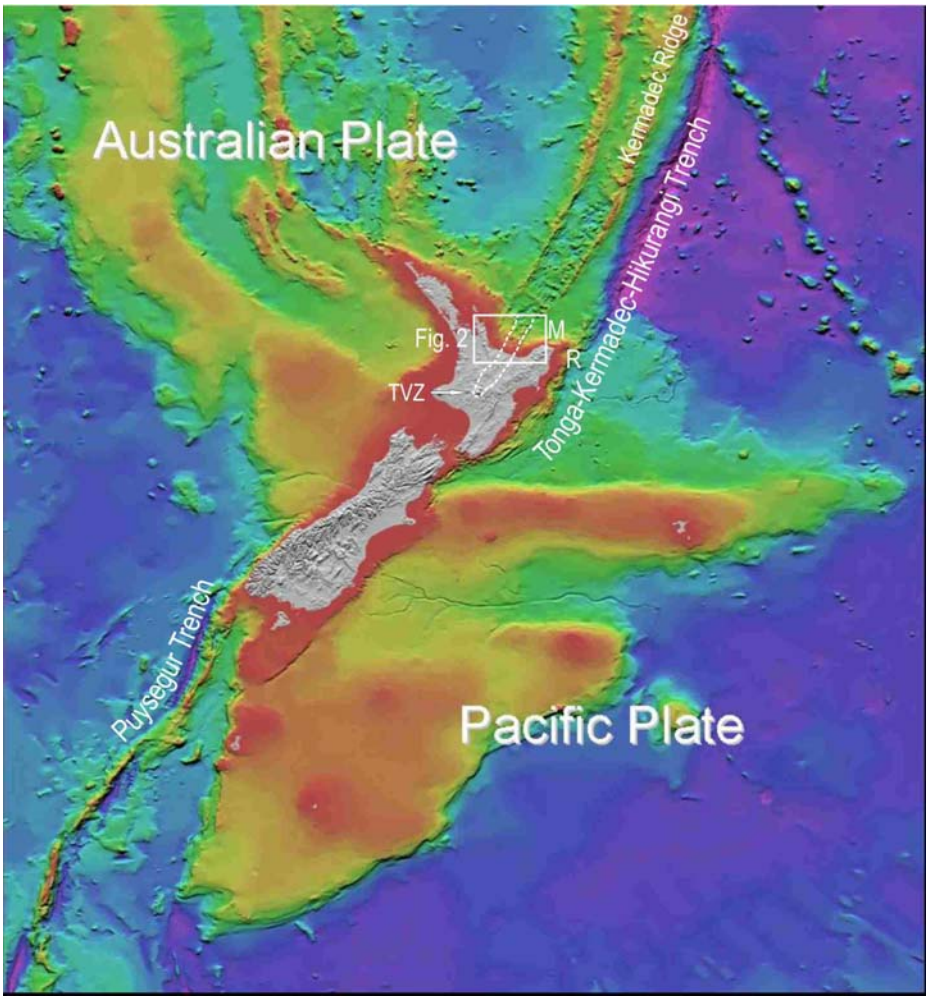

Figure 1: Geophysical setting for New Zealand. Note the plate convergence that crosses from east to west in central New Zealand. The white box indicates the study area of this paper. , (TVZ = Taupo Volcanic Zone; R = Ruatoria landslide; M = Matakaoa landslide)

As a result, it is not surprising that tsunamis have occurred relatively frequently along the coast of New Zealand in historic and prehistoric times (de Lange and Fraser 1999; Goff et al., 2001a). The record of prehistoric events has grown markedly over the past decade to include sites on the main and several offshore islands (e.g. McFadgen and Goff, in press; 2005; Goff et al., 2004; Bell et al., 2004; Nichol et al., 2004; Chagué-Goff and Goff, 2003). These geological data are useful for developing estimates of tsunami magnitude and frequency. They are also useful however as data points to compare with, and complement, hydrodynamic models (Walters and Goff, 2003).

In the end, tsunami runup effects depend on the initial or incident wave amplitude and direction, the wave period (or more generally the spectral content of the wave), and how the wave interacts with the ocean and shoreline topography. Where a harbor or coastal bay resonates with a similar period as the incident wave, large amplification of incident waves can be expected. In addition, offshore islands can cause a convergence of the waves and result in large amplitude waves on the adjacent coastal margin. In theory, hydrodynamic models should be able to provide realistic approximations of tsunami runup along the whole coastline. In the absence of groundtruthing it is difficult to know how close these approximations are to reality.

The objective of the work presented here is to evaluate potential tsunamigenic sources in the Bay of Plenty and determine the most significant source by comparing and contrasting independently obtained model and paleotsunami data. The potential sources are identified through existing geophysical data. Fault ruptures were simulated with elastic dislocation models (Okada, 1985; Wang et al, 2003), and sector collapse of seamounts and submarine landslides were simulated with a dynamic landslide model (Walters et al, 2006b). A high-resolution hydrodynamic model was used to simulate the effects of the resultant tsunami (Walters, 2005; Walters et al, 2006a). Finally, the results of paleotsunami studies were compared with model predictions to determine the most significant sources.

Potential Sources

The Bay of Plenty faces a diverse range of potential tsunamigenic sources either within the Bay of Plenty (Figure 2), along the plate boundaries (Figure 1), or remotely across the Pacific Ocean. Within the region a range of potential tsunamigenic sources have been reported in geophysical investigations that include seafloor mapping and seismic profiling of fault systems, mapping underwater volcanism and sector collapse, and mapping underwater landslides. These sources were summarized in Bell et al. (2004).

Return period is defined here as a qualitative measure of the average recurrence interval. A general methodology to determine these values is to construct a plot of magnitude versus the annual exceedence probability for each of the sources. For a given magnitude event, the corresponding probability then defines an average recurrence interval. However, there is no adequate data to define these plots, except for the detailed assessment of local faults in the Bay of Plenty (Lamarche and Barnes, 2005). Hence, the values for return period are rough estimates based on general knowledge of similar events.

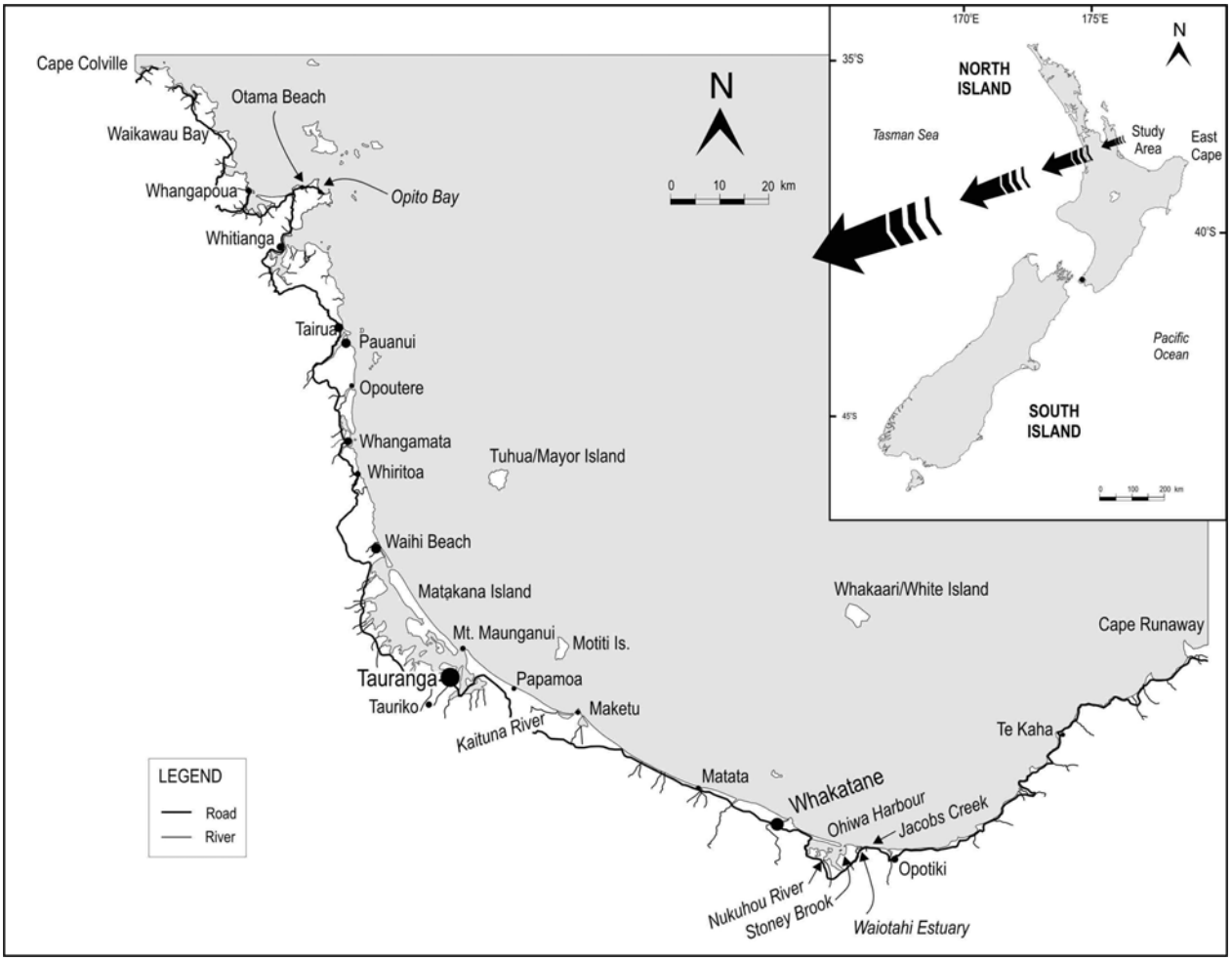

Figure 2: The Bay of Plenty – showing location of mainland paleotsunami sites and locations mentioned in the text

For the purpose of this study, the important potential tsunamigenic sources (local and regional) are categorized as:

1. Subduction zone earthquakes along the Tonga-Kermadec-Hikurangi trench associated with the Pacific/Australian plate boundary (Figure 1). This source occurs beneath the eastern margin of the Bay of Plenty and the Kermadec Ridge, where the Pacific Plate underthrusts (subducts) to the west. Historic earthquakes of magnitude M_w 8.0 to 8.3 have occurred along the Kermadec boundary (ITDB/PAC 2004) in the early 1900's. As a general rule of thumb, large subduction zone earthquakes in a particular area have return periods of 300 to 1000 years.

2. Regional active faults provide many candidates for sources within the Bay of Plenty (Lamarche and Barnes, 2005). They primarily include normal faults in the offshore Taupo Volcanic Zone (Figure 1). The major zone of active rifting extends between

Whakatane and Tauranga, with faults between Matata and Whakatane accommodating a significant proportion of the total crustal extension (Figure 2) (Wright, 1990; Lamarche et al., 2000). Normal faulting in this area rarely exceeds 2 m single event vertical displacement, but the larger boundary faults may be capable of larger seabed displacements. Typical return periods for these regional faults vary from a few hundred to 1000's of years (Lamarche and Barnes, 2005).

3. Landslide sources east and north of East Cape include giant landslide complexes such as Matakaoa and Ruatoria (Figure 2). Collot et al. (2001) have shown that the Ruatoria landslide was triggered approximately 170000 years ago and had a volume of about 3000 km^3. The Matakaoa landslide on the other hand contained at least three large landslides and probably dates to around 50000 years ago (Lewis et al., 1999; Carter and Lamarche, 2001). These slides included large slabs that slid down the continental shelf semi-intact and debris flows that inundated the abyssal plain. Large submarine landslides will undoubtedly produce large tsunamis, but these are highly complex events and much of the required data for modeling purposes are not available. Furthermore, with return periods in the 10's-100's of thousands of years, these events occur on a longer timeframe than the 500 to 1000 years considered here. However, smaller landslides are possible within the Matakaoa complex and in the submarine canyons of Bay of Plenty.

4. Offshore volcanic sources in the Bay of Plenty include Tuhua/Mayor Island and Whakaari/White Island. For Tuhua/Mayor Island, modeling studies indicate that the credible pyroclastic eruptions of a "Mt St Helens" scale (1 km^3) could produce a tsunami that would impact an area from Tairua to Maketu (Figure 2), with wave heights peaking at 0.5 m between Whangamata and Tauranga (de Lange, 1998; de Lange and Prasetya, 1999). An eruption ten times larger with a pyroclastic flow of Krakatau scale (10 km^3) would create waves that peak at around 5 m at the coast (de Lange and Prasetya, 1999). Recent geophysical data from Tuhua/Mayor Island indicates the last caldera collapse, associated with the largest eruption, occurred about 6,300 years ago (Houghton et al., 1992) and included the transport of pyroclastic flows into the sea. However, an examination of the detailed bathymetry (Figure 2) does not reveal any areas where large pyroclastic flows (>1 km^3) have occurred. Numerous smaller submarine volcanoes occur on the Bay of Plenty continental shelf and slope closer to the coast (within 100–150 km) (Gamble et al., 1993; Lamarche and Barnes, 2005). As a result, volcanic sources do not seem to have a significant impact.

5. Local landslides including sector collapse of seamounts, can provide sources within the Bay of Plenty. In particular, landslide sources at the heads of Tauranga and White Island Canyons were considered as possible sources (Figure 3). Landslide volumes however are relatively small; hence the tsunami that would be generated is also small. Seafloor geometry in the area would also ensure that the tsunami would be primarily directed offshore. As a result, this type of source has not been

considered further. Instead, a complete collapse of a seamount was modeled as an extreme case in order to gauge the relative size of a tsunami that could be generated. These could be a source of large amplitude waves because of the short distance to shore.

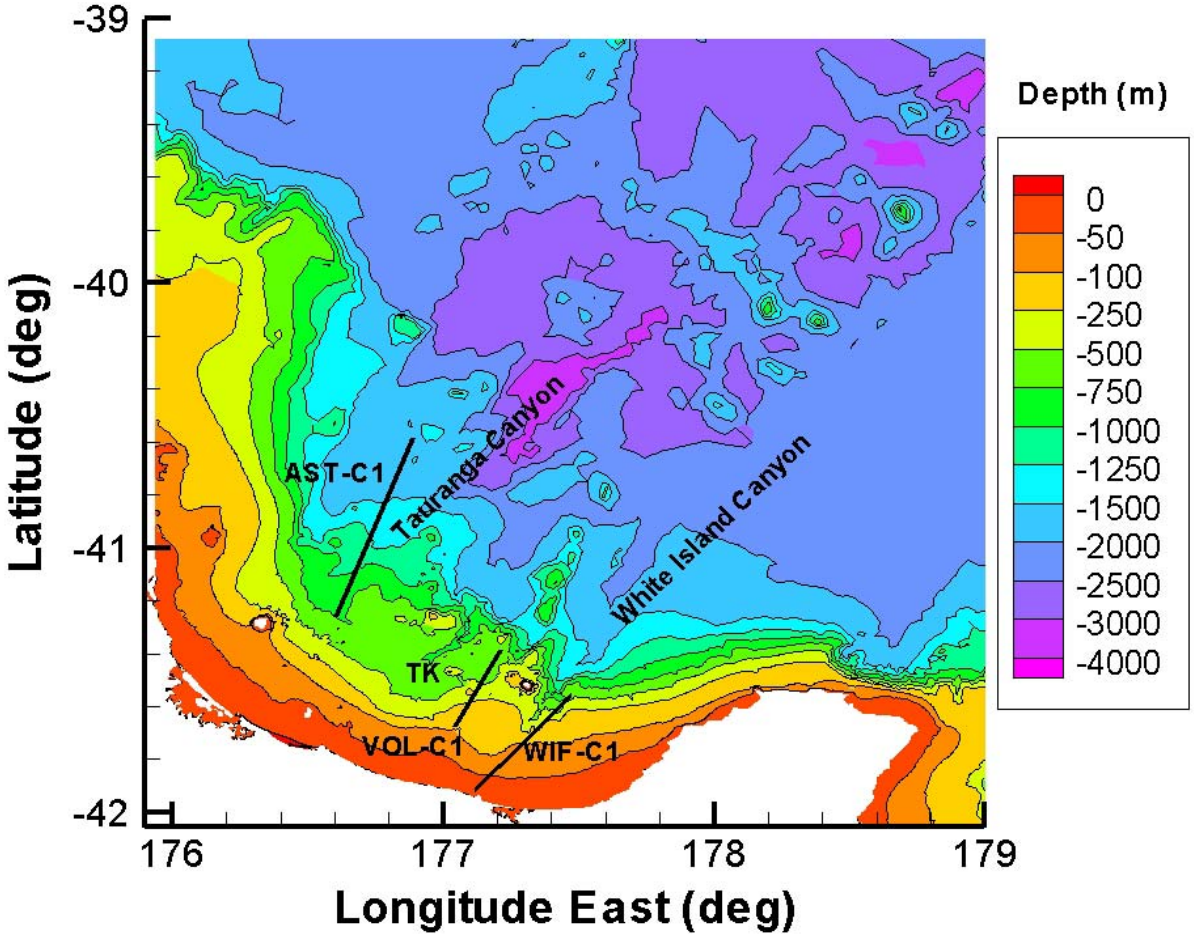

Figure 3: **High resolution bathymetry of the Bay of Plenty. AST-C1 = Composite Astrolabe fault, VOL-C1 = Composite Volkner fault, WIF-C1 = Composite White Island fault, TK=Tumokemoke Knoll.**

Of the remaining sources:

1. Upper plate faults along the Tonga-Kermadec-Hikurangi shelf margin were not judged capable of generating large tsunamis within the Bay of Plenty as compared to large subduction zone earthquakes due to their shorter wavelength, short fault length, and moderate vertical displacement.

2. Undersea volcanic sources in the Tonga-Kermadec-Hikurangi system can be represented as a point source for tsunamis. The amplitude of the waves from these volcanoes decreases rapidly with distance from the source and hence is not considered to be an issue here.

3. Pressure waves or pyroclastic flows from large onshore volcanic eruptions in the Taupo Volcanic Zone were not considered.

4. The primary source for a remote tsunami is South America. The historic record indicates that these events are unlikely to generate tsunamis of comparable size to local and regional events (de Lange and Fraser, 1999), so they too are not considered here.

Paleotsunami Data

A definitive identification of a paleotsunami deposit hinges on the use of as many data sources as possible. In most cases this relies largely on the recognition of as many paleoenvironmental characteristics as possible, including geological, archeological, and geomorphological parameters (c.f. McFadgen and Goff, in press; Goff et al., 2004; Witter et al., 2001). It is also useful to be able to identify a probable tsunami source. This task is made easier for areas with one coastline and a major offshore seismic source (e.g. west coast of North America, Chile), but is less clear cut for countries such as New Zealand with potential tsunami sources and coastline at all points of the compass. It is worth noting though that sufficient data now exist in New Zealand to allow tsunami sources to be estimated from palaeotsunami records.

Even a standard conception that a paleotsunami deposit represents ‘a deposit out of place’ (e.g. a sand layer sandwiched between peat) must be treated with caution since this visible identification is dependent upon the nature of both the material available for entrainment and the depositional environment. Therefore, perhaps counter-intuitively, a mud layer in sand can represent a paleotsunami (or paleostorm) deposit (Goff and Chagué-Goff, 1999).

The absence of some paleoenvironmental characteristics does not negate a paleotsunami interpretation, but rather it can be indicative of the particular context. For example, the absence of buried soil or vascular plants might mean that either the underlying material was devoid of vegetation, or that the nature of inundation removed the material prior to deposition of a ‘clean’ sediment. Hence it is useful to understand paleoenvironmental conditions at the time of deposition. In general terms, if the study site was relatively exposed to the sea it is possible that the last inundation removed evidence of earlier events and also has a limited number of potential paleoenvironmental characteristics. A more sheltered, low energy coastal wetland would be more likely to preserve evidence of multiple inundations and have more paleoenvironmental characteristics (e.g. Goff et al., 2001b).

The New Zealand paleotsunami database currently consists of over 200 sites (J. Goff, unpublished data). The database contains a range of information including archeological, geological, and geomorphological material. Each site contains details of location, age, elevation, distance inland, forms of evidence, possible/probable tsunami source, relevant references, general

comments concerning the evidence, and an indication of the veracity of the data. It is possible to differentiate between relative event magnitudes in the broad categories of <5.0 m (small), '>5.0-10.0 m (large)' and '>10.0 m (extreme)'. The latter category should be considered a catch-all for events greater than 10.0 m. In New Zealand the record of these extreme events ranges in height up to possibly 60.0 m. above mean sea level (Goff, 2003), although this should not be considered a maximum. The New Zealand record is far from complete and will continue to grow as more sites are studied and new analytical techniques are developed. Following a recent study of the Bay of Plenty area however (Bell et al., 2004), there is sufficient information available to undertake a comparison between independently obtained model results and geological data.

Paleotsunami deposits reported from the Bay of Plenty range in age from 9500 years BP to 1600-1700 AD. At least two of these events have had a significant region-wide impact, the most recent occurring in the 15th century (Bell et al., 2004). Data from the 15th century event are extensive, and include evidence collected from all mainland sites shown in Figure 2. These data were used to map estimated wave crest height around the Bay of Plenty. Estimated wave heights are based upon the maximum elevation of the deposit above sea level, estimated distance inland from paleoshoreline, and the wave height required for transport of the coarsest material (after Jaffe and Gelfenbaum, 2002).

Models

Tsunami Model

The numerical model used in this study is a general-purpose hydrodynamics and transport model known as RiCOM (River and Coastal Ocean Model). The model has been under development for several years and has been evaluated and verified continually during this process (Walters and Casulli, 1998; Walters, 2005; Walters et al., 2006a; 2006b). The hydrodynamics part of this model was used to derive the results described in this report.

The model is based on a standard set of equations - the Reynolds-averaged Navier-Stokes equation (RANS) and the incompressibility condition. In this study, the hydrostatic approximation is used so the equations reduce to the nonlinear shallow water equations.

To permit flexibility in the creation of the model grid across the continental shelf, a finite element spatial approximation is used to build an unstructured grid of triangular elements of varying-size and shape. The time marching algorithm is a semi-implicit numerical scheme that avoids stability constraints on wave propagation. The advection approximation is a semi-Lagrangian scheme, which is robust, stable, and efficient (Staniforth and Côté, 1991). Wetting and drying of intertidal or flooded areas occurs naturally with this formulation and is a consequence of the finite volume form of the continuity equation and method of calculating fluxes (flows) through the triangular element faces. At open (sea) boundaries, a radiation condition is enforced so that outgoing waves will not reflect back into the study area, but instead are allowed to realistically continue through this artificial boundary and into the open sea. The equations are solved with a conjugate-gradient iterative solver. The details of the numerical approximations that lead to the required robustness and efficiency may be found in Walters and Casulli (1998) and Walters (2005).

Coastline data were retrieved from the LINZ high resolution New Zealand coastline dataset which follows a boundary defined by the mean high water line. Bathymetric data were derived from surveyed data of coastal coverage with 10 m isobaths (to approximately 150 – 200 m depth) and 50 m contours at greater depths off the continental shelf. The coastline and contour data were combined to form a depth reference grid.

The model grid was generated using methods described in Henry and Walters (1993). A layer of elements is generated along the boundaries using a frontal marching algorithm (Sadek, 1980). The remaining interior points are filled in using the cluster concept described in Henry and Walters (1993). This grid was subsequently refined by a factor of four by subdividing each grid triangle successively into 4 new triangles using vertices at the mid-sides of the original triangle. Depth values are interpolated at each node from the reference dataset described above. The resulting model grid contains 365787 nodes and 722852 elements for the subduction zone events, and local, more refined grid for the remaining sources.

Fault Dislocation models

There were two dislocation models used in this study. The first is an analytical solution for a rectangular dislocation in an elastic media (Okada, 1985). The width, depth, strike, dip, and displacement are all considered constant. This type of model is more appropriate for the local normal faults in the Bay of Plenty where these parameters have been tabulated in Lamarche and Barnes (2005).

The second model is a more general numerical model developed by integrating Okada's (1985) point-source dislocation solution (Wang et al, 2003). This model is more appropriate for the curved dislocation surface and variable slip in a subduction zone fault.

Landslide Model

Laboratory experiments (Fleming et al, 2005) and models studies (Walters et al, 2006) have guided the creation of a series of dynamic landslide models. The models range from solid sliders, to viscous fluids, and to mixtures. For this study, the viscous fluid approximation was used where the landslide has internal Newtonian stresses and basal sliding with friction (Walters et al, 2006).

Results and Discussion

It is important to recall that the coastal effect of a tsunami depends on both the source characteristics and the coastal response characteristics. For remote tsunamis, maximum amplitudes and spectral content of the waves can be determined from historic data. This information combined with admittance information derived from the response patterns leads to reasonable estimation of effects (Walters and Goff, 2003). For local tsunamis, the situation is very different. In particular, the source characteristics are generally not well defined along the New Zealand coast.

Local fault events

A comprehensive summary of faults in the Bay of Plenty has been published by Lamarche and Barnes (2005). These faults are primarily normal faults in the offshore Taupo Volcanic Zone (Figure 1). The major zone of active rifting extends between Whakatane and Tauranga, with faults between Matata and Whakatane accommodating a significant proportion of the total crustal extension (Figure 2). The larger faults with significant seafloor traces include the Whakaari/White Island and Rangitaiki Faults in the offshore Whakatane Graben. Normal faulting in the Taupo Volcanic Zone rarely exceeds 2 m single event vertical displacement.

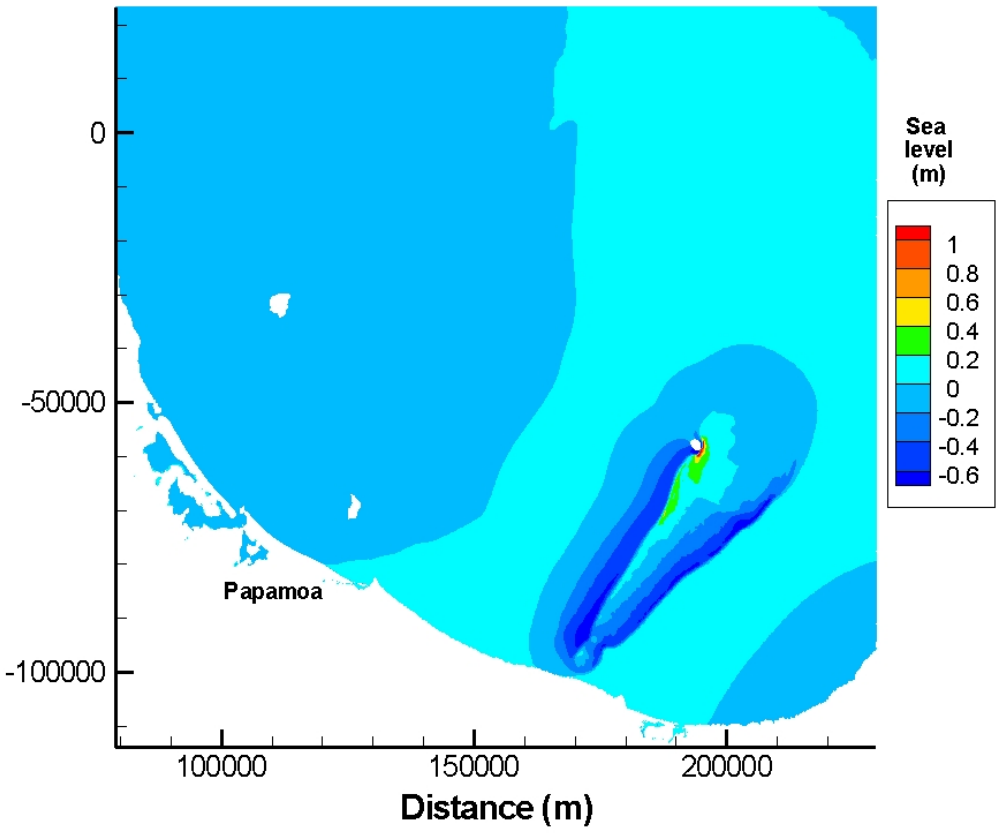

Figure 4: Composite White Island faults – 140 seconds after maximum single event displacement (note westward moving wave has just struck east coast of White Island).

Three representative faults were chosen based on their potential for producing relatively large wave heights (Figure 3). These included a composite of the White Island faults (WIF-C1), the composite Volkner faults (VOL-C1), and the composite Astrolabe faults (AST-C1). All the necessary parameters for an elastic dislocation model are provided in the report by Lamarche and

Barnes (2005). The rectangular-fault model of Okada (1985) was used to calculate seabed displacements for the three faults and these displacements were used as an initial condition for the tsunami model.

Because these faults are normal faults, they exhibit the greatest displacement downwards in the direction of dip (typically greater than 1 m), and a smaller positive displacement (typically 0.3 m) on the opposite side of the fault trace. As the wave separates and propagates in both directions away from the fault, the two waves have different characteristics. For the tsunami with a small positive leading wave (initially moving away from the direction of fault dip), the positive peak remains small and runup is not significant. However, for the other tsunamis with a negative leading wave, the positive peak is amplified and the runup in local areas can be up to 2 m. The illustrations in Figures 4 and 5 show snapshots in time near the start and end of the tsunami sequence for the White Island Fault composite fault (WIF-C1).

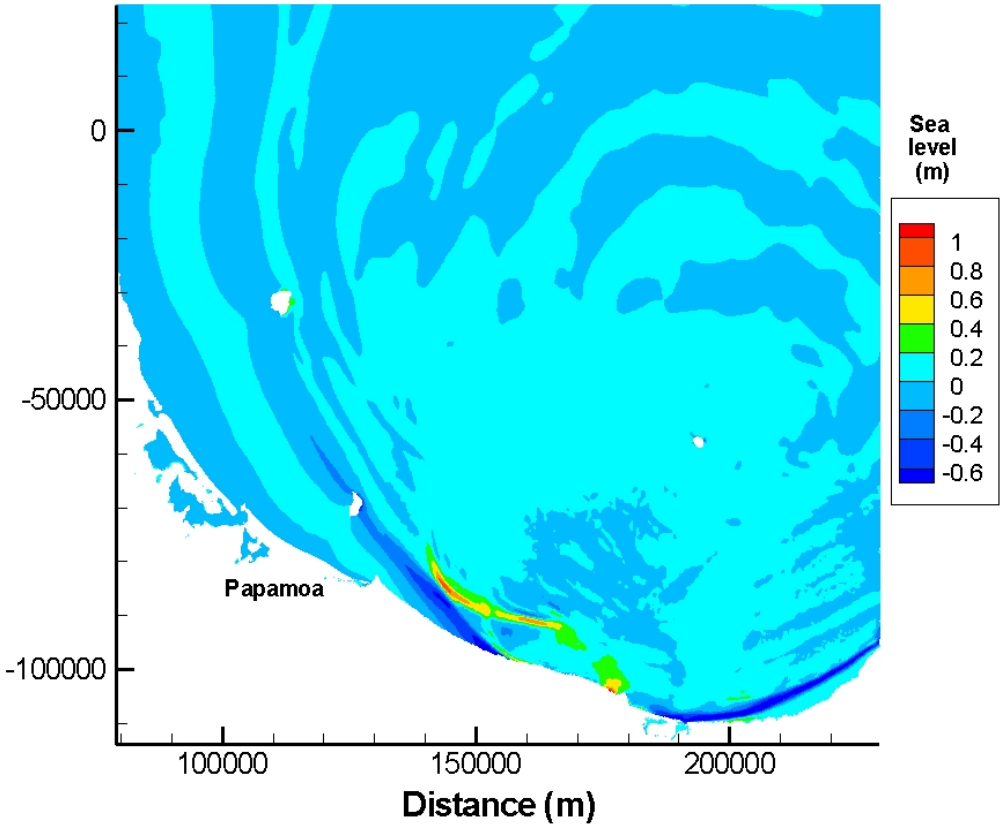

Figure 5: **Composite White Island fault – 1500 seconds after maximum single event displacement. Note the westward traveling wave with a leading trough has the largest positive wave crest height.**

Seamount collapse

The sector collapse of a seamount or submarine volcano acts as a point source and the resultant tsunami tends to decay rapidly with distance away from the source. Important factors that control the size of a tsunami are volume of the material that collapses, and the direction and depth of the collapse.

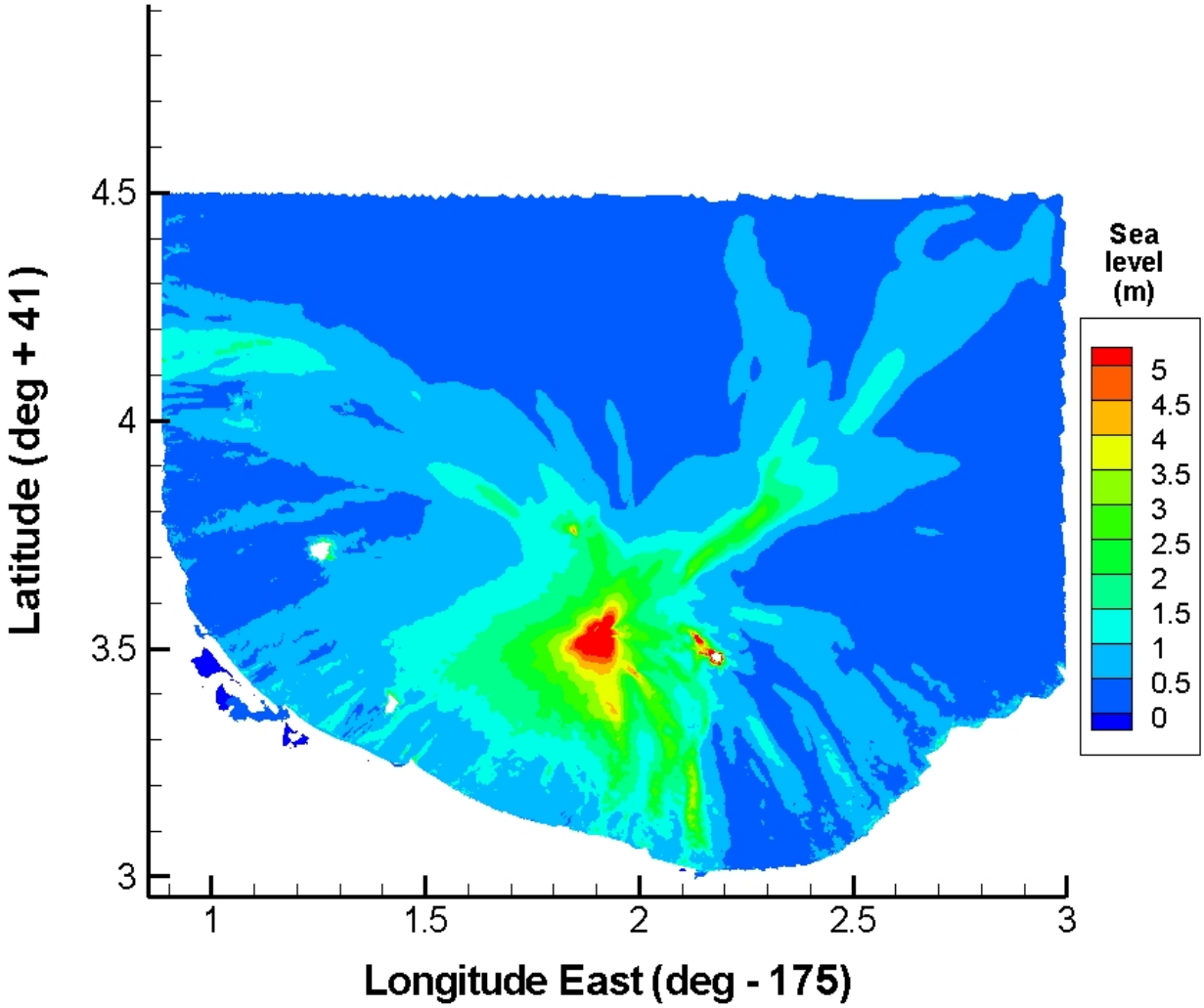

Figure 6: **Maximum water surface elevation for a collapse of Tumokemoke Knoll seamount. Waves peak at less than 1.5 m along the coastline (note change in scale).**

As an example, an entire collapse of the nearest large seamount, Tumokemoke Knoll was simulated as a material failure and subsequent landslide (Figure 3). The knoll is about 4 km in diameter at the base, about 300 m high from its base, and 200 m below mean sea level. The volume of material is approximately 1.2 km^3. This can be compared with the 10 km^3 of material from volcanic sources that is required to generate a 5 m tsunami (de Lange and Praysetya, 1999).

As expected, the tsunami decays rapidly with distance from the seamount source and the wave height is less than 1.5 m when it reaches the nearest shore (Figure 6).

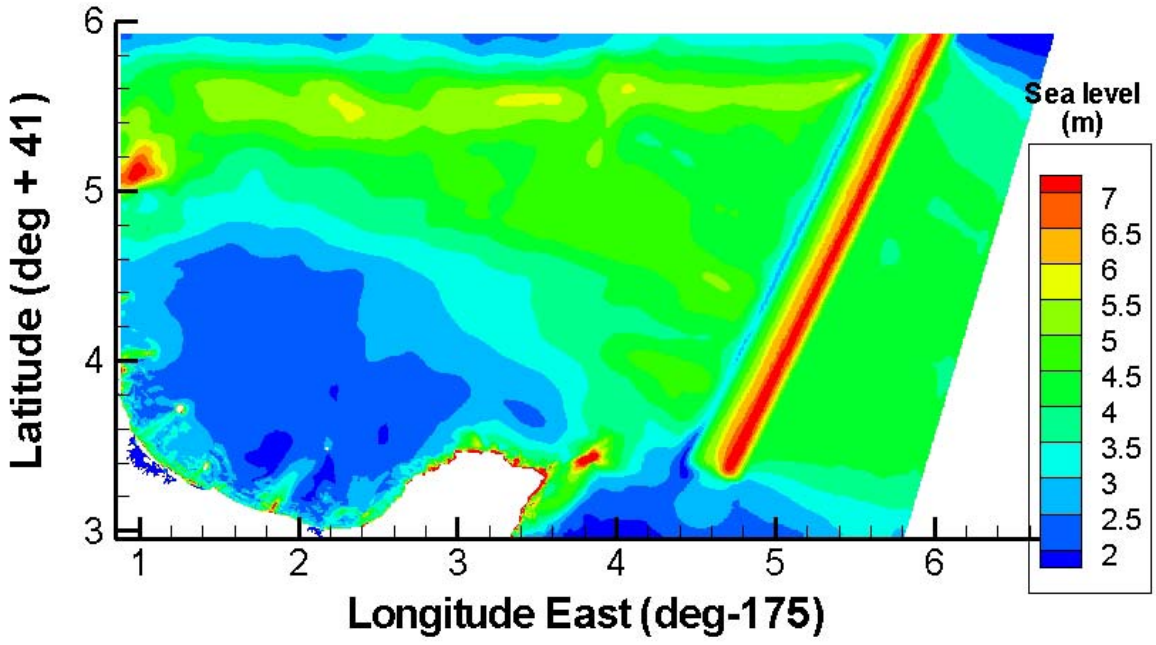

Figure 7: Maximum water surface elevations during a simulation of a subduction zone event. The reduced elevation on the north boundary is an artifact of the radiation boundary condition.

Subduction zone events

Most of the Bay of Plenty is directly exposed to tsunamis generated by subduction zone earthquakes immediately north of East Cape (the Kermadec-Hikurangi Trench). A fault-dislocation model (Wang et al, 2003) was used to model seabed displacement for events ranging from M_w 8.3 to M_w 8.7 (see Lamarche and Barnes (2005) for definitions). An event of M_w 8.5 however, seems likely to be near the maximum credible event for this source. On the basis of an empirical relation between maximum earthquake size, age of subducting plate, and convergence rate proposed by Ruff and Kamamori (1980), the Kermadec subduction zone would appear to be a very unlikely candidate for an event as large as Mw 8.5. Improvements to our knowledge of plate motion rate and age have put this empirical relation in question (Stein and Okal, 2006). The

devastating 2004 Sumatra earthquake and tsunami event serve as a wake-up call to remind us that giant earthquakes do occur in what are considered the most unlikely places for them. In fact, events with Mw 8.0 and 8.3 occurred farther north on the Kermadec trench early in the 20th century (ITDB/PAC 2004).

For the most likely maximum credible event, an M_w 8.5 fault rupture was modeled to strike the coast at Mean Sea Level (MSL) (Figure 7). Because fault movement is rapid with respect to surface wave propagation in this case, the seabed displacement was used as the initial water displacement for the tsunami that was created. The initial wave separates into two waves of roughly equal size - one propagating onshore and the other propagating offshore to become a remote tsunami elsewhere. The wave directed onshore is partially refracted around East Cape and comes ashore in the Bay of Plenty. The main part of the wave travels westward to the area around Tauranga and to the north. In the south part of the Bay of Plenty, the wave crest is stretched by refraction in the bay. Waves converge around Motiti Island and other islands, amplifying the tsunami on the adjacent coast (Figure 8).

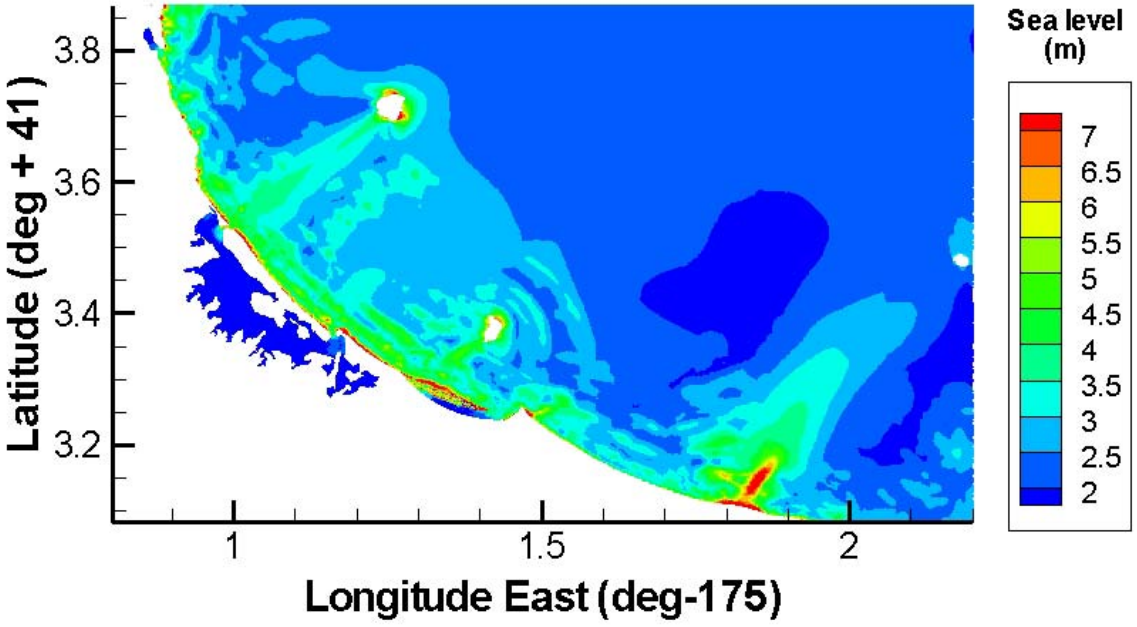

Figure 8: Maximum water surface elevation showing wave focusing behind Motiki Island.

The general pattern of tsunami crest height showed low values in the south part of the Bay of Plenty (1 to 3 m) and increasing height toward the north (5 to 8 m). There were local maxima in areas behind offshore islands. One local maximum had a height of 6 m onshore from Motiti Island, arriving 70 minutes or so after fault rupture. Waves breached the coastal sand dunes at this location.

A comparison between elevations derived from the paleotsunami data and the model results is shown in Figure 9. The model contains detailed topography around one of the data sites near Papamoa. Modeling tests indicated that an Mw 8.5 to 8.7 event would overtop the coastal sand dunes and inundate the site. As these are credible-sized events for this area, these results were used for comparison with the elevations derived from the data. Note that these results are preliminary in that other factors such as state of the tide and changes to the coastal dune system over the last 500 years has not yet been taken into account.

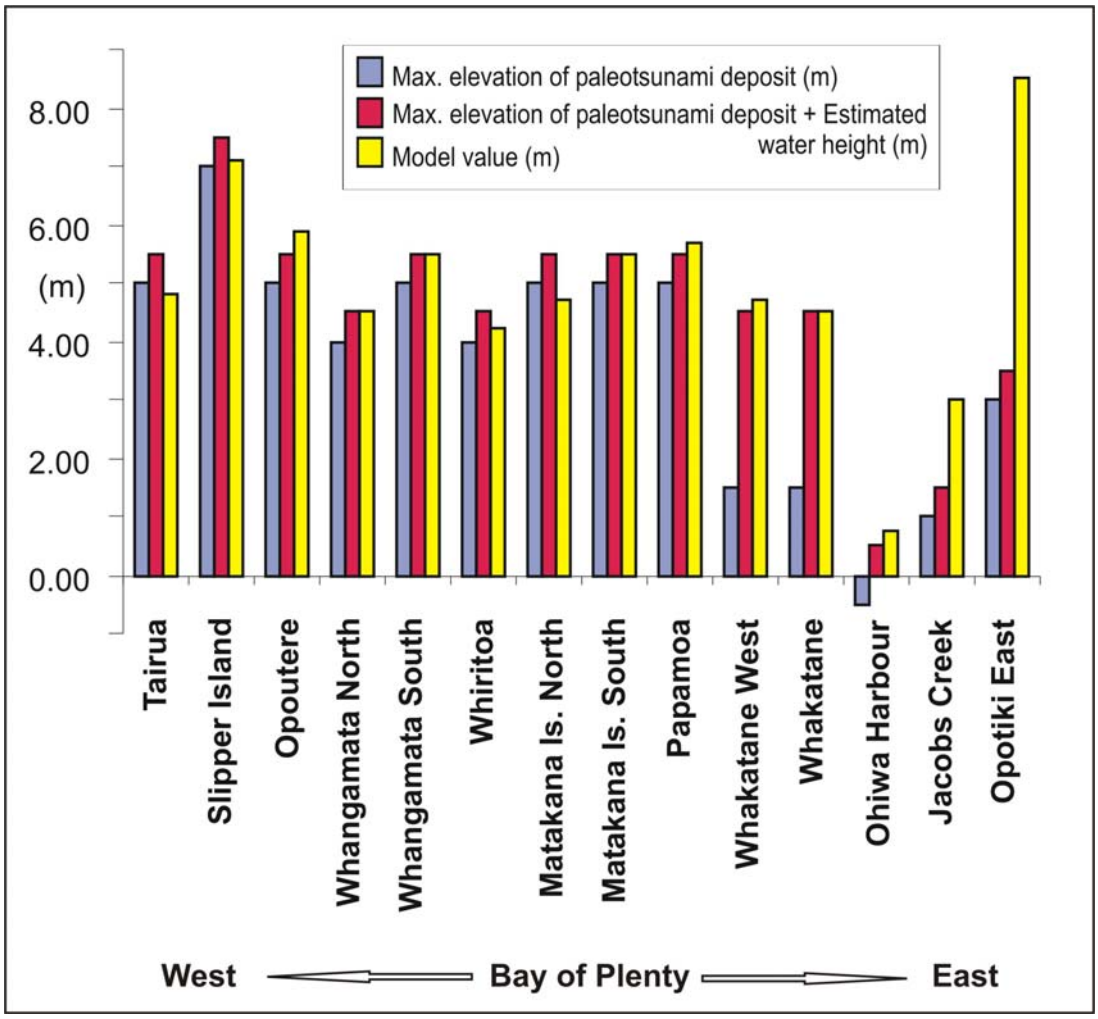

Figure 9: Summary diagram of comparison between model values (maximum water surface elevation at the shoreline) and palaeotsunami-related data.

There is a striking similarity in the spatial pattern in wave height between the paleotsunami data and the model results. As this pattern is sensitive to the incident amplitude and direction of the tsunami, it provides compelling evidence this data reflects the effects of a large subduction zone event extending north of East Cape. This pattern cannot be reproduced by other

combinations of sources in this area, and the wave crest heights are much too large for a remote tsunami.

The largest discrepancy between the data and the model elevations occurs in southern Bay of Plenty near Opotiki. This is an area where there is no coastal topography in the model and the shoreline is rather coarsely resolved. Even so, at Jacobs Creek there is a 2.5 m coastal barrier seaward of the site, hence the wave must overtop this barrier although the data site is at a lower elevation inland. At Opotiki East, the data site is in the lee of a large headland that would have considerably reduced wave height. Adding topographic detail would probably remove these discrepancies.

Conclusions

This paper presents an evaluation of potential tsunami sources for the Bay of Plenty. These sources include a subduction zone event, local fault ruptures, volcanic sources, seamount collapse, and local submarine landslides. Most of these events can produce tsunamis with crest heights of 1 to 2 m at the shoreline.

However, the most significant source is a subduction zone event along the Kermadec Ridge east of the Bay of Plenty. The pattern of wave height at the shoreline varies from 1 to 8 m and is in good agreement with wave height derived from independently gathered paleotsunami data. This suggests that subduction zone events are the most significant tsunamigenic source over timescales of 500 to 1000's of years.

Local faults described by Lamarche and Barnes (2005) can be locally important and can have a moderate wave crest height of 1 to 2 m.

Volcanic sources and pyroclastic flows are not generally of significance for emplaced volumes less than 1 km^3. Larger volumes seem to have a very low probability.

The seabed mapping shows many cases of sector collapse of seamounts. Model experiments with the collapse of Tumokemoke Knoll (1.2 km^3) showed that the tsunami decayed rapidly with distance away from the source. The maximum wave crest height at the shoreline was approximately 1.5 m although this was the seamount closest to shore. Hence, sector collapse is not very effective in generating significant tsunamis in the Bay of Plenty.

Submarine landslide volumes within the Bay of Plenty are relatively small; hence the tsunami that would be generated is also small. Seafloor geometry in the area would also ensure that the tsunami would be primarily directed offshore. As a result, this type of source was not considered significant. However, very large landslides (3000 km^3) have occurred on the continental shelf but the recurrence intervals were too long for these events to be considered here.

Acknowledgments

The authors acknowledge many informative discussions with Geoffroy Lamarche and Philip Barnes. Fraser Callaghan provided reference and model grids for this study. Environment Bay of Plenty provided logistical and financial support for some of this work.

References

Bell, R.G., Goff, J., Downes, G., Berryman, K., Walters, R.A., Chagué-Goff, C., Barnes, P. and Wright, I. (2004). Tsunami hazard for the Bay of Plenty and eastern Coromandel Peninsula. NIWA Client Report: HAM2004-084, 90pp.

Carter, L. and Lamarche, G. (2001). "The large Matakaoa Slide and its impact on the abyssal plain, near Hikurangi Margin, New Zealand". Presented to the European Union of Geosciences XI, Strasbourg, France.

Chagué-Goff, C. and Goff, J.R. (2003). Long- and short-term environmental changes in coastal wetlands, in Goff, J.R., Nichol, S., Rouse, H.L. (eds.) The *coast of New Zealand: Te Tai O Aotearoa*. Dunmore Press, Wellington, 215-236.

Collot, J-Y; Lewis, K.B., Lamarche, G. and Lallemand, S. (2001). The giant Ruatoria debris avalanche on the northern Hikurangi margin, New Zealand: results of oblique seamount subduction. *Journal of Geophysical Research 106*: 19271–19297.

de Lange, W.P. (1998). The last wave—tsunami. In: Awesome forces–The natural hazards that threaten New Zealand. (Ed.) Hicks, G.; Campbell, H., Te Papa Press, Wellington, p. 99-123.

de Lange, W. and Fraser, R.J. (1999). Overview of tsunami hazard in New Zealand. *Tephra 17*: 3-9.

de Lange, W.P. and Prasetya, G. (1999). Volcanoes and tsunami hazard–implications for New Zealand. *Tephra* 17: 30–35. Published annually by the Ministry for Civil Defence & Emergency Management.

Gamble, J.A., Wright, I.C. and Baker, J.A. (1993). Seafloor geology and petrology of the oceanic to continental transition zone of the Kermadec - Havre - Taupo Volcanic Zone arc system, New Zealand. *New Zealand Journal of Geology and Geophysics* 36: 417–435.

Goff, J.R. (2003). Joint Tsunami Research Project: Stage 1. GeoEnvironmental Client report: GEO2003/20028, Christchurch. 49pp.

Goff, J.R. and Chagué-Goff, C. (1999). A Late Holocene record of environmental changes from coastal wetlands. Abel Tasman National Park. New Zealand. *Quaternary International 56*: 39-51.

Goff, J., Chagué-Goff, C. and Nichol, S. (2001a). Palaeotsunami deposits: A New Zealand perspective. *Sedimentary Geology* 143: 1-6.

Goff, J., Nichol, S. and Chagué-Goff, C. (2001b). Environmental changes in Okarito Lagoon, Westland. Department of Conservation Internal Series No. 3, 30pp.

Goff, J.R., Wells, A., Chagué-Goff, C., Nichol, S.L. and Devoy, R.J.N. (2004). The elusive AD 1826 tsunami, South Westland, New Zealand. *New Zealand Geographer* 60: 14-25.

Heath, R.A. (1976). The response of several New Zealand harbours to the 1960 Chilean tsunami. *In:* Heath, R.A., Cresswell, M. (eds) Tsunami Research Symposium 1974. *Bulletin of the Royal Society of New Zealand 15*: 71–82.

Henry, R.F., and Walters, R.A. (1993). A geometrically-based automatic generator for irregular triangular networks. *Communications in Applied Numerical Methods 9.*

Houghton, B.F., Weaver, S.D., Wilson C.J.N. and Lanphere, M.A. (1992). Evolution of a Quaternary peralkaline volcano: Mayor Island, New Zealand. Journal of Volcanology and Geothermal Research 51: 217–236.

ITDB/PAC (2004). Integrated Tsunami Database for the Pacific. Version 5.12 of December 31 2004. CD-ROM, Tsunami Laboratory, ICMMG SD RAS, Novosibirsk, Russia.

Jaffe, B. E., and Gelfenbaum, G. (2002). Using tsunami deposits to improve assessment of tsunami risk. Solutions to Coastal Disasters '02, Conference Proceedings, ASCE, p. 836-847.

Lamarche, G. and Barnes, P. (2005). fault characterisation and earthquake source identification in the offshore Bay of Plenty. NIWA Client report: WLG2005-51, 57pp, 36 figs.

Lamarche, G., Bull, J., Barnes, P., Taylor, S. and Horgan, H. (2000). Constraining fault growth rates and fault evolution in the Bay of Plenty, New Zealand. *EOS, Transactions of the American Geophysical Union 81*: 481, 485- 486.

Lewis, K. B., Collot, J-Y. and Goring, D. (1999). Huge submarine avalanches: is there a risk of giant waves and, if so, where? *Tephra 17*: 21–29.

McFadgen, B.G. and Goff, J.R. (in press). Tsunamis in the archaeological record of New Zealand. *Sedimentary Geology.*

McFadgen, B.G. and Goff, J.R. (2005). An earth systems approach to understanding the tectonic and cultural landscapes of linked marine embayments: Avon-Heathcote Estuary (Ihutai) and Lake Ellesmere (Waihora), New Zealand. *Journal of Quaternary Science* 20: 227-237.

Nichol, S., Goff J.R. and Regnauld, H. (2004). Sedimentary evidence for a regional tsunami on the NE coast of New Zealand. *Geomorphologie: Relief, Processus, Environnement* 1: 35-44.

Okada, Y. (1985). Surface deformation due to shear and tensile faults in a half-space, *Bulletin of the Seismological Society of America 75:* 1135-1154.

Ruff, L. and Kamamori, H. (1980). Seismicity and the subduction process. *Physics of Earth Planetary Interior* 23: 240-252.

Sadek, E.A. (1980). A scheme for the automatic generation of triangular finite elements. *International Journal of. Numerical Methods in Engineering* 15: 1813-1822.

Staniforth, A. and Côté, J. (1991). Semi-Lagrangian integration schemes for atmospheric models - a review. *Monthly Weather Review* 119: 2206-2223.

Stein, S. and Okal, E. (2006). Spatial distribution of the largest megathrust earthquakes: Variations in plate tectonic parameters or sampling bias? In Abstract volume of USGS Tsunami Sources Workshop, April 21-22, 2006, Menlo Park.

Walters, R.A. (2005); A semi-implicit finite element model for non-hydrostatic (dispersive) surface waves. *International Journal for Numerical Methods in Fluids* 7: 721-737.

Walters, R.A., Barnes, P. and Goff, J. (2006a). Locally generated tsunami along the Kaikoura coastal margin: Part 1. Fault ruptures. *New Zealand Journal of Marine and Freshwater Research* 40: 1-17.

Walters, R.A., Barnes, P., Lewis, K., Goff, J. and Fleming, J. (2006b). Locally generated tsunami along the Kaikoura coastal margin: Part 2. Submarine landslides. *New Zealand Journal of Marine and Freshwater Research* 40: 18-34.

Walters, R.A., and Casulli, V. (1998). A robust, finite element model for hydrostatic surface water flows. *Communications in Numerical Methods in Engineering* 14: 931-940.

Walters, R. and Goff, J.R. (2003). Assessing tsunami hazard on the New Zealand coast. *Science of Tsunami hazards,* 21 (3), 137-153.

Wang, K., Wells, R., Mazotti, S., Hyndman, R.D., and T. Sagiya (2003). A revised dislocation model of interseismic dislocation of the Cascadia subduction zone. *Journal of Geophysical Research* 108(B1), 2026, doi:10.1029/2001JB001227.

Witter, R.C., Kelsey, H.M., and Hemhill-Haley, E. (2001). Pacific storms, El Niño and tsunamis: competing mechanisms for sand deposition in a coastal marsh, Euchre Creek, Oregon. *Journal of Coastal Research 17*, 563-583.

Wright, I.C. (1990). Late Quaternary faulting of the offshore Whakatane Graben, Taupo Volcanic Zone, New Zealand. New Zealand Journal of Geology and Geophysics 33: 245–256.

THE POTENTIAL OF TSUNAMI GENERATION ALONG THE MAKRAN SUBDUCTION ZONE IN THE NORTHERN ARABIAN SEA. CASE STUDY: THE EARTHQUAKE AND TSUNAMI OF NOVEMBER 28, 1945

George Pararas-Carayannis
Honolulu, Hawaii, USA

ABSTRACT

Although large earthquakes along the Makran Subduction Zone are infrequent, the potential for the generation of destructive tsunamis in the Northern Arabian Sea cannot be overlooked. It is quite possible that historical tsunamis in this region have not been properly reported or documented. Such past tsunamis must have affected Southern Pakistan, India, Iran, Oman, the Maldives and other countries bordering the Indian Ocean.

The best known of the historical tsunamis in the region is the one generated by the great earthquake of November 28, 1945 off Pakistan's Makran Coast (Balochistan) in the Northern Arabian Sea. The destructive tsunami killed more than 4,000 people in Southern Pakistan but also caused great loss of life and devastation along the coasts of Western India, Iran, Oman and possibly elsewhere.

The seismotectonics of the Makran subduction zone, historical earthquakes in the region, the recent earthquake of October 8, 2005 in Northern Pakistan, and the great tsunamigenic earthquakes of December 26, 2004 and March 28, 2005, are indicative of the active tectonic collision process that is taking place along the entire southern and southeastern boundary of the Eurasian plate as it collides with the Indian plate and adjacent microplates. Tectonic stress transference to other, stress loaded tectonic regions could trigger tsunamigenic earthquakes in the Northern Arabian Sea in the future.

The northward movement and subduction of the Oman oceanic lithosphere beneath the Iranian micro-plate at a very shallow angle and at the high rate is responsible for active orogenesis and uplift that has created a belt of highly folded and densely faulted coastal mountain ridges along the coastal region of Makran, in both the Balochistan and Sindh provinces. The same tectonic collision process has created offshore thrust faults. As in the past, large destructive tsunamigenic earthquakes can occur along major faults in the east Makran region, near Karachi, as well as along the western end of the subduction zone. In fact, recent seismic activity indicates that a large earthquake is possible in the region west of the 1945 event. Such an earthquake can be expected to generate a destructive tsunami.

Additionally, the on-going subduction of the two micro-plates has dragged tertiary marine sediments into an accretionary prism - thus forming the Makran coastal region, Thick sediments, that have accumulated along the deltaic coastlines from the erosion of the Himalayas, particularly along the eastern Sindh region near the Indus River delta, have the potential to fail and cause large underwater tsunamigenic slides. Even smaller magnitude earthquakes could trigger such underwater landslides. Finally, an earthquake similar to that of 1945 in the Makran zone of subduction, has the potential of generating a bookshelf type of failure within the compacted sediments – as that associated with the "silent" and slow 1992 Nicaragua earthquake – thus contributing to a more destructive tsunami. In conclusion, the Makran subduction zone has a relatively high potential for large tsunamigenic earthquakes.

INTRODUCTION

Large earthquakes along the Makran Subduction Zone (MSZ) have generated destructive tsunamis in the past (Berninghausen, 1966). Although the historic record is incomplete, it is believed that tsunamis from this region had significant impact on several countries bordering the Northern Arabian Sea and the Indian Ocean. The tsunami generated along the MSZ on November 28, 1945 was responsible for great loss of life and destruction along the coasts of Pakistan, Iran, India and Oman (Qureshi, 2006; Pakistan Meteorological Department 2005; Mokhtari and Farahbod, 2005; Pararas-Carayannis, 2006a). The effects of this tsunami on other countries bordering the Indian Ocean have not been adequately documented.

Reports on the potential for tsunami generation along the Makran coast of Pakistan have been cursory. Based on a thorough review of recent geophysical surveys and seismic data, the present study analyzes the potential tsunami generation mechanisms along the MSZ by reviewing subduction processes of the Oman oceanic lithosphere underneath the Iranian microplate and - more specifically - the seismotectonics of the east and west segments, including the section in the Gulf of Oman. Furthermore, the study examines the seismo-dynamics of compressional collision of the India and Eurasia plates along the northwestern boundary of India in the vicinity of the Northern Arabian Sea - as potential sources of future tsunamis and evaluates the tsunami risk from major earthquakes along coastal Karach, the deltaic Indus region and the grabens of Northwestern India. Finally, the study evaluates the possible effects of the extensive sedimentation from major rivers in the region on subduction processes.

THE TSUNAMI OF 28 NOVEMBER 1954 ALONG THE MAKRAN COAST OF PAKISTAN IN THE NORTHERN ARABIAN SEA

On November 28, 1945, an earthquake, off Pakistan's Makran Coast (Balochistan) generated a destructive tsunami in the Northern Arabian Sea and the Indian Ocean. More than 4,000 people were killed in Pakistan by both the combined effects of the earthquake and the tsunami. However, the tsunami was responsible for most of the loss of life and the great destruction, which occurred along the coasts of Iran, Oman and northwestern India (Pararas-Carayannis, 2006b).

THE EARTHQUAKE

The great earthquake occurred at 21:56 UTC (03:26 IST), on 28 November 1945). Its epicenter was off the Makran coast at 24.5 N 63.0 E (24.2 N, 62.6 E according to USGS, in the northern Arabian Sea, about 100 km south of Karachi and about 87 kms SSW of Churi (Baluchistan), Pakistan. The quake's focal depth was 25 kms.

The earthquake's Richter Magnitude (Ms) was 7.8. The Moment Magnitude (Mw) was later given as 7.9 and reevaluated to be 8.1 (Pacheco and L. Sykes, 1992). The quake was recorded by observatories in New Delhi, Kolkata (Calcutta) and Kodaikanal. Its intensity was high throughout the region. It was strongly felt in Baluchistan and the Las Bela area of Pakistan. It was reported that in the western and southern sections of Karachi the strong surface motions lasted for about 30 seconds.

According to eyewitness reports, people were "thrown out of their beds", doors and windows rattled, and windowpanes broke. The underwater cable link between Karachi and Muscat (Oman) was damaged, disrupting communications. The lighthouse at Cape Moze - 45 miles from Karachi - was also damaged. The earthquake was strongly felt also at Manora, where the lighthouse was damaged. It was moderately felt in Panjgaur and Kanpur.

Other Earthquake Effects

The earthquake is reported to have caused the eruption of a mud volcano a few miles off the Makran Coast of Pakistan (Wadia, 1981). The eruption formed four small islands. A large volume of gas emitted at one of these islands, is reported to have sent flames "hundreds of meters" into the sky (Times of India 1945; Mathur, S.M. "Physical Geology of India). Such mud volcanoes are not uncommon in the Sindh region of the Makran coast. Their presence indicates the existence of high petroleum deposits. They are known to discharge flammable gases such as methane, ethane and traces of other hydrocarbons. The observed flames resulted from emitted natural gas which caught fire after the earthquake.

Fig 1. The Makran coast of Pakistan, showing location of the submarine communication cable cut by the earthquake (after Qureshi, 2006)

Historical Earthquakes and Tsunamis in the Northern Arabian Sea

Most of the earthquakes in this region of Southeast Asia occur mainly on land along the boundaries of the Indian tectonic plate and the Iranian and Afghan micro-plates. At least 28 earthquakes with magnitudes close to 7 or over 7 are known to have occurred in this region from 1668 to the present time (Ambrasseys and Bilham, 2003). According to historical records, in 893-894 A.D an earthquake with an estimated moment magnitude of 7.5 occurred in the Debal (lower Sindh) region of what is now Pakistan killing 150,000 people and destroying several towns. There is no data on whether it generated a tsunami. Also, historic records indicate that a large earthquake in late October/early

November 325 BC generated a tsunami which impacted the fleet of Alexander the Great, which was in the vicinity of the Indus river delta at that time (Pararas-Carayannis, 2006a).

THE TSUNAMI

Generating Area of the 1945 Makran Tsunami

The large earthquake is believed to have ruptured almost the entire length of the MSZ's eastern segment. The length of its rupture is estimated at about 300-350 km. A major tsunami was generated which was destructive in Pakistan, India, Iran and Oman. The approximate location and size of the tsunami generating area is shown in Fig. 1 below.

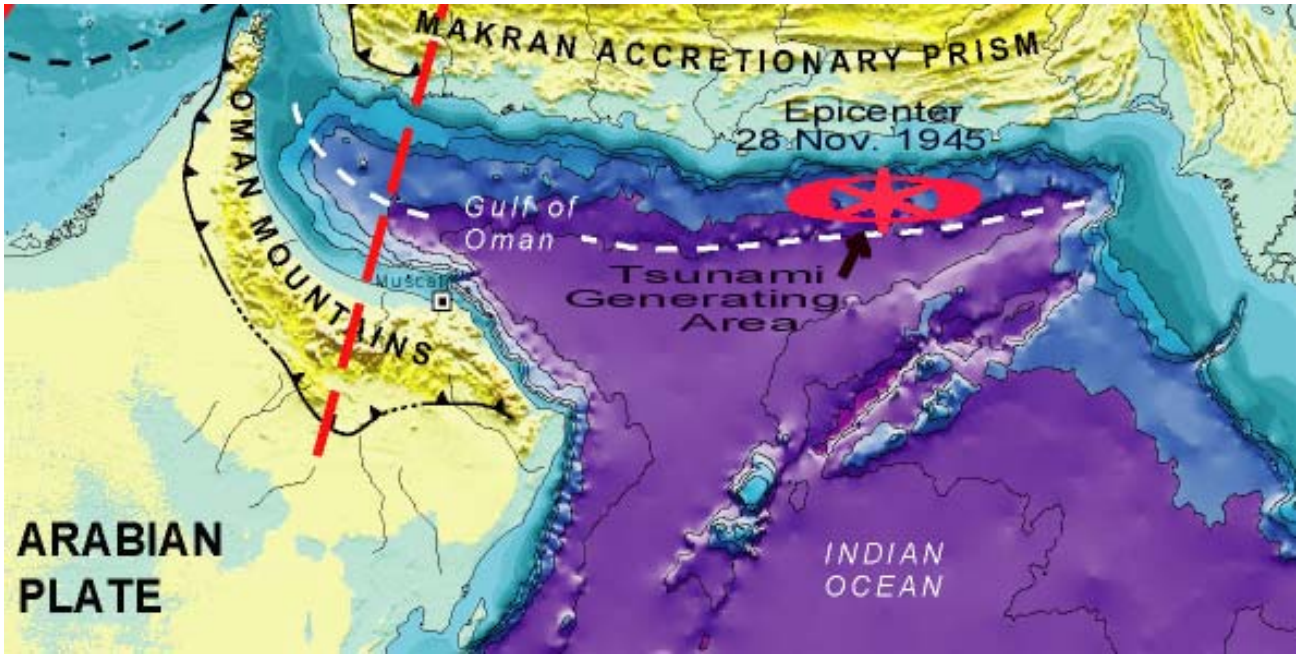

Fig. 2 The generating area of the 28 November 1945 tsunami off the Makran coast of Pakistan.

Effects of the November 28, 1945 Tsunami in Pakistan, India, Iran, and Oman

PAKISTAN - The tsunami reached a maximum run up height of 13 m (40 feet) along the Makran coast. The waves destroyed fishing villages and caused great damage to port facilities. More than 4,000 people died from the combined effects of the earthquake and the tsunami, but most deaths were caused by the tsunami. The tsunami destroyed completely Khudi, a fishing village about 30 miles west of Karachi, killing its entire people. At Dabo Creek, 12 fishermen were swept out to sea.

Elsewhere along the Makran coast there was considerable destruction and loss of life. Many people died at the towns of Pasni and Ormara but no details are available. Many more were washed out to sea. At Pasni, the waves destroyed government buildings, rest houses and postal and telegraph facilities. The tsunami was recorded at Gwadar, but there is no report on damages.

Karachi was struck by waves of about 2 m (6.5 feet) in height. According to reports the first wave was recorded at 5:30 am local time, then at 7:00am, 7:15am and finally at 8:15am. The last wave at 8:15 was the largest. The tsunami arrived from the direction of Clifton and Ghizri. There was no reported damage to the port and boats in the harbor of Karachi. However, at Keamari the waves flooded a couple of compounds along the harbor's oil installations.

INDIA - Waves as high as 11.0 to 11.5 m struck the Kutch region of Gujarat, on the west coast of India, causing extensive destruction and loss of life. Eyewitnesses reported that the tsunami came in like a fast rising tide.

The tsunami reached as far south as Mumbai, Bombay Harbor, Versova (Andheri), Haji Ali (Mahalaxmi), Juhu (Ville Parle) and Danda (Khar). According to reports the first wave was observed at 8:15am (local time) on Salsette Island in Mumbai. In Mumbai the height of the tsunami was 2 meters. Fifteen (15) persons were washed away. There was no report on damage at Bombay Harbor. Five people died at Versova (Andheri, Mumbai), and six more at Haji Ali (Mahalaxmi, Mumbai), Several fishing boats were torn off their moorings at Danda and Juhu.

IRAN – The tsunami caused extensive flooding of low-lying areas but no details are available.

OMAN - There was considerable loss of life and destruction but no details are available. The tsunami was recorded at Muscat.

THE POTENTIAL OF TSUNAMI GENERATION ALONG THE MAKRAN SUBDUCTION ZONE AND THE KUTCH GRABEN IN THE NORTHERN ARABIAN SEA

The active, subduction zone along the Makran coast of Pakistan and Iran has produced many tsunamigenic earthquakes in the Northern Arabian Sea in the past and is a potential source region for future destructive tsunamis. As demonstrated by the 1945 event, the region is capable of generating tsunamigenic earthquakes with moment magnitudes up to Mw 8.1. Also, large earthquakes along the Kutch Graben of India have caused major sea flooding and destruction of coastal areas. Extensive sedimentation by major rivers has created unstable continental slope conditions, so the potential of tsunami generation from such sources cannot be overlooked. Understanding the seismotectonics of the region and the subduction processes along the MSZ in particular, is useful in assessing future large/great earthquakes and tsunami hazards in the Indian Ocean.

OVERALL TECTONIC SETTING

Migration of the Indian tectonic plate and collision with the Eurasian tectonic plate has developed a diffuse zone of deformation and seismicity in the entire South Asia region. Continuous compression due to continent-continent convergence along the Himalayan arc boundary has resulted in major thrust or reverse type of faulting which has caused upward displacement of the Indian plate, the formation of the Himalayan Mountain Range and the Tibetan Plateau. High compression and seismic activity characterize the entire tectonic boundary along both the eastern and western sections of the thrust.

Continuing active collision along the northwestern boundary at the foothills of the Himalayan mountains caused the destructive October 8, 2005 earthquake in Pakistan (Pararas-Carayannis, 2005).

The continental convergence has further deformed and folded the western boundary, creating fractured microplates, great faults, large grabens and a major subduction zone. A complicated pattern of tectonic micro-plates and areas of both subduction and upthrust characterize the region. Complex, kinematic earth movements along the boundaries of such active zones have caused numerous destructive earthquakes in India, Pakistan, Afghanistan, Iran and Tibet in recent years. Earthquakes along the Makran Subduction Zone and in the Kutch Graben region of India are infrequent but have the potential of generating destructive tsunamis – some with far reaching impact.

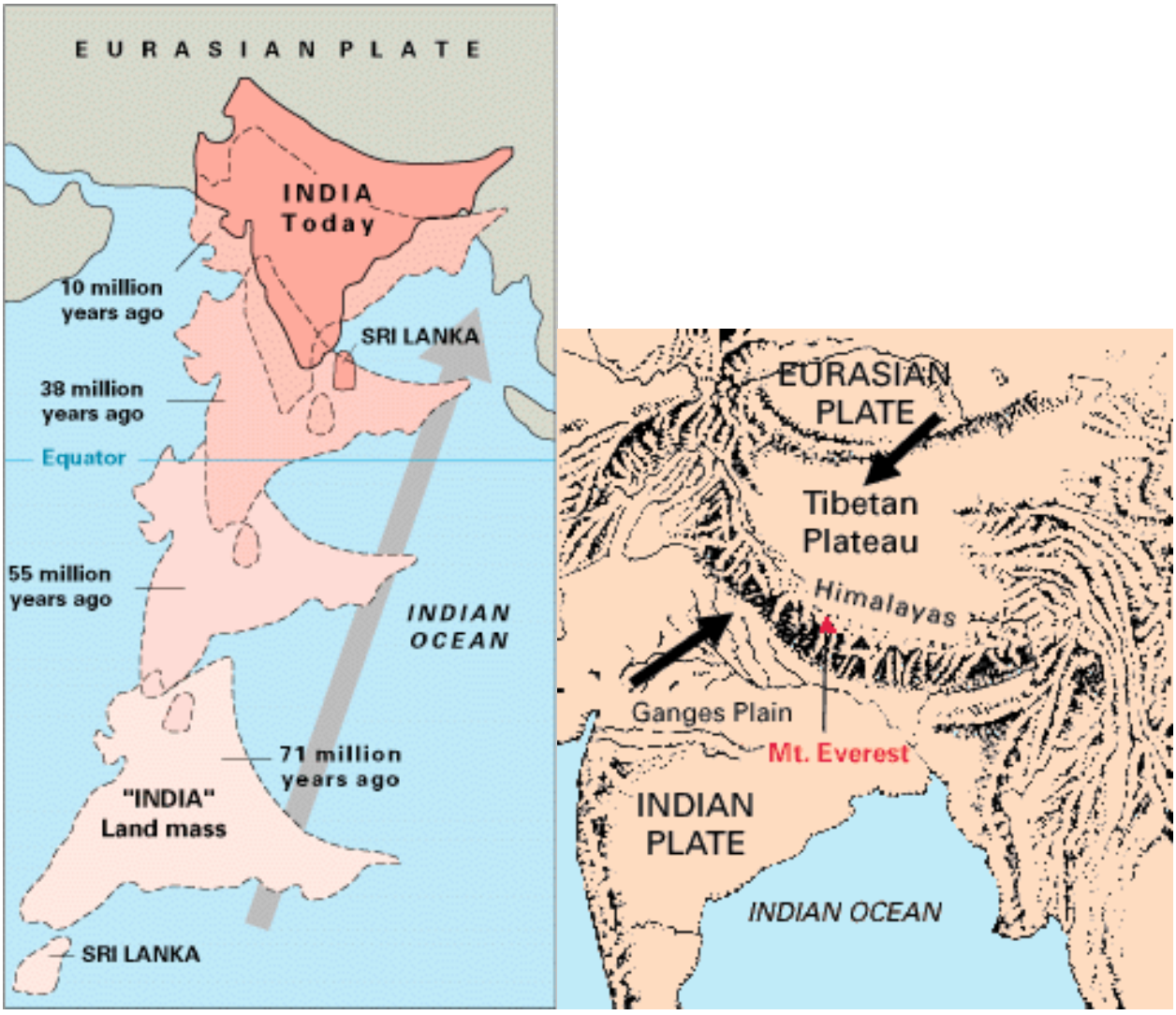

Fig. 3. The India tectonic plate has been drifting and moving in a north/northeast direction, for millions of years colliding with the Eurasian tectonic plate and forming the Himalayan Mountains. (USGS graphics)

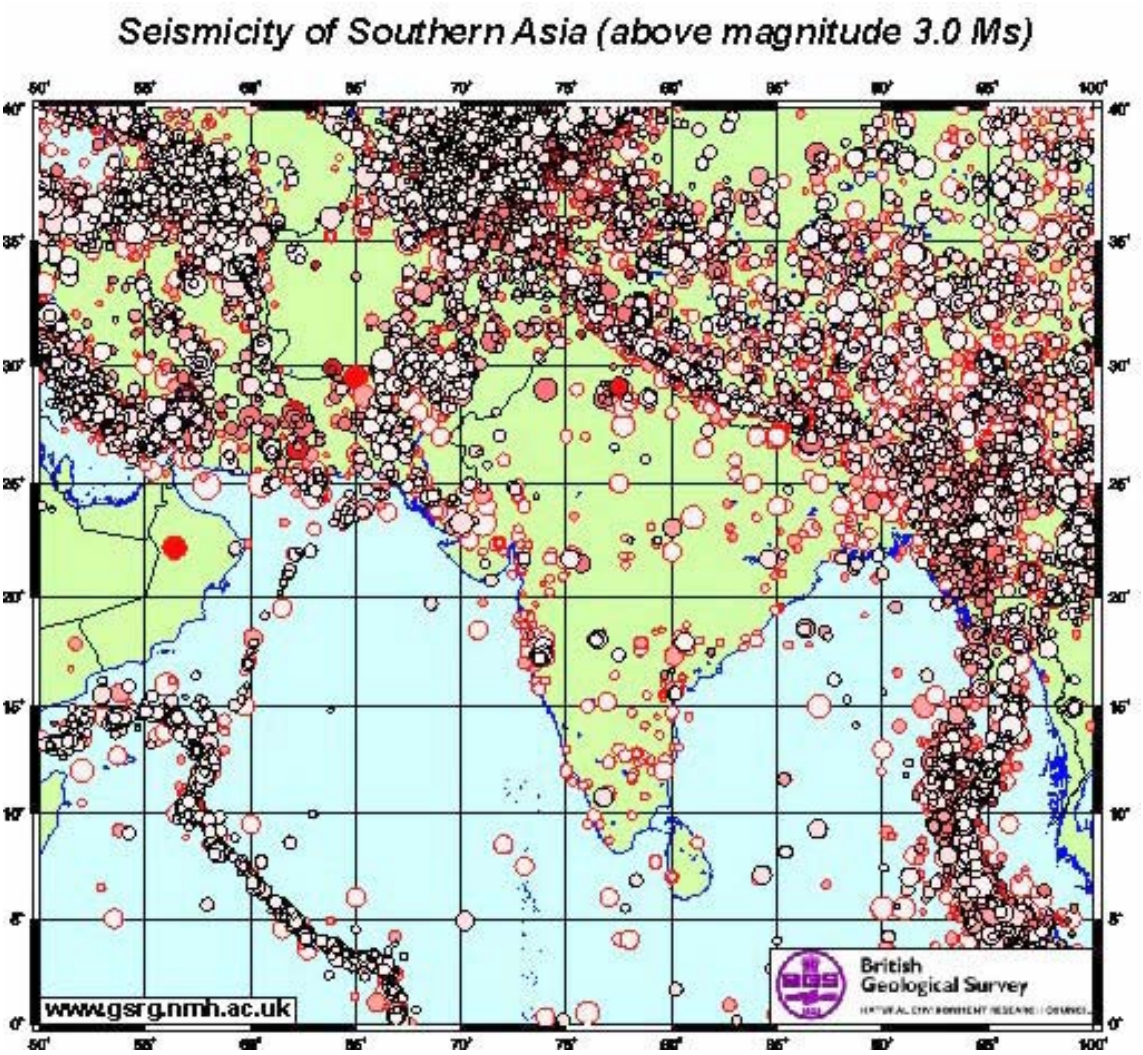

Fig. 4 British Geological Survey graphic of the seismicity of Southern Asia of the Carlsberg Midoceanic Ridge and of the southern portion of the Arabian Peninsula and the Red Sea.

MORPHOTECTONICS OF THE EURASIAN PLATE'S MAKRAN MARGIN

Active tectonic convergence of the India plate with the Arabian and Iranian microplates at a rate of about 30 to 50 mm/y (Platt et al. 1985) has created an extensive and complex tectonic plate margin in Southcentral Asia along the Makran coasts of Iran and Pakistan. The east-west oriented complex is one of the largest accretionary wedges on earth. It is more than 800 km long, bounded to the east and west by large transform faults which define the plate boundaries. The present front includes the Makran Subduction Zone (MSZ) and its associated topographic trench which, to a large extent, is buried by sediments. Also, the margin includes the Makran Accretionary Prism (MAP), the Makran

Coastal Range (MCR) and the Chegai Volcanic Arc. To the west of the Accretionary Prism, continental collision has formed the Zagros fold and thrust belt (Regard et al., 2003).

The Gulf of Oman and the Makran offshore region have been extensively surveyed over the years with swath mapping, high-resolution and single-channel reflection seismics, ocean-bottom seismology, micro-seismicity monitoring, magnetics, gravity and 2D seismic data collection (GEOMAR, Germany, the University of Cambridge and the National Institute of Oceanography, Pakistan, - Cruise (SONNE-123), 1997, 2000; Dorostian & Gheitanchi; Hutchinson et al 1981).

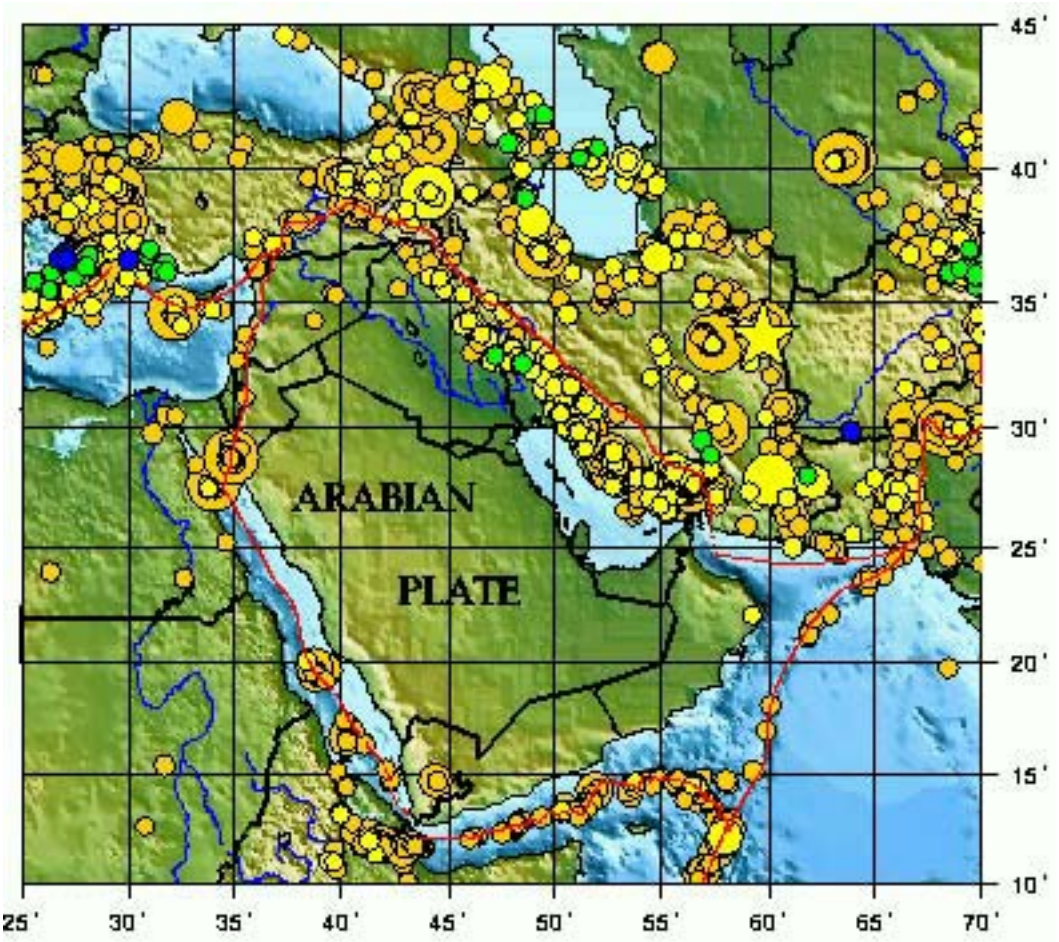

Fig. 5 Distribution of earthquake epicenters along the boundaries of the Pakistan, Afghanistan, Iran and Arabian microplates.

The Makran Subduction Zone (MSZ)

The Makran Subduction Zone (MSZ) in the Northern Arabian Sea has been formed by the northward movement of the Oman oceanic lithosphere and its under thrusting of the Iranian micro-plate at a very shallow angle of about 20 degrees. The east-west trending MSZ is more than 800-km-long. The trench associated with the present accretionary front does not have much of a morphological relief as other trenches around the world's oceans. A very thick sedimentary column enters the subduction zone (Closs et al., 1969, White and Louden, 1983). Extensive erosion of the Himalayan

mountain ranges and the numerous rivers which flow into the North Arabian Sea have buried the trench with sediments with thickness of up to 7 km. The deeper structure of the MSZ, the wedge sediments and the subducted oceanic crust has been surveyed recently by wide-angle and seismic reflection (Kopp et al., 2000). The effects of this extensive sedimentation on the seismotectonics of the region and the potential tsunami generation will be examined in a subsequent section.

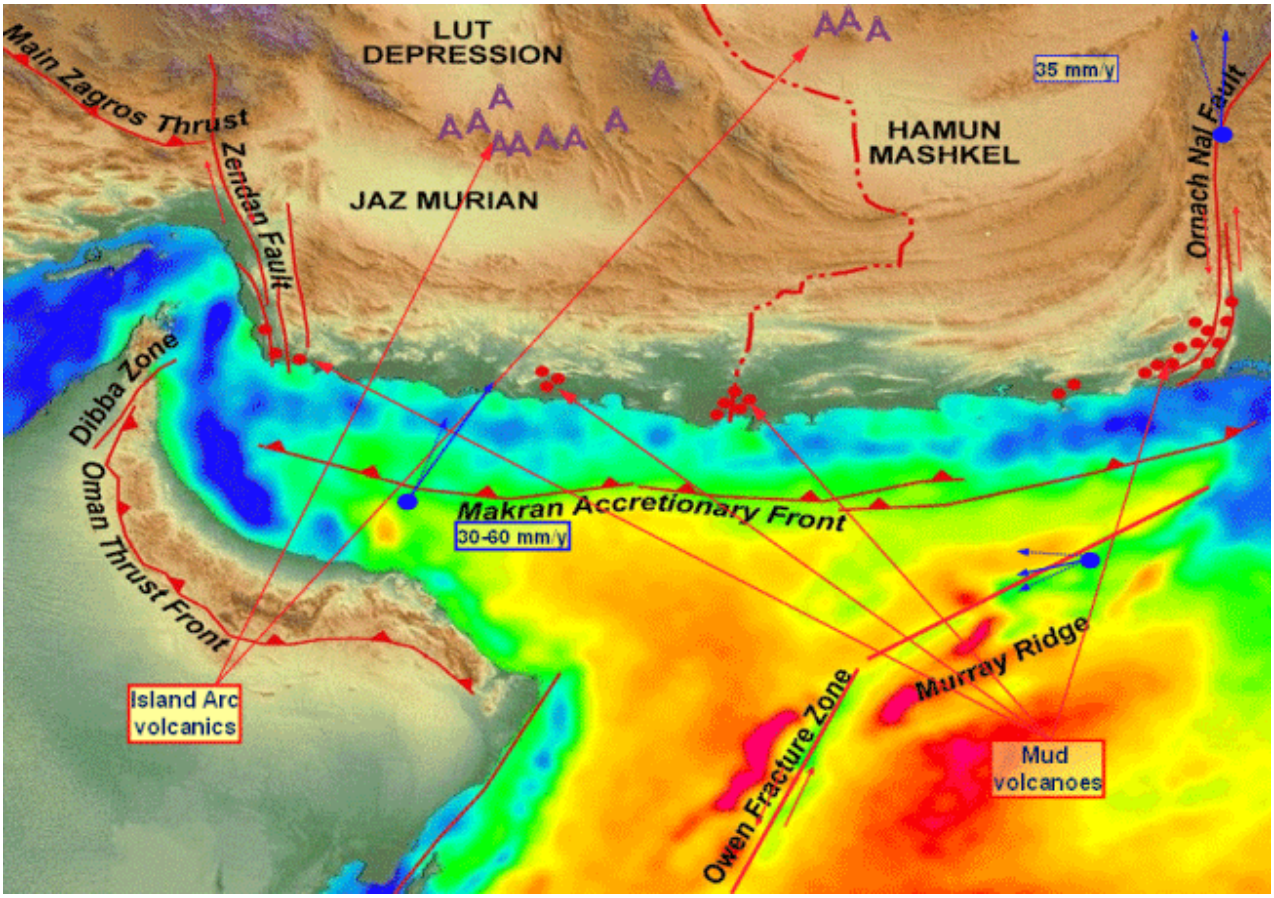

Fig. 6 The Makran Accretionary Prism and the Zone of Tectonic Subduction in the Northern Arabian Sea

The Makran Accretionary Prism (MAP)

The morphology of the coastal region is further complicated by the extreme sediment accretion from the erosion in the Himalayas (Closs et al., 1969, White and Louden, 1983; Platt et al., 1985; Minshull et al., 1992, Fruehn et al., 1997). The active tectonic convergence of the Oman oceanic lithosphere with the Iranian micro-plate has dragged thick tertiary marine sediments into a very extensive accretionary prism complex at the southern edge of the Asian continent (White and Louden, 1983; Platt et al., 1985). Studies of the morphotectonics of the MAP using swathmapping and 3.5 kHz Parasound echo sounding (Huhn et al., 1998) have provided a better assessment of the tectonic plate movements and interactions.

The MAP complex is more than 900 km long and it is highly fractured. It has the same east-west orientation as the MSZ and is bounded on both sides by large transform faults associated with tectonic plate boundaries. The MAP is the largest of its kind in the world, with up to 7 km of sediments deposited in the Gulf of Oman to the west, and major rivers contributing vast amount of sediment to the offshore region in the east.

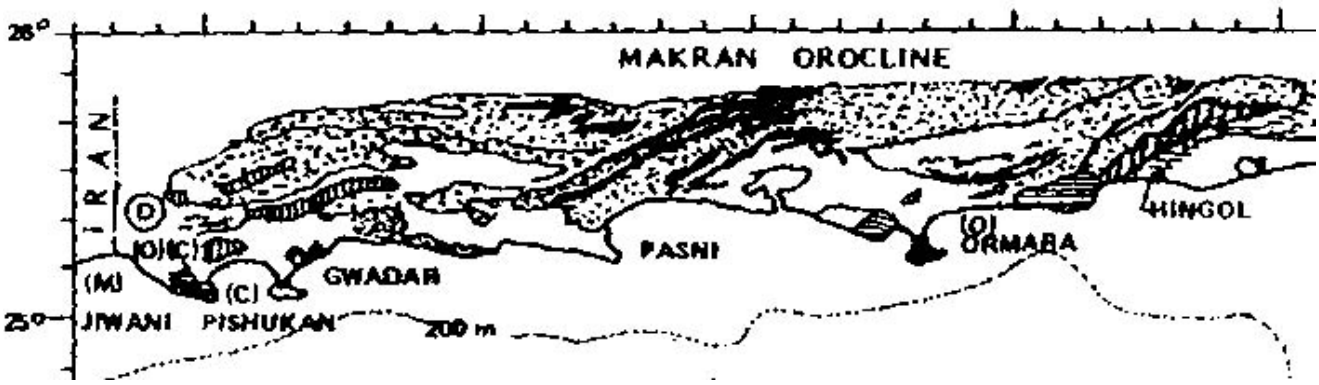

Fig. 7. Tectonic compression along the Makran Accretionary Prism has formed an extensive orocline, The Makran Coastal Range in southern Pakistan.

Along the Balochistan section of the Makran coast of Pakistan there is less sedimentation. Several small river deltas have been formed and the continental shelf of the Arabian Sea in this region measures only 15-40 km in width. However, in the eastern Sindh region, the Indus River has formed one of the largest deltas in the world. Past meandering of Indus have formed extensive deltas east of Karachi and have altered significantly ancient shorelines. In this region of the Northern Arabian Sea, extensive sedimentation has widened the continental shelf to about 150 km.

The Makran Coastal Range (MCR)

The same active tectonic convergence of the Oman oceanic lithosphere beneath the Iranian micro-plate has lifted the tertiary marine sediments into a very extensive coastal mountain range at the southern edge of the Asian continent (White and Louden, 1983; Platt et al., 1985). The Makran Coastal Range (MCR) is a narrow belt of highly folded and densely faulted mountain ridges which parallel the present shoreline and extend for about 75 percent of the total coast length for about 800 km (500 mi) in both the Balochistan and Sindh Provinces. The steep mountains rise to an elevation of up to 1,500 m (5,000 ft). The coast is rugged with uplifted terraces, cliffs and headlands.

The Chegai Volcanic Arc (CVA)

The same tectonic mechanism has resulted in the formation of the Chagai volcanic arc, which extends into Iran on the west and truncates against the Chaman transform fault on the east. The Koh-e- Sultan volcano and other volcanic cones in the Chagai area are side products of this active subduction (Bakht, 2000; Schoppel, 1977). . Koh-e-Sultan was a formidable volcano once, but it hadn't erupted in 800 years. However, at the present time there is no evidence of very active volcanism – as along

other tectonic convergence zones – and the Koh-e-Sultan volcano appears to be in a dormant stage. Even if volcanoes on the Chegai arc become active again, they are too far removed from the coast to pose any threat for tsunami generation.

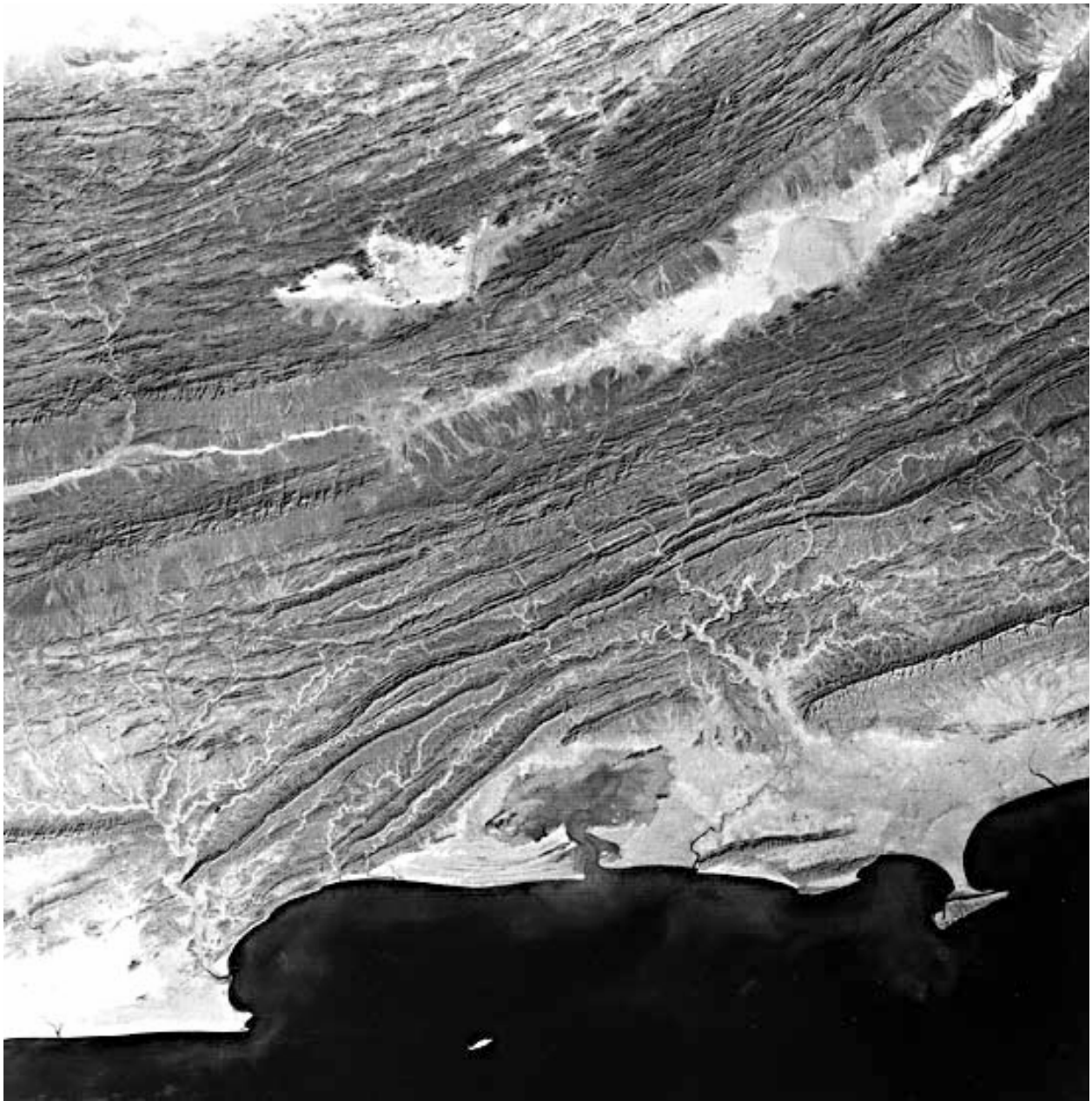

Fig. 8 **NASA** Satellite photo of a section of the Makran rugged and tectonic coastline showing uplifted terraces, headlands, sandy beaches, mud flats, rocky cliffs, bays and deltas. Numerous mud volcanoes are present along the shores.

The Kutch, Bombay, Cambay and Namacia Grabens

East of the Makran Accretionary Prism and the zone of tectonic subduction, lateral transition between subduction and collision of the India and Arabia tectonic plates at about 42mm/yr has formed the Kutch, Bombay, Cambay and Namacia Grabens, in northwestern India (Wadia, 1981). Although these grabens are not directly related to the Makran seismotectonics, they are included in this report because they are potential tsunami sources in the Northern Arabian Sea. These grabens are bounded by thrust and subsidence faults that are close to coastal regions, where significant earthquakes occurred in the past and will occur again in the future. The Kutch graben region has produced several large earthquakes - the latest in 2001 (Pararas-Carayannis, 2001).

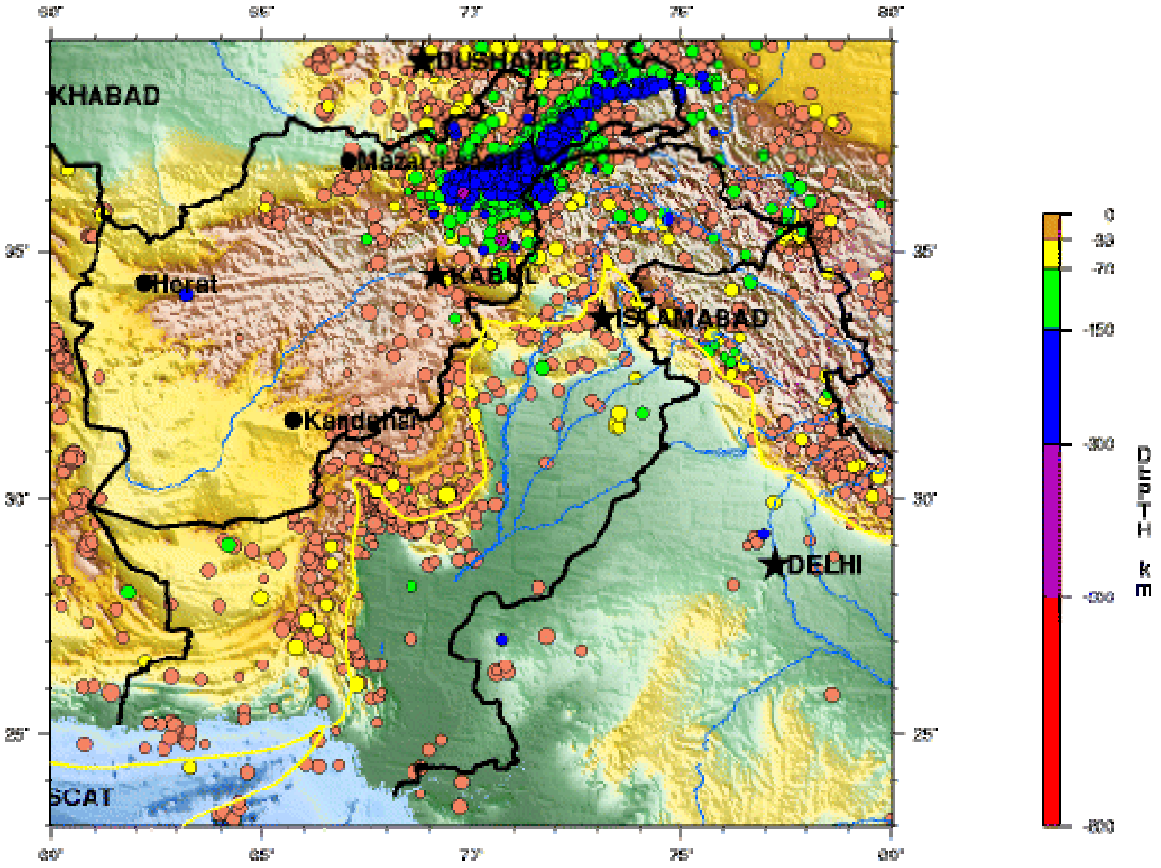

Fig. 9. Seismicity of Pakistan, 1990-2000 (Pakistan Seismological Agency)

SEISMO-DYNAMICS OF COMPRESSIONAL COLLISION AND SUBDUCTION AT EURASIA'S SOUTH TECTONIC MARGIN ALONG THE MAKRAN COASTS OF PAKISTAN AND IRAN

The seismo-dynamics of the Southcentral Eurasian plate's margin along the Makran coast are complex because of compressional collision of major and minor tectonic plates. The entire region is traversed by thrust and transform faults, formed by great tectonic stresses. Major and great earthquakes occur with frequency. The following review of major faults can help identify potential tsunamigenic sources in the region.

Major Faults and Potential Tsunamigenic Source Regions

Most of Pakistan's major faults are on land and most earthquakes occur in the north, the northwestern and the western sections of the country, along the boundary of the Indian tectonic plate with the Iranian and Afghan micro-plates (Quittmeyer and Jacob, 1979; Jadoon, 1992). Major inland thrust zones exist along the Kirthar, Sulaiman and Salt mountain ranges. The devastating October 8, 2005 Earthquake occurred in the Hazara-Kashmir syntaxial bend – the region of maximum collision in the north (Pararas-Carayannis, 2005).

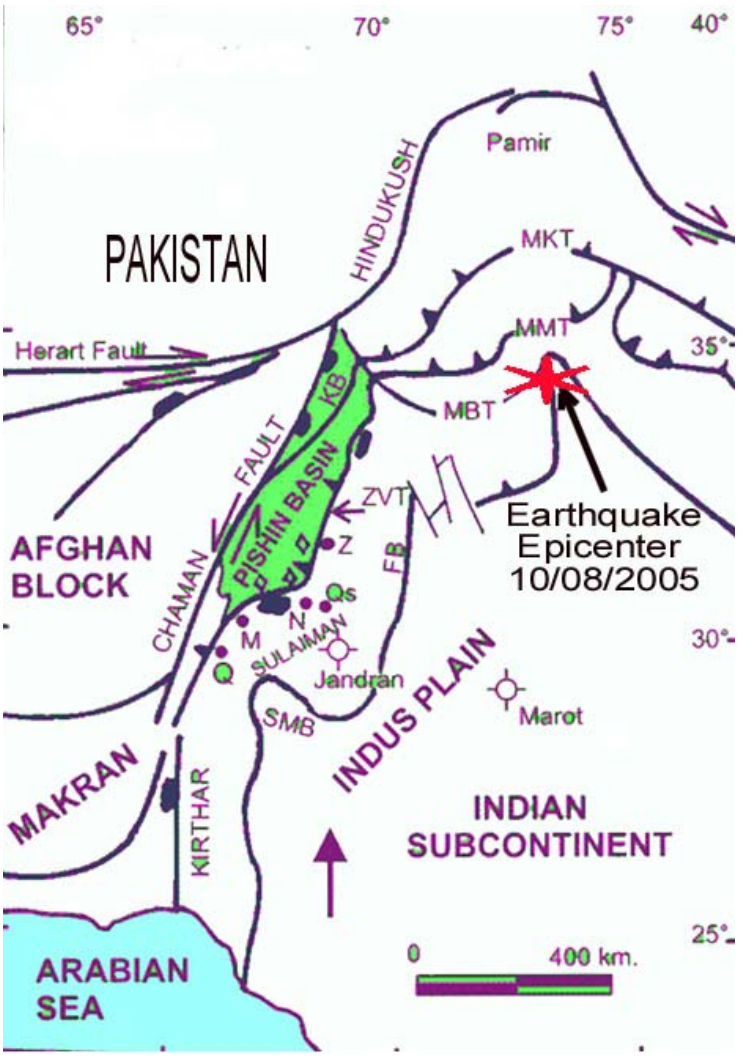

Fig. 10 Major faults in Pakistan

Fewer earthquakes occur along faults near the Makran Continental Margin. However, some of these earthquakes can be major or great in magnitude and some have the potential of generating tsunamis - either by the nature of their tectonic crustal movements or by the triggering of underwater landslides.

Segmentation of the Makran Subduction Zone

Deformation along the entire length of the MSZ appears to be uniform - which indicates that the rate of subduction does not change appreciably from east to west. However there is a large change in seismicity, degree of deformation, as well as significant variations in rupture histories between the eastern and western MSZ (Minshull et al., 1992; Dorostian & Gheitanchi). Each region exhibits a different seismicity pattern. Also, recent geological studies indicate that two Paleozoic continental blocks dominate the overriding tectonic plate. The boundary between these two blocks is approximately coincident with the transition and the differences in seismicity between the eastern and western MSZ.

Also, recent surveys of the Makra accretionary wedge using swathmapping and 3.5 kHz Parasound echo sounding (Huhn et al., 1998), indicate that a sinistral, strike-slip fault crosses the wedge obliquely and continues to the abyssal plain. The significance of these findings is that this fault separates the MSZ, into two different segments - the western which has very low seismicity, from the eastern where the seismicity is significantly higher. Also, this unique morphotectonic feature has led to the postulation that the north-easternmost part of the Arabian plate, is actually a separate micro plate that moves independently. Two recent shallow earthquakes in this central region exhibited right-lateral strike-slip motion, (Dorostian & Gheitanchi, Iran & Institute of Geophysics, Tehran Univ.) which also supports that there are two major segments to the MSZ - each behaving differently, but still capable of generating large tsunamigenic earthquakes. Therefore, the apparent variation in seismicity between the eastern and western segments of the MSZ may be due to differences in slip mechanisms of two different tectonic microplates.

Eastern Segment: The length of the eastern MSZ segment is estimated at about 350-400 km. Most of the 14 known earthquakes have occurred along this segment. Of these, only the great (Mw 8.1) earthquake of 1945 was instrumentally recorded (Byrne et al. 1992).

Also, there appears to be a pattern in seismic activity prior to major earthquakes on the eastern segment. Large earthquakes are preceded by increased activity of smaller events. For example, for ten years prior to the 1945 Makran earthquake, there was a concentration of seismic activity in the vicinity of its epicenter.

Western Segment: The western segment of the MSZ has not generated any known tsunamigenic earthquakes. However, recent seismic activity indicates that a large earthquake is possible in the region west of the 1945 event. Such an earthquake could generate a destructive tsunami.

Since the western segment is an extension of the eastern rupture of an active subduction zone in a region where major earthquakes have occurred recently in Iran, Afganistan and Pakistan, its relative seismic quietness over a long period is somewhat puzzling and posing several questions. Why has this region remained aseismic? Is the western segment locked and building stress for a great event in the future? Is it possible that the western segment is significantly different from the eastern and experiences largely aseismic slip at all times? Can an earthquake as great as the 1945 occur along the western segment? Is this segment of the MSZ a potential source of destructive tsunamis in the North Arabian Sea and the Indian Ocean? A review of the geophysical and geological processes and the findings of recent surveys on both segments of the MSZ can help answer some of these questions and help evaluate the potential for tsunami generation along the western region.

Comparison of the Eastern and Western Segments: The seismodynamics of the western segment of the MSZ are complex. The presence of late Holocene marine terraces along sections of the coasts of both eastern and western Makran could be construed as proof that both segments of the arc are able to produce large plate boundary earthquakes.
The absence of earthquakes along the plate boundary on the western segment indicates that either entirely aseismic subduction occurs or that the megathrust plate boundary is currently locked.

Aseismic deformation has been inferred elsewhere along the north-south convergence between the plates of Arabia to the south and Eurasia to the north. For example, earthquake and geodetic data indicate greater aseismic deformation in the Zagros region in Southern Iran than that in the Alborz-Kopet-Dag regions of northern Iran, where deformation results primarily from earthquake activity (Masson et al., 2005). The implication from these findings is that aseismic subduction and deformation must also occur south of the Zagros fault along the western subduction boundary of the MSZ, in the Gulf of Oman. This could account for the lack or seismic activity on the western segment of the MSZ. Of course, this does not mean complete absence of earthquakes along thrust faults on the western segment of the MSZ and of the MAZ – only that aseismic deformation occurs most of the time. Occasional major earthquakes can be expected and these have the potential to generate tsunamis that could be particularly destructive in the Gulf of Oman.

EFFECTS OF SEDIMENTATION ON SUBDUCTION PROCESSES AND THE GENERATION OF TSUNAMIGENIC EARTHQUAKES.

A better understanding of the complex processes of sediment transport and the effect of sedimentation on shear stresses and interactions along tectonic boundaries of subduction zones, can lead to improved evaluation of seismic and tsunami risks. Also, continental slope instability due to extensive sedimentation from major rivers in the region adds to the tsunamigenic potential from underwater landslides.

Aside from tectonic stresses, sedimentation may be partly responsible for the observed differences in seismicity between the eastern and western segments of the MSZ. Therefore a comparison of the sedimentary structure of the eastern and western MSZ helps shed some light on how subduction processes may be affected and the potential for the generation of tsunamigenic earthquakes.

Effects of Sedimentation on Aseismic Subduction

As with other subduction zones, the aseismic region on the entire MSZ lies within that part of the accretionary wedge that consists of largely unconsolidated sediments with seismic velocities less than 4.0 km/s. This region in the overlying accretionary wedge remains aseismic during and between great earthquakes. Thus, the extensive forearc and accretionary wedge seem to have significant effects on the type of boundary slips that can be expected along the MSZ - and thus on the frequency and intensity of potential tsunamigenic earthquakes in the Northern Arabian Sea region.

Fig. 11 Major rivers in Southern Pakistan contribute enormous amounts of sediments and turbidite deposits

Fine turbidite deposits in the offshore region may affect the mechanics of subduction processes near the deformation boundary of the tectonic plates. As mentioned previously, the subducted oceanic crustal structure of the MSZ has been partially studied with seismic velocity models from four wide-angle seismic lines that image the wedge sediments and with collection of seismic reflection data (Kopp et al. 2000). The data indicates that fine turbidite sediments bypass the accretionary ridges and are transported to greater depths offshore and may be responsible for the sparse earthquake activity associated with subduction in different segments of the subduction zone. Such turbidite bypass occurs primarily in the western region. Essentially, these findings suggest that fine sediments are available to lubricate the western segment plate boundary sufficiently to allow slow slippage most of the time. Such mechanism could account for the suspected aseismic slip of the tectonic plates along the western segment.

However, if the plate boundary is locked or partially locked, this would suggest that great earthquakes with long repeat times might be possible also along the western segment. Based on the present studies and surveys, it appears that both seismic and aseismic slips occur along subsegments of the western plate boundary and that a portion of the western segment may be locked.

However, the size of the earthquakes in the western segment - and thus the potential for tsunami generation – may be limited by other factors. Because of additional fracturing and segmentation of the western segment, earthquakes would be expected to have shorter ruptures and deeper focal depths.

Effects of Sedimentation on Earthquake Rupture Velocity and Tsunami Generation.

If the above-stated hypothesis of lubrication by sediments is correct, then the following explanation can be provided for the seismicity differences between the eastern and western segments of the MSZ and their potential for producing tsunamigenic earthquakes. In the eastern segment of MSZ, thrust earthquakes occur along the plate boundary where the sediments appear to be more consolidated, dewatered or lithified and thus, more likely to stick or lock before the stress is released by an earthquake. The earthquakes appear to be shallower in focal depth. Also, the consolidated sediments along the plate boundary would have a tendency to slow the rupture velocity of an earthquake. Additional, "en echelon", bookshelf type of sediment failure along an earthquake's rupture zone - would account for slower rupture velocity and for greater tsunamigenic efficiency. Such appears to have been the case in the Andaman Sea segment of the rupture of the December 26, 2004 earthquake along the Great Sunda Trench. The rupture velocity was much less in the Andaman Sea segment than in the Sumatra segment - which was not as heavily sedimented.

Also, such slower rupture occurred along the Mid-America Trench when the September 2, 1992 Nicaragua tsunamigenic earthquake struck. It is believed that block motions of consolidated sediments were associated with bookshelf faulting which contributed to the slow, silent and deadly tsunami-earthquake. The block motions were extremely shallow and occurred within subducted sediments where there was a lot of shear - thus the rupture was slower in speed (Pararas-Carayannis, 1992). The same slower rupture occurred in the Andaman Sea segment of the Great Sunda Subduction Zone in December 2004. In both of these cases, the degree of sediment consolidation along the plate boundary appears to have been a key factor in locking slippage on the megathrust region of the tectonic boundary, then releasing greater energy when the stress thresholds were exceeded.

The eastern segment of the MSZ appears to behave in a similar way. There is more sedimentation closer to the Indus and other major rivers in the east. The sediments are much thicker. The earthquake rupture velocities would be expected to be slower and the tsunamigenic efficiency would be expected to be greater because of potential bookshelf type of fault failures along the Makran coastal area.

Furthermore, the existence of thrust earthquakes along the MSZ indicates that either the sediments along the plate boundary in the eastern segment become sufficiently well consolidated and dewatered at about 70 km from the deformation front, or that older, lithified rocks are also present within the forearc so that stick-slip sliding behavior along the subduction boundary becomes possible when the stress exceeds a critical level. Thus, a repeat of a great tsunamigenic earthquake like the 1945 event is very possible. Earthquake ruptures may be as long as 300 km long and moment magnitudes could be as much as 8.

In contrast to the eastern segment, the plate boundary along the western segment of MSZ has not produced great earthquakes and there have been no recordings of shallow events. Most of the earthquakes along the western segment occur on the down going plate at intermediate, rather than shallow depths. This would suggest that dewatering and lithification of sediments occur at greater depth along the decollment surface of the plate boundary and, because of the greater focal depth, such earthquakes would not be as efficient tsunami generators as those along the eastern segment. Also,

there appears to be much more fracturing along the western segment, which would suggest that future earthquakes may have shorter ruptures and lesser magnitudes.

In spite of these observations, a large quantity of unconsolidated sediments does not necessarily mean a lower potential for great thrust earthquakes along a subduction boundary. It is rather the overall structural distribution of consolidated and unconsolidated sediments along the boundary that become the key factors.

At the present time there is not sufficient data to evaluate better the effect of sediments on subduction dynamics in this region. The western segment of the MSZ could produce a great earthquake but more likely it could rupture as a number of segments in somewhat smaller-magnitude events. On the basis of the above evaluation, it can be concluded that the western segment of the MSZ is a potential source region of infrequent major earthquakes and potentially destructive local tsunamis. However, because of the shorter crustal ruptures, earthquakes on the western segment would not be as great as the 1945 event on the eastern segment. Maximum expected ruptures would be less than 100 km long and earhquake magnitudes would be up to 7.

REGIONAL EVALUATION OF THE POTENTIAL FOR TSUNAMI GENERATION IN THE NORTHERN ARABIAN SEA

Based on the above discussion of earthquake data, geology morphotectonics and subduction processes, the following is a regional assessment of the tsunami generation potential in the Northern Arabian Sea, and the possible tsunami near and far- field effects elsewhere in the Indian Ocean. In addition to the source seismodynamics, a factor that could also contribute to the destructiveness of a tsunami generated in the Northern Arabian Sea would be the relatively large astronomical tide, which is about 3-3.5m (10-11 feet) along the Makran coastline. A tsunami arriving during high tide at a coast in the northern Arabian Sea could be expected to be significantly more destructive because of this high tidal range.

Potential for Tsunami Generation along the Makran Subduction Zone (MSZ)

Although the Makran Subduction Zone in the Northern Arabian Sea is an active seismic zone, large tsunamigenic earthquakes have been relatively rare. It is quite possible that tsunamis in this region have not properly reported or documented. A thorough analysis of historical records may reveal that many tsunamis occurred in the past. Such tsunamis could have affected Southern Pakistan, India, Iran, Oman, the Maldives and other countries bordering the Indian Ocean.

Overall, the seismicity of the Makran region is relatively low compared to the neighboring regions, which have been devastated regularly by large earthquakes (Jacob and Quittmeyer, 1979). Although infrequent, major and great earthquakes have occurred along the MSZ throughout geologic history and in recent times. Several tsunamis must have been generated in the past along this active zone but have not been adequately documented. As already mentioned a large magnitude earthquake generated the oldest known tsunami in the region in 325 B.C. and not in 326 B.C. as reported in the literature (Pararas-Carayannis, 2006a). It is believed that the tsunami destroyed part of Alexander the Great's fleet while on its journey back to Mesopotamia after the India campaign (Lietzin 1974, Murty and Bapat, 1999, Pararas-Carayannis, 2006a).

Large tsunamigenic earthquakes can be expected mainly on the eastern portion of the subduction zone. As previously described, the great earthquake (Mw 8.1) of November 28, 1945 on the MSZ generated a very destructive tsunami in the North Arabian Sea. According to the literature, the earthquake was a thrust event that ruptured approximately one-fifth of the entire length of the MSZ, which would be approximately 200 – 250 km. (Byrne et al. 1992). What was reported may be an underestimate. Although no centroid solution could be obtained for this event, the revised moment magnitude of Mw 8.1 would suggest a longer rupture - in the order of 300-350 Km (Pararas-Carayannis, 2006b). Nine other smaller earthquakes are known to have occurred in the eastern Makran with similar thrust mechanisms. The 1945 event's magnitude of 8.1 appears to be the upper limit of tsunamigenic earthquakes this region can produce along the plate boundary. The limiting factors appear to be an apparent segmentation of the MSZ and the large volumes and spatial distribution of both consolidated and unconsolidated sediments. The significance of the sediments to the subduction dynamics was discussed previously. In brief, tsunamis generated along the eastern segment of the MSZ can be expected to be destructive in Pakistan and other countries bordering the Northern Arabian Sea and the Indian Ocean.

Along the western segment, the dynamics of subduction are different. Although aseismic subduction may be occurring, there are subsections which may be locked and have the potential to generate earthquakes with magnitudes up to 7 and local tsunamis along the Makran coast of Iran and Pakistan as well as along the north coast of Oman.

Potential for Tsunami Generation along the Makran Accretionary Prism (MAP) from Gas Hydrate Collapses

The MAP region exhibits high internal deformation, layering and compaction of sediments (Fruehn et al., 1997). As reported previously, the 1945 Makran earthquake caused the eruption of a mud volcano a few miles off the Makran Coast. It was reported that a large volume of gas was emitted which caught fire and sent flames "hundreds of meters" into the sky. The observed flames probably resulted from emitted natural gas, which caught fire after the earthquake. This event and geologic studies of the MAP stratigraphy (Harms et al., 1984) indicate that the region has high petroleum deposits, including gases such as methane, ethane and traces of other hydrocarbons. The ocean floor of the continental margin along the MAP is thick with sediments in an oil producing area of the world. The unique geology, morphology of the sea floor and the thick sedimentary layers on the MAP region indicate that thick methane gas hydrate layers must exist in this region. Therefore, the explosion of gas hydrate deposits has the potential to generate tsunamis or to trigger submarine landslides that could generate tsunamis in the region.

Potential for Tsunami Generation along the Makran Coastal Range (MCR)

The Owen Fault Zone is a transform fault in the Arabian Sea that is associated with the active tectonic boundary of the India and Arabia plates. It extends from the Gulf of Aden in a northeast direction towards the Makran coast where it enters the coast in the Balochistan region. Then it continues as a land fault known as the Chaman Fault – an extensive system that extends in a north-northeast direction along Pakistan's western frontier with Afghanistan. The Chaman fault begins near Kalat, in the northern Makran Range, passes near the city of Quetta and continues to Kabul, Afghanistan. The Balochistan province in and around Quetta is the region of highest seismicity. On

May 30, 1935, a great earthquake (Mw 8.1) along this fault destroyed the city of Quetta and killed about 30,000 people (Ramanathan and Mukherji, 1938). Up to the October 8, 2005 earthquake this had been the deadliest in Pakistan. Large earthquakes along the Owen Fault Zone or the Chaman closer to the Makran coastal range are infrequent, but have the potential of generating major earthquakes and tsunamis.

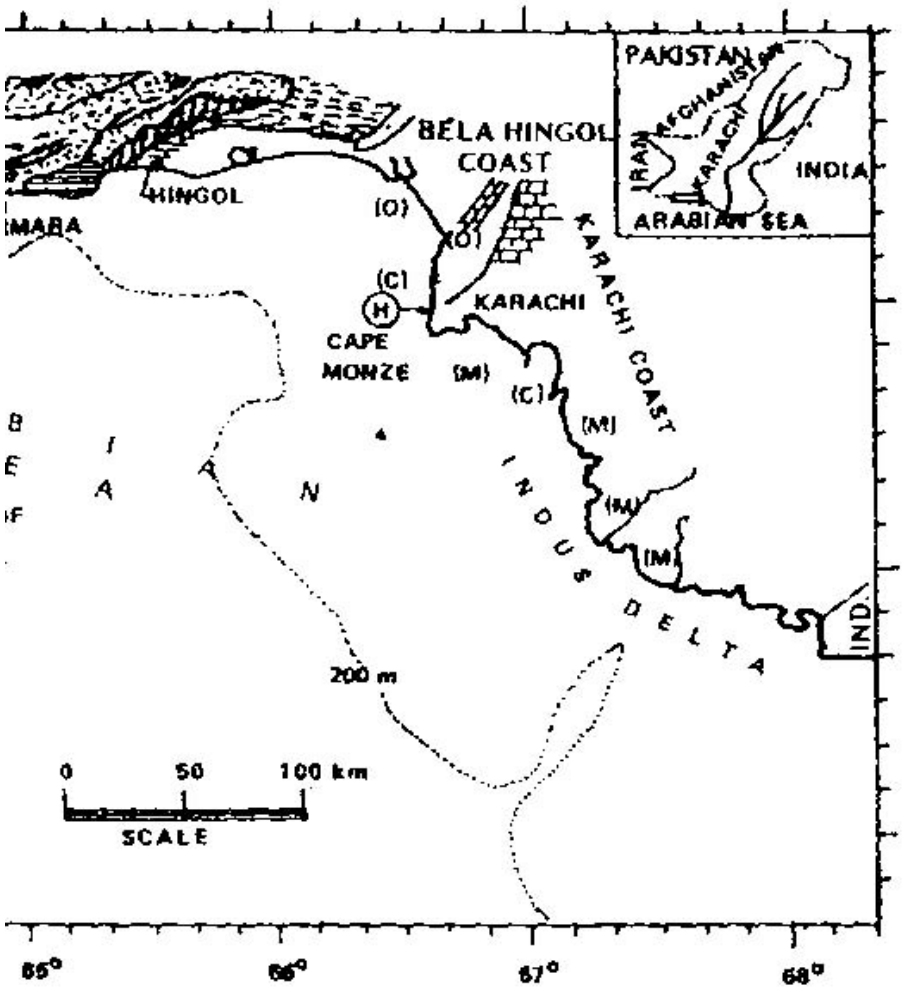

Fig. 12 The Karachi and Deltaic Indus Region

Potential for Tsunami Generation along the Karachi and the Deltaic Indus Region

Around Karachi and other parts of deltaic Indus, there are several thrust faults which have the potential of generating major earthquakes and local tsunamis. Unfortunately, most tsunamis in this region have not been adequately documented.

A major thrust fault which runs along the southern coast of the Makran coast and parts of deltaic Indus is believed to be of the same character as the West Coast fault along the coast of Maharashtra, India. The Allah Bund is a major fault that traverses Shahbundar, Jah, Pakistan Steel Mills, and

continues to the eastern parts of Karachi - ending near Cape Monz. This fault has produced many large earthquakes in the past in the deltaic areas along the coast, causing considerable destruction. For example, a major earthquake on this fault destroyed Bhanbhor in the 13th century. Another major earthquake in 1896 was responsible for extensive damage in Shahbundar. There is no record of whether any tsunamis were generated near the coastal regions. However, because of the proximity of this fault to sections of deltaic areas, it is possible that past earthquakes have generated landslides and local tsunamis.

Another major fault near Karachi is an extension of the one that begins near Rann of the Kutch region of India. Still another one is the Pubb fault which ends into the Arabian Sea near the Makran coast. Finally, a major fault in the lower Dadu district, near Surajani, is also in the vicinity of Karachi.

In brief, destructive local tsunamis can be generated near Karachi and the deltaic Indus area because of the proximity of thrust faults to coastal areas, the nature of crustal movements of major earthquakes, and the unstable, heavily-sedimented, coastal slopes of this deltaic region.

Potential for Tsunami Generation along the Kutch, Bombay, Cambay and Namacia Graben Regions of India

Lateral transition between subduction and collision of the India and Arabia tectonic plates has formed the Kutch, Bombay, Cambay and Namacia Grabens, in northwestern India (Wadia, 1981). In the Kutch region, remote sensing and gravity investigations have determined a spatial pattern of tectonic lineaments along which 7 big earthquakes (M>6) occurred in the last 200 years (Srivastava and Ghosh, Indian Scool of Mines). Although infrequent, several destructive earthquakes in the coastal Sindh region occurred in 1524, 1668, 1819, 1901, 1956, and as recently as 25 January 2001 (Pararas-Carayannis, 2001).

The larger earthquakes involved extensive vertical crustal uplift over land areas paralleling the orientation of the Kutch Graben. For example, the 1819 earthquake in Rann of the Kutch, bordering the Sindh region, was associated with thrust uplift of up to 30 feet along the Allah Bund fault and slippage depression of up to 10 feet along coastal fault plains. Although poorly documented as having generated a tsunami, the 1819 event was reported as having resulted in major sea inundation, destruction of coastal settlements, and permanent changes to the coastline and the drainage of major rivers, such as Indus. Probably the 1524 earthquake in the same region also resulted in major inundation by the sea.

In conclusion, earthquakes associated with thrust and subsidence faulting in the coastal region of the Kutch Graben and along the major fault, which runs along the west coast of Maharashtra, India, have the potential of generating local tsunamis. Also, earthquake events on the Kutch Graben have the potential of triggering undersea landslides and local tsunamis in the offshore region. The tsunami hazard for this northwest region of India has been underestimated and needs to be properly evaluated.

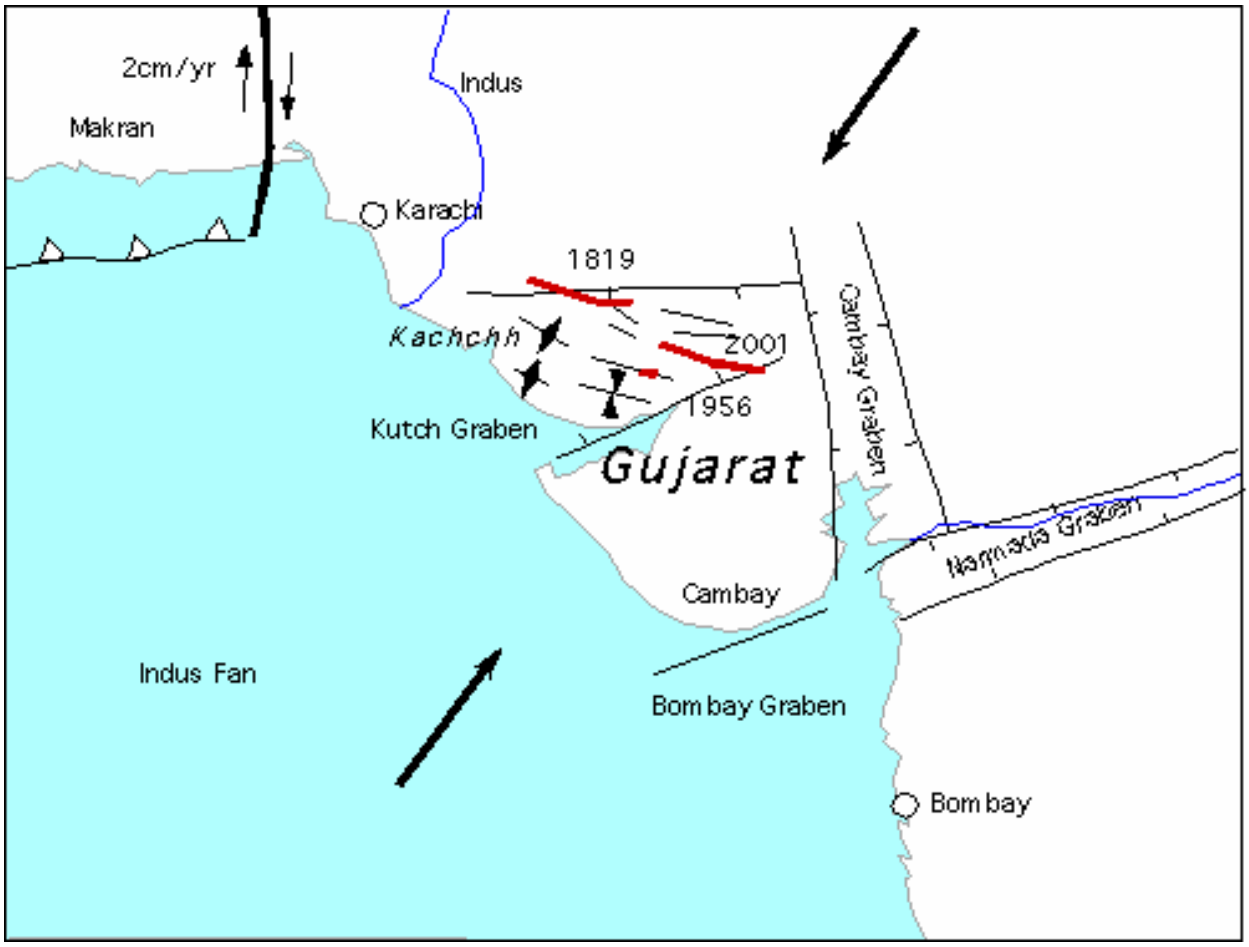

Fig. 13 The Kutch, Bombay, Cambay and Namacia Graben Regions of India

SUMMARY AND CONCLUSIONS

Active tectonic convergence of the India plate with the Arabian and Iranian microplates has created an extensive and complex tectonic plate margin in Southcentral Asia along the Makran coasts of Iran and Pakistan. The east-west oriented tectonic plate margin complex includes one of the largest accretionary wedges on earth. It is more than 900 km long, bounded to the east and west by large transform faults which define the plate boundaries. The present margin includes the Makran Subduction Zone (MSZ) and its associated topographic trench, the Makran Accretionary Prism (MAP), the Makran Coastal Range (MCR) and the Chegai Volcanic Arc. To the west of the MAP, continental collision has formed the Zagros fold and thrust belt. To the east, lateral transition between subduction and collision of the India and Arabia tectonic plates has formed the Kutch, Bombay, Cambay and Namacia Grabens, of northwestern India. Tsunamis generated in these regions of the Northern Arabian Sea can have a significant near and far field impacts.

The MSZ is a relatively active and can produce destructive tsunamigenic earthquakes. Its seismic history indicates significant variations in rupture histories primarily in two segments. Large

earthquakes occur mainly on the eastern segment. The earthquake of November 28, 1945 had a moment magnitude Mw 8.1 and a rupture estimated at about 300-350 km long. It generated a destructive tsunami. Waves of up to 13 m (40 feet struck Pakistan and waves as high as 11.5 m struck the Kutch region of India. Waves of 2 m struck as far south as Mumbai. Also Iran and Oman were struck. The magnitude of 8.1 of the 1945 event is the upper limit of earthquakes this region can produce along this plate boundary. The limiting factors are the apparent segmentation of the MSZ and the large volumes and spatial distribution of both consolidated and unconsolidated sediments. The degree of sediment consolidation along the plate boundary appears to be a key factor in locking slippage on the megatrhrust region, then releasing greater energy when the stress thresholds are exceeded.

The sediments are thicker and the continental shelf wider along the eastern segment of the MSZ because of the proximity to the Indus and other major rivers. The existence of thrust earthquakes indicates that either the sediments along the plate boundary in the eastern segment become sufficiently well consolidated and dewatered at about 70 km from the deformation front, or that older, lithified rocks are present within the forearc so that stick-slip sliding behavior becomes possible when the stress exceeds a critical level. Thus, great tsunamigenic earthquakes with magnitudes up to Mw 8 and ruptures of 300-350 km can be expected to occur in the future.

In contrast, the plate boundary along the western segment of the MSZ has not produced great earthquakes and there have been no recordings of shallow events. The present absence of earthquakes indicates either entirely aseismic subduction or those subsegments of the megathrust plate boundary are currently locked. It is more likely that both seismic and aseismic slippage is occurring. The extensive forearc and accretionary wedge seem to have a significant effect on the type of boundary slips that can be expected along or near the western segment - and thus on the frequency and intensity of potential tsunamigenic earthquakes in this region. Surveys of the area indicate that the mechanics of subduction processes near the deformation boundary on the western segment may be affected by the introduction of fine turbidite deposits which, perhaps, lubricate the decollment surface of the subduction boundary. Such deposition and lubrication could account for the aseismic slip and the sparse earthquake activity along sections of the western segment of the MSZ.

Also, most of the earthquakes on this segment occur on the downgoing plate at intermediate, rather than shallow focal depths. This would suggest that dewatering and lithification of the sediments occur at greater depth along the decollment surface. Because of the greater focal depth, such earthquakes would not be as efficient tsunami generators as those along the eastern segment that have shallower focal depths The size of earthquakes - and thus their potential for tsunami generation – may be limited by other factors. There appears to be much more fracturing along the western segment of the MSZ. Earthquakes would be expected to be smaller-magnitude events (less than 7) and to have shorter ruptures (less than 100 km) along subsegments. In spite of these observations, a large quantity of unconsolidated sediments does not necessarily mean a lower potential for great thrust tsunamigenic earthquakes along a subduction boundary. It is rather the overall structural distribution of consolidated and unconsolidated sediments along the boundary that become the key factors. At the present time there is not sufficient data or surveys to fully evaluate the effect of sediments on the subduction dynamics of this region. On the basis of the above evaluation, it can be concluded that the western segment of the MSZ is a potential source region of infrequent major earthquakes and of potentially destructive local tsunamis.

The MAP region is another potential source of local tsunamis. Its unique geology, morphology of the sea floor, thick sedimentary layers and its proximity to vast sources of oil and natural gas deposits

indicate the presence of thick methane gas hydrate layers. Explosion of gas hydrate deposits has the potential to trigger submarine landslides that could generate local tsunamis.

Another potential source for tsunamis in the North Arabian Sea is near Karachi and the deltaic Indus. Local tsunamis would be generated because of the proximity of thrust faults to coastal areas, the nature of crustal movements of major earthquakes, and the unstable, heavily-sedimented, coastal slopes of this deltaic region.

Finally, the Kutch Graben region of India has produced several large earthquakes in the past and there is a record of extensive "sea flooding" associated with the 1819 earthquake. Thus, earthquakes associated with thrust and subsidence faulting in the coastal region of the Kutch Graben or along a major fault - which runs along the west coast of Maharashtra - have the potential of causing tsunamis directly or by triggering undersea landslides. Similarly further south, thrust and subsidence faults on the Bombay, Cambay and Namacia Grabens, have the potential to generate local tsunamis, particularly from landslides triggered by major earthquakes.

REFERENCES

Ambrasseys, N. and Bilham, R., 2003, "Earthquakes and Associated Deformation in North Baluchistan 1892-2001", Bulletin of the Seismological Society of America, Vol .93, No. 4, p. 1573 - 1605.

Bakht S. M. 2000. An Overview of Geothermal Resources of Pakistan. Proceedings World Geothermal Congress 2000, Kyushu - Tohoku, Japan, May 28 - June 10, 2000

Berninghausen, W.H., 1966. "Tsunamis and Seismic Seiches reported from regions adjacent to the Indian Ocean", BSSA, Vol 56, No.1, 1966.

Byrne Daniel E., Sykes Lynn R. Davis Dan M., 1992. Great thrust earthquakes and aseismic slip along the plate boundary of the Makran subduction zone. JOURNAL OF GEOPHYSICAL RESEARCH, VOL. 97, NO. B1, PAGES 449–478, 1992

Closs, H., Bungenstock, H., Hinz, K., 1969. Ergebnisse seismischer Untersuchungen im nrdlichen Arabischen Meer: ein Beitrag zur internationalen Indischen Ozean Expedition. METEOR Forschungsergebnisse, Reihe C, 2, 28 pp. Flueh, E. R., Kukowski, N., Reichert, C. (Editors). FS Sonne Cruise Report SO-123 - MAMUT, Maskat - Maskat 07.09. - 03.10.1997, GEOMAR Rep. 62, 292 pp.

Dorostian A., Gheitanchi M. R., Seismicity of Makran. Report of College of Science, & Institute of Geophysics, Islamic Azad Univ. North Tehran Branch, Iran (undated).□□

Regard V. Bellier O., Thomas J.-C., Abbassi M.R., Mercier J. L., Shabanian E., Feghhi Kh., Soleymani Sh., Bonnet S., Bourlès D. L., Braucher R., and J. Martinod, 2003. Tectonics of a Lateral Transition Between Subduction and Collision:The Zagros-Makran Transfer Deformation Zone (SE IRAN) European Geophysical Society 2003. Geophysical Research Abstracts, Vol. 5, 01210, 2003

Fruehn, J., White, R. S. and Minshull, T. A., 1997. Internal deformation and compaction of the Makran accretionary wedge, Terra Nova, 9: 101-104.

GEOMAR, Germany, the University of Cambridge and the National Institute of Oceanography, Pakistan, - Cruise (SONNE-123), 1997, 2000

Huhn K. , Kukowski N. , Schillhorn T. and E. Flueh, 1998. Morphotectonics of the Makran accretionary wedge imply new aspects for the plate tectonic situation in the northeast Indian Ocean. http://www.geomar.de/add_info/former_info/abstracts98/agu98abstracts.html

Harms, J. C., Cappel, H. N. and Francis, D. C., 1984. The Makran coast of Pakistan: Its stratigraphy and hydrocarbon potential. In: Haq, B. U. and Milliman, J. D. (Editors), Marine Geology and Oceanography of Arabian Sea and Coastal Pakistan: 3-27.

Hutchinson, I., Louden, K. E., White, R. S., 1981. Heat flow and age of the Gulf of Oman, Earth Planet. Sci. Lett., 56: 252-262.

Jacob, K. H. and Quittmeyer, R. L., 1979. The Makran region of Pakistan and Iran: Trench-arc system with active plate subduction. In: Farah, A. and de Jong, K. A. (Editors), Geodynamics of Pakistan: 305-317.

Jadoon, I.A.K., 1992, "Ocean/continental transitional crust underneath the Sulaiman Thrust Lobe and an evoluationary tectonic model for the Indian/Afghan Collision Zone", Pakistan Journal of Hydrocarbon Research, v.4, no.2, p.33-45.

Kopp C., Fruehn J., Flueh,E. R., Reichert, C., Kukowski N., Bialas J. and D. Klaeschen. 2000. Structure of the Makran subduction zone from wide-angle and reflection seismic data. Proceedings, 8th International Symposium on Deep Seismic Profiling of the Continents and Their Margins, Edited by R. Carbonell, J. Gallart and M. Torne, Tectonophysics, vol 329 Pages 171-191

Kopp C., Fruehn, J. Flueh E. and C. Reichert. 1998. Seismic Images of the Makran Subduction Zone

Mathur, S.M. "Physical Geology of India"□□

Minshull, T. A., White, R. S., Barton, P. J. and Collier, J. S., 1992. Deformation at plate boundaries around the Gulf of Oman, Marine Geology, 104: 265-277.

Mokhtari, M. and Farahbod, A.M. 2005. Tsunami Occurrence in the Makran Region. Tsunami Seminar, Tehran, 26 February 2005

Murty. T. and A. Bapat, 1999 "Tsunamis on the coastlines of India", International Tsunami Symposium, May 1999 (Abstract).

Pacheco and L. Sykes, 1992. "Seismic Moments of Great Shallow Earthquakes 1900-1990 with Magnitude > 7", Seismological Society of America, 1992.

Pararas-Carayannis, G. 2006a. Alexander the Great – Impact of the 325 B.C, Tsunami in the North Arabian Sea Upon his Fleet.
http://drgeorgepc.com/Tsunami325BCIndiaAlexander.html

Pararas-Carayannis, G. 2006b. The Earthquake and Tsunami of 28 November 1945 in Southern Pakistan http://drgeorgepc.com/Tsunami1945Pakistan.html

Pararas-Carayannis, G., 2005. "The Earthquake of 8 October 2005 in Northern Pakistan" http://www.drgeorgepc.com/Earthquake2005Pakistan.html

Pararas-Carayannis, G., 2001, "The Earthquake of 25 January 2001 in India" http://www.geocities.com/CapeCanaveral/Station/8361/Quake2001India.html

Pararas-Carayaniis, G. 1992. The Earthquake and Tsunami of 2 September 1992 in Nicaragua http://drgeorgepc.com/Tsunami1992Nicaragua.html

Platt, J. P., Leggett, J. K., Young, J., Raza, H. and Alam, S., 1985. Large-scale sediment underplating in the Makran accretionary prism, Southwest Pakistan, Geology, 13: 507-511.

Quittmeyer, R.C., and Jacob, K.H., 1979. "Historical and Modern Seismicity of Pakistan, Afghanistan, N.W. India and S.E. Iran," Bulletin of the Seismological Society of America, 69/3, pp. 773-823, 1979.

Qureshi R. M. 2006. Vulnerability of Pakistan Coast to Tsunami. Possible Applications/Role of Nuclear Techniques RCARO Workshop (20 - 24 February, 2006) Daejon, Korea

Masson F., Chery J., Hatzfeld D., Martinod J. Vernant P., Tavakoli F., and M. Ghfory-Ashtiani, 2005. Seismic versusasesimsic deformation in Iran inferred from earthquakes and geodetic data. Geophys. J. Int. (2005) 160, 217-226

Regard V., Bellier O., Thomas J.-C., Abbassi M.R., Mercier J. L., Shabanian E., Feghhi Kh. , Soleymani Sh. , Bonnet S., Bourlès D. L., Braucher R. and J. Martinod, 2003. Tectonics of a Lateral Transition between Subduction and Collision: The Zagros-Makran Transfer Deformation Zone (SE Iran), European Geophysical Society 2003, Geophysical Research Abstracts, Vol. 5, 01210, 2003

Ramanathan, K., and Mukherji, S., 1938, "A seismological study of the Baluchistan, Quetta, earthquake of May 31, 1935", Records of the Geological Survey of India, Vol. 73, p. 483 – 513.

Schoeppel, R.J., 1977 Prospects of Geothermal power in Saindak area, Baluchistan province, Pakistan. Final report for Oil and Gas Development Co. 15p.

Srivastava V. K. and Ranjana Ghosh. Mapping of tectonic lineaments and analysis of earthquake occurrences in Kutch region of Indian subcontinent using GIS and Remote Sensing techniques. Report of the Dept. of Applied Geophysics, Indian School of Mines

Times of India Newspaper archives (Mumbai), India, November 1945

Wadia, D.N., 1981, "Geology of India", Tata-McGraw-Hill, New Delhi.

White, R. S., Louden, K. E., 1983. The Makran Continental Margin: Structure of a Thickly Sedimented Convergent Plate Boundary. In: J. S. Watkinsand C. L. Drake (Editors), Studies in Continental Margin Geology. Mem. Am. Ass. Petrol. Geol. 34: 499-518.

2006: STATUS OF TSUNAMI SCIENCE RESEARCH AND FUTURE DIRECTIONS OF RESEARCH

Barbara H. Keating
President of the Tsunami Society
University of Hawaii
Rm. 314 HIG, 2525 Correa Rd.
Honolulu, HI 96822

ABSTRACT

In 2005, Dr. Robert Wiegel compiled "Tsunami Information Sources". The compilation has been made available via a website and has been published as an issue in *Science of Tsunami Hazards*. The compiled references have been assigned keyword descriptions, and compiled in order to review the breath and depth of Tsunami Science publications.

The review indicates that tsunami research involves eight major scientific disciplines: Geology, Seismology, Tsunami Science, Engineering, Disaster Management, Meteorology and Communications. These disciplines were subdivided into many topical subjects and the results were tabulated.

The topics having the largest number of publications include: tsunamigenic earthquakes, numerical modeling, field surveys, engineering models, harbor, bay, and canal modeling and observations, energy of tsunamis, workshops, tsunami warning centers, instrumentation, tsunami catalogs, tsunami disaster mitigation, evaluation of hazards, the aftermath of tsunamis on humans, and AID provided to Tsunami Damaged Communities.

Several areas of research were identified as likely directions for future research, including: paleotsunami studies, risk assessments, instrumentation, numerical modeling of earthquakes and tsunami, particularly the 2004 Indian Ocean event. There is a dearth of recent publications available on tsunami hazards education for the general public.

1. INTRODUCTION

Dr. Robert Wiegel published a bibliography of Tsunami citations in a *University of California Berkeley Hydraulic Engineering Laboratory Report, UCB/HEL-2005-1*. This report entitled, "Tsunami Information Sources," was also published as an issue of the *Science of Tsunami Hazards* (2006). The report compiled tsunami science publications, particularly:

1) Bibliographies, Books and Pamphlets, Catalogs, Collections, Journals and Newsletters, Maps, Organizations, Proceedings, Symposium and Workshops, Videos and photographs (pages 2-13).
2) Articles, Papers, Reports (pages 13-15).

An analysis of the publications listed under Item 2, "Articles, Papers and Reports," was made in order to determine: key areas of research, significant trends in research, and likely future trends (what's hot and what's not).

This analysis was initiated in order to facilitate a comparison of citations, describing tsunami deposits in Keating et al. (2006 in press) with the Wiegel (2005) compilation. This initial effort was then expanded into an overall review of tsunami literature. While this summary was being prepared in the spring of 2006, a second compilation was published, Wiegel (2006b). This second publication includes citations added since the first report and references from publications that fall into the categories of Planning and Engineering Design for Tsunami Mitigation/Protection, and Tsunami Propagation Near-shore. A re-analysis of the entire database is warranted, preferably an analysis involving collaboration between both authors (Wiegel and Keating), and with an expanded computerized indexing involving multiple keywords.

The results of the research, demonstrate that current research is focused in only a few areas and it also suggests that there is a deficiency in educational material on tsunami hazards available in the literature.

2. METHOLOGY

The bibliography of articles, papers, and reports compiled by Wiegel (2005 and 2006a) consists of citations of tsunami publications. In order to assess the general nature of the publications, each citation (on pages 13-115 of Wiegel, 2005) was assigned a keyword from the title to provide a general category for the major emphasis of each paper; for example, edge wave, long periods, resonance curve, and so on. After the keywords were identified, the citations were divided into disciplinary categories (see Fig. 1), including: Geology, Disaster Management, Communications, Engineering, Seismology, Numerical Modeling, Tsunami Science, and Meteorology, and then tabulated. The distribution of publications by discipline shows there are comparable numbers of publications within the disciplines of: Geology, Engineering, Seismology,

Numerical Modeling and Tsunami Science. The citations within each discipline were further subcategorized into topics.

This analysis is based upon several assumptions including: 1) the title of a professional publication will adequately reflect the general subject matter of the paper, 2) a single keyword will adequately describe a publication, and 3) each publication is significant and should be incorporated into the status review. Unfortunately, these assumptions are not valid in many cases. Many of the publications within the bibliography had insufficient information in the title for classification or inclusion in any of the topics used and thus many citations were excluded from this analysis.

In addition, it was found that a single keyword is often inadequate, for example "The Numerical Modeling of Run-up from the 1946 Tsunami in Hilo" would be listed under the discipline of Tsunami Science and the topic Numerical Modeling. A publication entitled, "The Earthquake and Tsunami Involved with the 1975 Kalapana Tsunami" would be tabulated under discipline of Seismology and the topic of Tsunamigenic Earthquake. While a publication titled "The Numerical Modeling of the Tsunami and Earthquake Associated with the 1975 Kalapana Earthquake" would be included under the discipline category of Tsunami Science and the topic of Numerical Modeling. A title such as "The Tsunami Deposits Associated with the 1975 Kalapana Earthquake" would be categorized under the discipline of Geology and subtopic Field Surveys." Finally, the assumption that "the publication is significant and should be incorporated into the review" is impossible to address, based solely upon a title.

Figure 1. This pie chart diagram shows the distribution of tsunami publications by scientific discipline. The numbers on the chart indicate the percentages of the total.

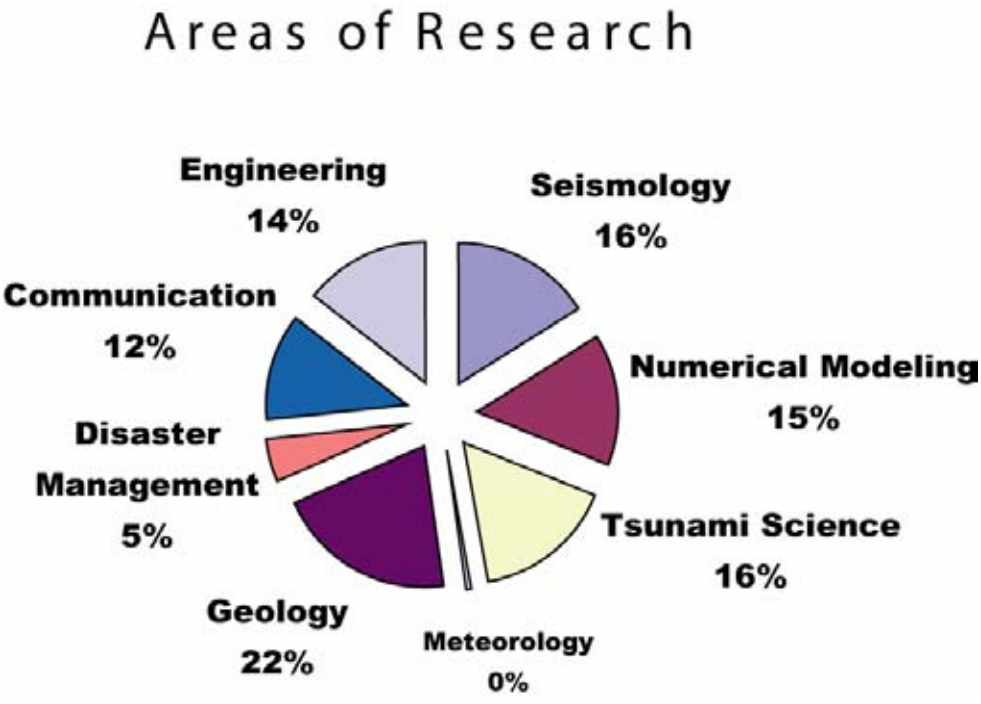

No digital database of publications is ever complete for more data becomes available as the database is being constructed. In building a data base on tsunami deposits (Keating et al., 2006) utilized most of the digital search engines available over the Internet. The results vary greatly from one digital database to another (e.g., Web of Science, Georef, Geobase, etc). Many older publications simply are not available digitally, thus it often proves to be a frustrating experience when searching for older publications. The incomplete nature of the digital databases reflects how they are constructed, emphasizing the addition of the newest publications, over incorporating older material. Also, the sources of citations are different for various databases (now downloaded directly from publishers). These problems reflect the youth of digital databases. As the scientific citations within databases increase and the search engines improve, analyses of publications will become more comprehensive.

3. RESEARCH CATEGORIES

3.1 Subdivision of Disciplines into Research Topics

The greatest number of publications (Fig. 1) falls under the discipline of Geology (n= 504), followed by Seismology, Tsunami Science, Engineering and Wave modeling. Each discipline category (listed at left in Fig.2) can be further subdivided into Research Topics. The breakdown by research topic for each of the scientific disciplines is shown in the center column of Fig. 2. Geologic publications (n= 516) were subdivided into nine topical areas. The most frequently published topic, in the discipline of Geology, is geological field surveys of tsunami and paleo-tsunamis (n= 295; see Fig. 2), followed by composite topic of landslides and turbidity currents (n= 136). Within the Engineering Discipline there are 361 publications (Fig. 2). The majority of these publications (n=212) focus on modeling studies.

The research topic most frequently referred to in the discipline of Seismology is the topic Tsunamigenic Earthquakes (n= 149). The second most frequent research topic that was included in the title was the composite category of Ruptures, Faulting, and Thrusts (n= 74).

Under the category of Tsunami Topics (summarized in Figure 2) there are 915 publications. The largest numbers of publications deals with Numerical Modeling (n= 301). Tsunami Observations (N= 142) is the second most popular topic. Wave studies entail a total of 265 publications (Figure 2). The largest number of these studies involves wave behavior in harbors, bays, and canals (n= 95).

Figure 2. (Next Page) This illustration is a histogram, showing the number of publications analyzed by discipline (left column) and topic (center column). On the right is a plot of the number of publications per topic. The horizontal bars show varying shades of stippled patterns indicating the various disciplines involved. The topics of greatest interest (largest number of publications) are labeled on the histogram.

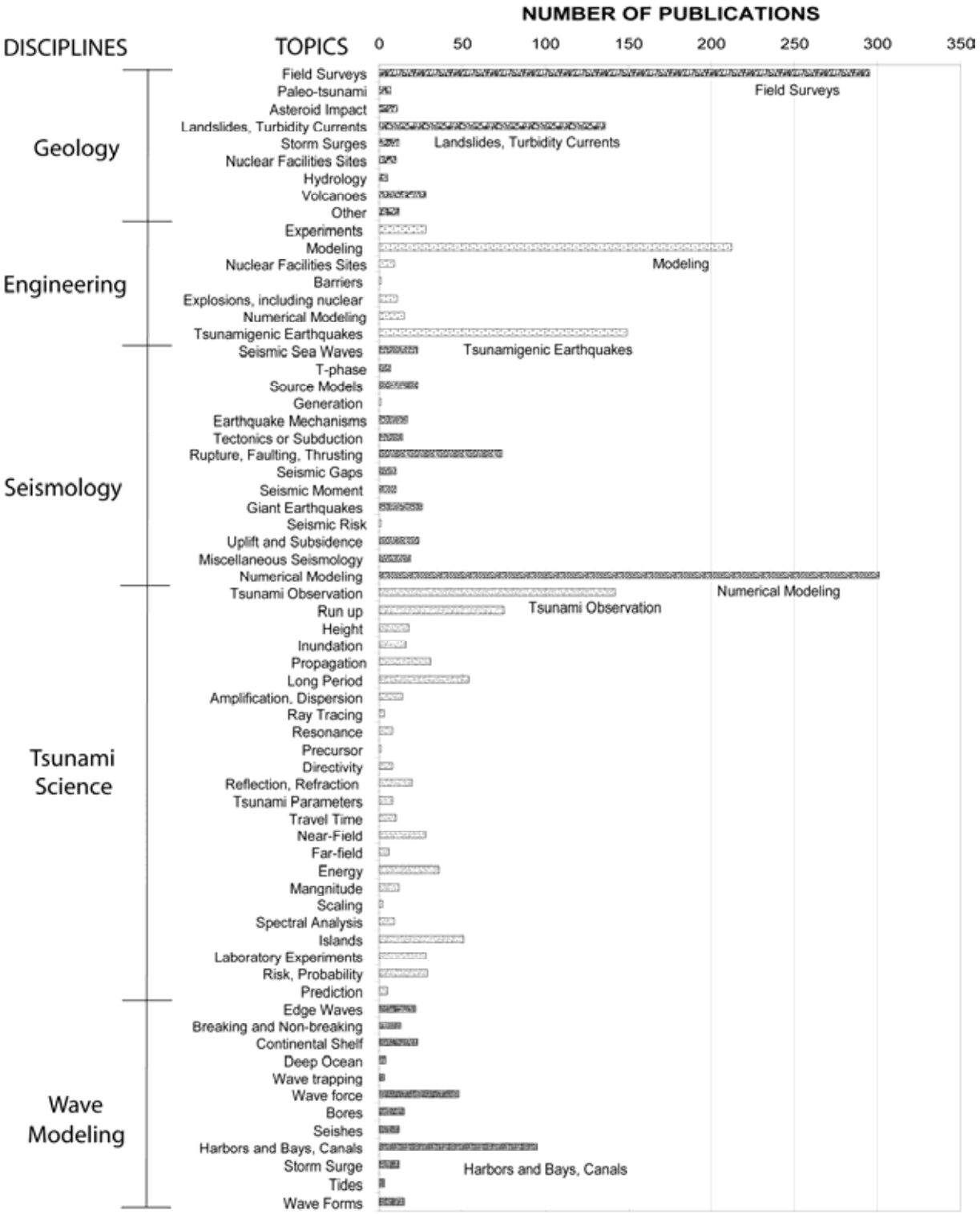
NUMBER OF PUBLICATIONS
DISCIPLINES
TOPICS
0
50
100
150
200
250
300
350
Geology
Field Surveys
Paleo-tsunami
Asteroid Impact
Landslides, Turbidity Currents
Storm Surges
Nuclear Facilities Sites
Hydrology
Volcanoes
Other
Field Surveys
Landslides, Turbidity Currents
Engineering
Experiments
Modeling
Nuclear Facilities Sites
Barriers
Explosions, including nuclear
Numerical Modeling
Tsunamigenic Earthquakes
Modeling
Seismology
Seismic Sea Waves
T-phase
Source Models
Generation
Earthquake Mechanisms
Tectonics or Subduction
Rupture, Faulting, Thrusting
Seismic Gaps
Seismic Moment
Giant Earthquakes
Seismic Risk
Uplift and Subsidence
Miscellaneous Seismology
Numerical Modeling
Tsunamigenic Earthquakes
Numerical Modeling
Tsunami Science
Tsunami Observation
Run up
Height
Inundation
Propagation
Long Period
Amplification, Dispersion
Ray Tracing
Resonance
Precursor
Directivity
Reflection, Refraction
Tsunami Parameters
Travel Time
Near-Field
Far-field
Energy
Mangnitude
Scaling
Spectral Analysis
Islands
Laboratory Experiments
Risk, Probability
Prediction
Tsunami Observation
Wave Modeling
Edge Waves
Breaking and Non-breaking
Continental Shelf
Deep Ocean
Wave trapping
Wave force
Bores
Seishes
Harbors and Bays, Canals
Storm Surge
Tides
Wave Forms
Harbors and Bays, Canals

3.2 RISK REDUCTION CATEGORIES

The majority of publications discussed to this point could be referred to as hazards science and engineering. Publications dealing with human or societal impact, and disaster management and are separated into the basic categories of risk reduction (Fig. 3). These categories include: Disaster Preparedness, Disaster Response, Disaster Recovery, Disaster Mitigation, and Development. These tsunami-related publications were further subdivided into topics such as: Resilience, Crises Management, Removal and Wreckage, Rebuilding, and Mitigation, Evaluation of Hazards, Safety Studies, Emergency Services, Medical Care, Evacuation, Response, Assessment, Survival, Preparation, Prevention, and Protection. A new field of research involves human response to tsunami. The tropics involving human behavior are included in Disaster Response and Recovery.

Instrumentation has been incorporated with the category of Hazards Science since instruments are the tools of scientists. However the topic is also associated with warning systems (Disaster Preparedness Category). The Instrumentation topic only contains only 48 publications. This is surprising since the monitoring of earthquakes and tsunami is extremely dependent upon instrumentation. The topics of maps and bathymetry, photography, indexes, glossary, lists, catalogs, history, data processing and computer codes have also been listed under the category Hazards Science. Finally, publications on re-insurers, insurance, land management, political demands, AID, and dealing with bureaucrats and reporters have been included under the categories Disaster Mitigation and Development.

In summary, the topics having the most publications include categories such as field surveys, source mechanisms, numerical modeling and studies involving tsunami effects on harbors, bays and canals. The least number of publications fall in the categories of seismic and tsunami risk, precursors and/or predictions, and education. This suggests a need for increased efforts in the topics of education and tsunami risk.

4. INTERACTIONS

While, much of the material that has been published in the "Tsunami Information Sources", and summarized here, is basic research, any knowledge related to tsunami research directly or indirectly benefits society. Thus it is important to reflect on how Tsunami research contributes to Public Risk Reduction. An interesting report on several aspects of Hazard Management associated with the 2004 Indian Ocean Tsunami is available on the Internet (Cosgrave et al., 2006).

The interaction between science, disaster management policy and education has been summarized in Figure3 where each category of activities contributes directly to a reduction of deaths, injuries and property loss (Risk Reduction). The principle components of risk reduction are illustrated within this figure as a series of overlapping circles. This concept of "circles within a circle" represents the overlapping areas of expertise needed to facilitate risk reductions. The illustration includes: Science, Disaster Preparations, Disaster Response, Disaster Recovery, Disaster Mitigation, Development and Environmental Change. In large part, the publications of tsunami scientists and engineers falls in the category of "Science". In order to facilitate risk reductions, individual scientists should work with, and provide technical information, to all others workings toward the goal of Risk Reduction.

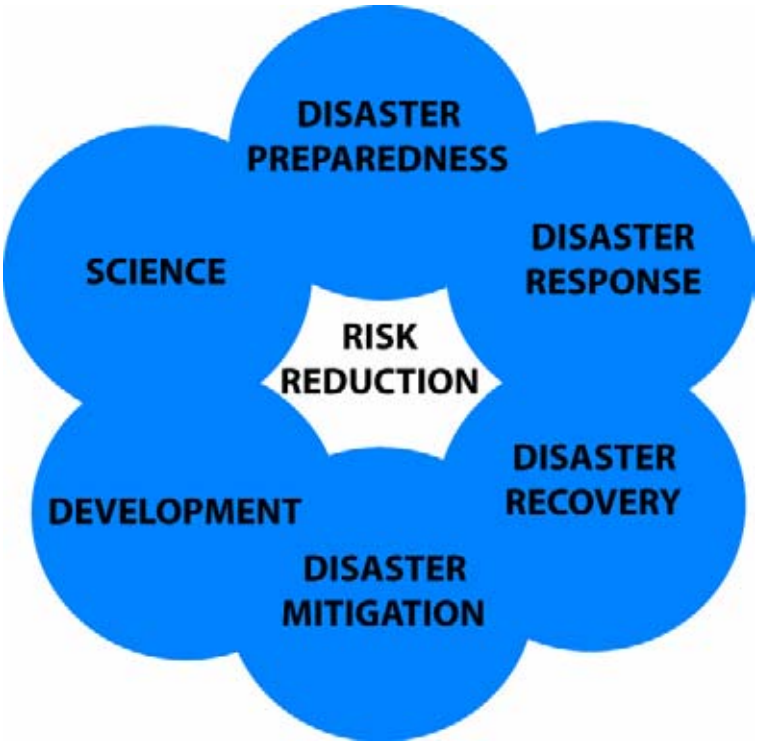

FIGURE 3. The illustration above shows the principle components of Risk Reduction with the research topics reviewed in this manuscript included in the illustration. An effort to reduce damage from natural disasters (and particularly tsunamis) involves cooperation between individuals working in all fields.

In order to present a review of tsunami science within this risk reduction framework, the scientific disciplines, as well as topics (and number of publications) have been applied (in Figure 4) to the Risk Reduction scheme, just discussed.

3.2 STRIKING LACK OF EDUCATION PUBLICATIONS

Education is listed under the heading Development and topic Educational Efforts. The total number of publications is four. This is number is woefully inadequate.

Despite the devastating loss of lives during the 2004 Indian Ocean Tsunami, the experience proved that many people did survive because they had a rudimentary knowledge of tsunami. In order to prevent deaths due to tsunami we need both Tsunami Warning Centers and PUBLIC EDUCATION.

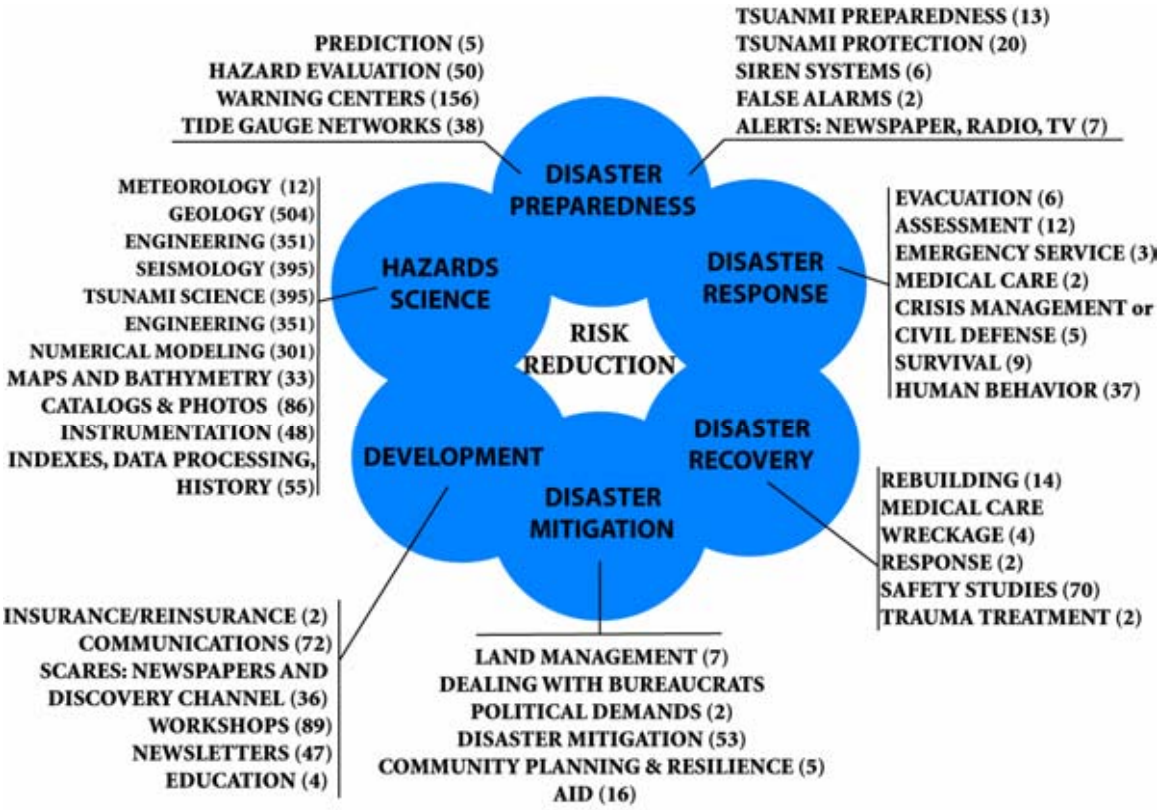

Figure 4. A basic risk reduction scheme is shown above as overlapping shaded circles. Lists of disciplinary and topical categories have been added to the margins of the figure, with the number of publications (listed in parenthesis). These results are based upon a keyword analysis of citations within the "Tsunami Information Sources"(Wiegel, 2005 and 2006a).

An experience of unwise human behavior from Honolulu can provide important insights into the global need for tsunami hazards education. During the last tsunami warning in Honolulu, an estimated 400 surfers went to the shore to surf the tsunami waves. Had even a moderate tsunami occurred many of these 400 surfers would have landed in the lobbies of the Waikiki Hotels and other sites of devastation and would have contributed significantly to the casualties. To remedy this situation, a CD was produced that warns surfers and divers of the dangers of tsunami (He'e Nalu, in references). This CD has been distributed to the public through surf and dive shops. The majorities of individuals living in Hawaii moved here or were born after the last destructive tsunami in Hawaii and many lack knowledge of the devastating effects of tsunami inundation.

4. FUTURE DIRECTIONS

In 2003, a summary of publications related to tsunami deposits (Fig. 5) was presented at the fall meeting of the Am. Geophysical Union (Keating, 2003). The data available at that time demonstrated an exponential expansion of publications on tsunami deposits. This expansion should continue into the foreseeable future, partially fueled by

the research associated with the 2004 Indian Ocean Tsunami. It is likely that continued research into establishing the recurrence rates of tsunami, in tsunami inundation prone areas, will allow us to better assess risk, regionally and locally.

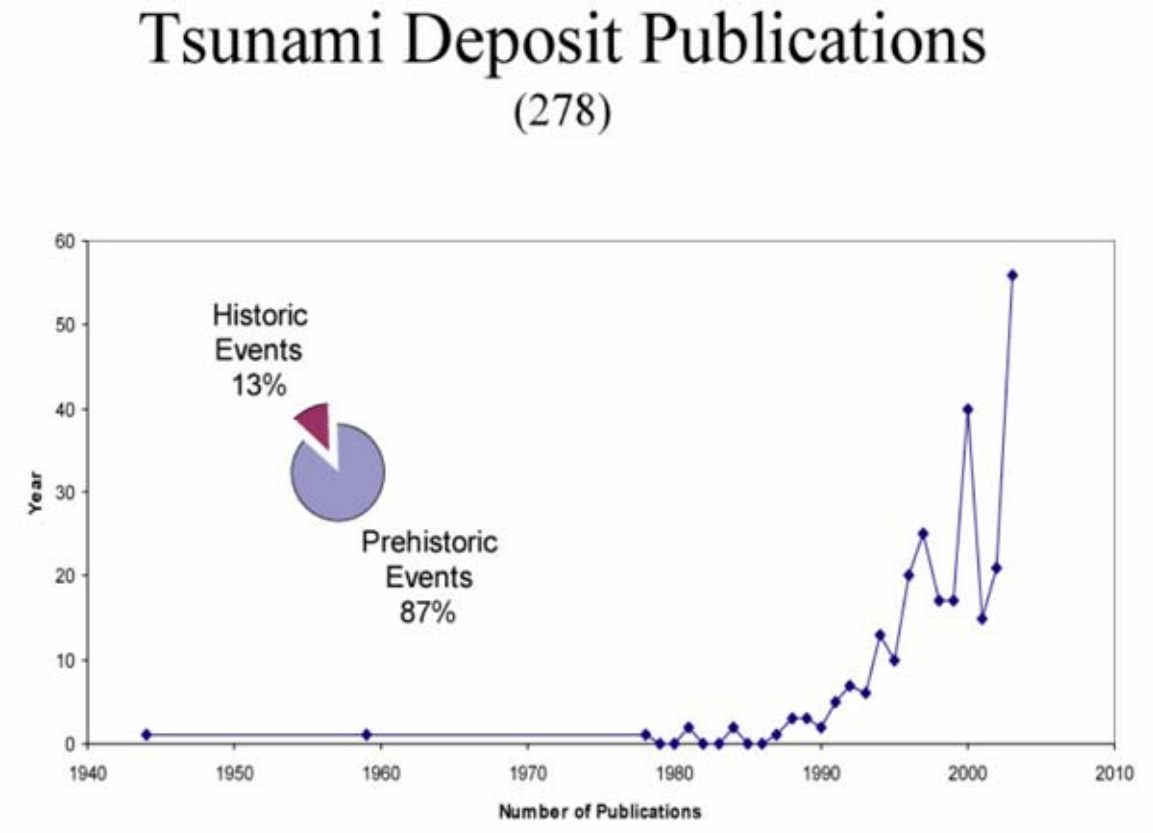

FIGURE 5. This illustration shows the number of publications describing tsunami deposits that were published between 1940 and 2003. Based upon the rapid increase in publications, the topic of paleo-tsunami recorded in sedimentary deposits is clearly one of the fastest growing areas of tsunami research.

5.1 RISK ASSESSMENT

In the past two years, there has been a series of devastating natural disasters (a giant tsunami, earthquakes, tornadoes, hurricanes on the Gulf coast and elsewhere) that challenge the capabilities of the insurance and re-insurance industries to cover the costs of natural disasters. It has become obvious that society as a whole needs accurate risk assessment (and management) that is based upon reliably determined rates of tsunami reoccurrence. Furthermore, the reoccurrence rate must be established at a regional level and perhaps a local level. Adequately funded paleo-tsunami deposit studies might allow us to make valid risk assessments for highly populous, and therefore highly expensive, risk management areas.

5.2 STORM VS. TSUNAMI DEPOSITS

In order to establish reoccurrence rates for tsunami we must be able to differentiate storm deposits from tsunami deposits. In consultation with scientists at the University of South Florida, the author and collaborators have begun to look at this issue and the investigations appear very promising.

5.3 INSTRUMENTATION

NOAA has actively been developing a system of deep ocean pressure monitoring systems (Tsunameter system or DART buoys). These instruments have a potential to allow rapid monitoring and evaluation of tsunami, facilitating warnings and evacuation (Bernard, 2005). This advance in instrumentation could lead to more timely and more accurate warnings and thus save lives. And it will lead to many new publications!

5.4 LANDSLIDES

Another instrumental advance that has impacted tsunami research is the utilization of side-scan sonar to map landslides and slumps on the seafloor in areas that were likely to be tsunamigenic. The sea floor images have proven extremely useful in the study of landslides on continental slopes and volcanic edifice failures. It is vitally important that these mapping efforts be coupled with site surveys to establish rock properties, ages, rock types, mechanical properties, etc. Additionally, landslide research has been an important focus in tsunami research in the recent past and is likely to remain an important area of study.

5.5 INTEGRATED INVESTIGATIONS

Many scientists have been involved in scientific investigations associated with the 2004 Indian Ocean Tsunami. Because so many scientists within different disciplines were involved, it is likely that multi-investigator projects will develop that link together observations and measurements on the ground to modeling in the laboratory. In particular, studies of tsunami sediment transport may be linked to models of the carrying power, or destructive power, of the tsunami waves.

5. CONCLUSION

Our understanding of tsunami largely results from direct observation of waves and their effect on shorelines and structures and on the numerical modeling of earthquakes and tsunami. The seismic studies related to the 2004 Indian Ocean Tsunami indicate that extremely long ruptures, actually a series of connected ruptures in space and time, of the sea floor are possible and can generate huge tsunami. Careful numerical analyses of the earthquake and resultant tsunami from the 2004 Indian Ocean event will dominate tsunami publications for the next several years.

6. ACKNOWLEDGMENT

Many thanks to Dr. Robert Wiegel for his efforts in compiling the Tsunami Information Sources and providing the important compilation for publication in the *Science of Tsunami Hazards*. This summary was supported by a grant for the University of Hawaii Office of the Vice-Chancellor of Research. I thank Matt Wanink for his assistance in producing the figures and the Power Point Presentation for the Tsunami Symposium, 3. The publication summarizes an oral presentation given within the Tsunami Society Business Meeting in the 3rd Tsunami Symposium, Honolulu, HI, May 23-26, 2006.

6. REFERENCES

Bernard, E. N., 2005, The U. S. National Hazard Mitigation Program: A Successful State-Federal Partnership, in (E. N. Bernard, ed) "Developing Tsunami Resilient Communities, The National Tsunami Hazard Mitigation Program," Springer Pub., Dordrecht, p. 5-24.

Cosgrave, J., 2006, Tsunami Evaluation Coalition: Initial Findings, Website: www.alnap.org/tec/, pp. 1-16.

Keating, B. H., 2003,What should mega-tsunami deposits look like? Abstract, E.O.S., Trans. American Geophysical Un., Fall Meeting Program, OS21D-07, page F810.

He'e Nalu, but never try to surf a tsunami, produced by the Center for the study of Active Volcanoes and the Pacific Tsunami Museum, Distributed free by the Hawaii Civil Defense System. CD.

Wiegel, R. L., 2005, Tsunami Information Sources, University of California, Berkeley Hydraulic Engineering Lab, Report UCB/HEL. 2005-1, pp. 1-115. Also available at: http:www.lib.Berkeley.edu/WRCA/tsunamis.html.

Wiegel, R. L., 2006a, Tsunami Information Sources, Science of Tsunami Hazards, 24, 2, 58-171.

Wiegel, R. L., 2006b, Tsunami Information Sources, Part 2, University of California, Berkeley Hydraulic Engineering Lab, Report UCB/HEL. 2006-1, pp. 1-36.

Science of Tsunami Hazards, Vol 24, No. 5 (2006) ISSN 8755-6839

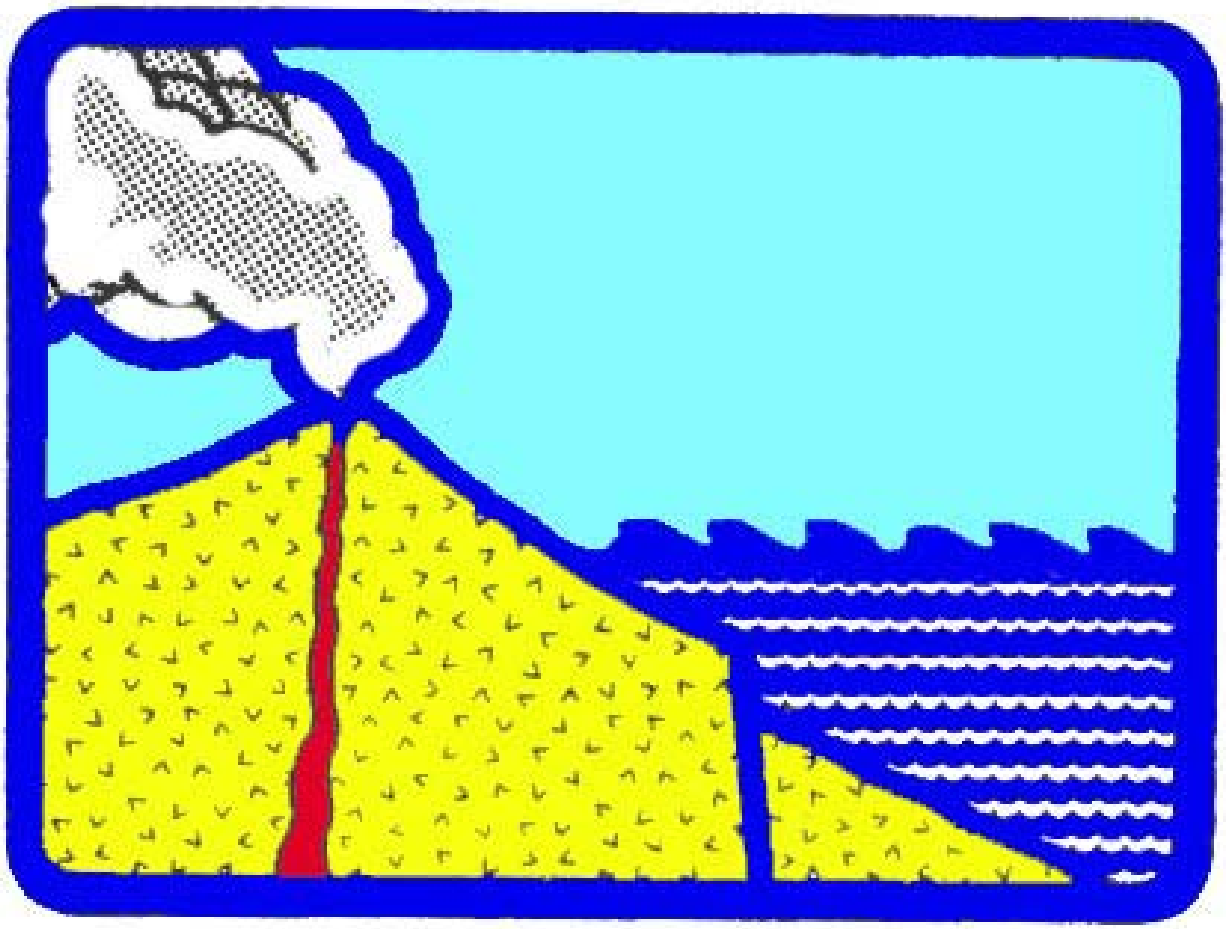

2523 Correa Rd, UH/SOEST, Rm 215 HIG
Honolulu, HI 96822, USA

WWW.STHJOURNAL.ORG